Award Number: **W81XWH-10-1-0791**

TITLE: **Improving Joint Function Using Photochemical Hydrogels for Articular Surface Repair**

PRINCIPAL INVESTIGATOR: **Mark A. Randolph**

CONTRACTING ORGANIZATION: **Massachusetts General Hospital**
Boston, MA 02114

REPORT DATE: **February 2017**

TYPE OF REPORT: **Final**

PREPARED FOR: U.S. Army Medical Research and Materiel Command
Fort Detrick, Maryland 21702-5012

REPORT DOCUMENTATION PAGE

Form Approved
OMB No. 0704-0188

PLEASE DO NOT RETURN YOUR FORM TO THE ABOVE ORGANIZATION.

30SEP2010-30NOV2016

1. REPORT DATE *(DD-MM-YYYY)*	2. REPORT TYPE	3. DATES COVERED *(From - To)*
02-28-2017	Final Report	~~XXXXXXXXXXXXXX~~

4. TITLE AND SUBTITLE
Improving Joint Function Using Photochemical Hydrogels for Articular Surface Repair

5a. CONTRACT NUMBER
W81XWH-10-1-0791

5b. GRANT NUMBER
OR090275

5c. PROGRAM ELEMENT NUMBER

6. AUTHOR(S)
Randolph, Mark A.; marandolph@mgh.harvard.edu

5d. PROJECT NUMBER

5e. TASK NUMBER

5f. WORK UNIT NUMBER

7. PERFORMING ORGANIZATION NAME(S) AND ADDRESS(ES)
Massachusetts General Hospital
Boston, MA 02114

8. PERFORMING ORGANIZATION REPORT NUMBER

9. SPONSORING/MONITORING AGENCY NAME(S) AND ADDRESS(ES)
U.S. Army Medical Research and Materiel Command
Fort Detrick, Maryland 21702-5012

10. SPONSOR/MONITOR'S ACRONYM(S)

11. SPONSOR/MONITOR'S REPORT NUMBER(S)

12. DISTRIBUTION/AVAILABILITY STATEMENT
Approved for Public Release; Distribution Unlimited

13. SUPPLEMENTARY NOTES

14. ABSTRACT
The goal of this project was to develop a novel means to regenerate the articular cartilage and restore normal function of the joint. A strategy that can generate durable hyaline articular cartilage, which will be predominantly type II collagen, and is capable of integrating with the surrounding cartilage matrix (without fissures) could improve the long-term outcome of joint surface repair. Several photochemically crosslinkable gels were developed and tested in vitro and in vivo in mice including collagen, fibrin, PEG thiol-ene, and gelatin methacrylamide. All have shown satisfactory cell viability and some cartilage formation. A modification to using dynamic culture as a bioreactor has resulted in the formation of aggregates of chondrocytes called dynamic Self-Regenerating cartialge (dSRC) that can be encapsulated in the gels. This has resulted in superior cartilage formation and has been tested in two swine in a pilot study. In the final year, 3 and 6-month swine studies were performed to assess the utility of this approach for generating articular cartilage for joint surface repair.

15. SUBJECT TERMS
Cartilage; articular; collagen gel; poly(ethylene)glycol gel; photochemical crosslinking

16. SECURITY CLASSIFICATION OF:			17. LIMITATION OF ABSTRACT	18. NUMBER OF PAGES	19a. NAME OF RESPONSIBLE PERSON
a. REPORT	b. ABSTRACT	c. THIS PAGE			USAMRMC
U	U	U	UU	90	19b. TELEPHONE NUMBER *(Include area code)*

Reset

Table of Contents

Page

1. INTRODUCTION

Injuries to the cartilage surfaces of joint are particularly problematic because, unlike bone and other vascular tissues comprising the joint, cartilage is avascular and possesses limited capacity for repair and self-regeneration. Consequently, injury to cartilage in the articulating joints from trauma results in scar formation and possible arthritic changes that can lead to pain, stiffness, and loss of structure and function. These joint injuries not only limit physical activity and mobility of those afflicted, but the inability to move freely can cause deep psychological scars and loss of independence when individuals have to depend on family and healthcare providers for constant assistance to perform daily life functions. The level of functional capability in the injured limb and ultimate quality of life depend on the successful outcome of joint surface regeneration performed as a secondary procedure weeks or even months after the initial injury. The return of function and the probability of return to active duty rely on successful restoration of the entire joint including the articular surface, and therefore, joint function. Lesions in the joint surface are commonly treated with microfracture, autologous cell implantation (ACI), or osteoarticular autograft transfer system (OATS). To date, however, the outcomes of many restorative procedures are very unsatisfactory and an improved method for joint repair is a clear unmet need in military medicine. **The goal of our research was to introduce a novel means to regenerate the articular cartilage and restore normal function of the joint.** A strategy that can generate durable hyaline articular cartilage, which will be predominantly type II collagen, and is capable of integrating with the surrounding cartilage matrix (without fissures) could improve the long-term outcome of joint surface repair. *The scope of this research was to develop regenerative medicine approaches involving biocompatible hydrogel scaffolds seeded with autologous cells that provide three-dimensional environments favorable for promoting chondrogenesis for joint surface repair.* Five peer-reviewed publications have resulted from this project thus far. Another manuscript is in draft form and we anticipate possibly 1 or 2 additional manuscripts will result from this project.

2. KEYWORDS

Cartilage; articular; collagen gel; poly(ethylene)glycol gel; photochemical crosslinking

3. ACCOMPLISHMENTS

(a) Major goals of the project

Task 1 Test of photochemically crosslinked gels to produce cartilage and bone using chondrocytes and osteoblasts

Subtask 1.1.a Prepare animal protocols for ACURO
Animal protocols for the use of mice and swine were approved in July 2010 prior to the beginning of the award. These documents were submitted to ACURO.

Milestone #1 Animal approvals from ACURO
ACURO approval for the use of mice was received on October 25, 2010 and approval for the use of swine on November 10, 2010.

Subtask 1.1.b Perform implantation of photochemically crosslinked collagen and PEG gels with chondrocytes and osteoblasts
Subtask 1.1.c Evaluate cartilage and bone matrix produced in vivo in mice

Candidate photochemically crosslinked hydrogels for encapsulating chondrocytes or chondrocyte precursor cells were tested. The algorithm for making and testing the gels is presented in Figure 1. If the gels performed well in making neocartilage in mice, we would then proceed to swine studies. If not, our plan would be modified to re-examine cartilage production in vitro and in mice before proceeding. Photochemically crosslinked gels were made using collagen, gelatin methacrylamide, and poly(ethylene) glycol thiol-ene gels. The photochemically crosslinked collagen gels demonstrated increased resistance to collagenase digestion over uncrosslinked gels, but had little effect on changing the bulk modulus (stiffness) of the gels. This work was published in the Journal of Biomedical Materials Research Part A (Omobono et al., Biomed Mater Res A. 2015 Apr;103(4):1332-8. doi: 10.1002/jbm.a.35266. PubMed PMID: 25044419) and reported in the 2014 annual report (Appendix 1). Testing of the PEG thiol-ene gels showed changes in the shear moduli were related to the weight percent of the gels. In vitro studies showed good viability of swine articular chondrocytes following the polymerization process. Modifications were made to the gel to tether TGF-β1 to the molecular backbone to promote matrix formation by encapsulated chondrocytes. This work was published in 2014 in the Journal of Biomedical Materials Research Part A (Sridhar et al., J Biomed Mater Res A. 2014 Dec;102(12):4464-72. doi:10.1002/jbm.a.35115. Epub 2014 Feb 26.) (Appendix 2). Additional modifications were made in the PEG thiol-ene formulation and published in Advanced Healthcare Materials in 2015 (Sridhar et al., Adv Healthc Mater. 2015 Apr 2;4(5):702-13. doi: 10.1002/adhm.201400695. Epub 2015 Jan 21.) (Appendix 3). Another formulation included norbornene-functionalized gelatin to tailor the degradation of the crosslinked gel and published in Regenerative Engineering and Translational Medicine (Sridhar et al., Regen. Eng. Transl. Med. DOI 10.1007/s40883-015-0002-3) (Appendix 4). In year 4 we began testing a new photochemically crosslinkable gel formulation, gelatin methacrylamide (GelMA). This material was tested in vitro and in vivo in mice in year 5 showing cell survival and new cartilage matrix formation in vivo using chondrocytes (Figure 2). The material supported chondrocytes and permitted new cartilage matrix formation, but will require additional modifications if it were to be used in the subsequent swine studies. No further studies were performed with GelMA during the course of this project.

In year 4 we developed a new strategy to grow immature cell aggregates, originally referred to as chondrons, but now termed dymanic Self-Regenerating Cartilage (dSRC). These dSRC aggregates promoted contiguous new cartilage matrix to form. A complete study of these dSRC combined with photochemically crosslinked collagen was completed in year 5 and reported below. The dSRC/collagen gel formulation was pilot tested in swine with favorable outcomes showing new cartilage formation in the defects using cells in gels compared to empty defects and defects with gels alone. The results of the mice study and the pilot swine study were reported in 2016 (Meppelink et al., Tissue Eng Part A. 2016 Jul;22(13-14):962-70. doi:10.1089/ten.TEA.2015.0577. PubMed PMID: 27324118.) (Appendix 5). Additionally, one of our initial goals was to generate new cartilage that would integrate with existing native cartilage. To this end, we studied the mechanical environment of the interface of the dSRC with surrounding native cartilage with confocal strain mapping. The results of these studies have been reported at several meetings and a manuscript has been drafted for publication (Appendix 6).

Milestone #2 Outcomes of cartilage and bone formed in test gels using chondrocytes and osteoblasts in mice

Milestone #2 completed

Subtask 1.2.a Initiate 3-month pilot study in swine with photochemically crosslinked collagen and PEG gels with bilayer of chondrocytes and osetoblasts

Subtask 1.2.b Evaluate cartilage and bone matrix formation in 3-month swine study

Seven swine were enrolled in a study evaluating the use of dSRC implanted with photochemically crosslinked collagen gels. Three chondral defects were made in the patellar groove of the left knee joint in each swine. dSRC were made by dynamic culture of the cells for 14 days. The sites of treatment and the type of treatment were randomized. Treatments were: 1) cells in photochemically crosslinked gels; 2) photochemically crosslinked gels not containing cells; and 3) empty defects. Defects treated with dSRC in the gel showed early stages of regeneration of the cartilage surface as demonstrated in the defects treated with cells (C1 and C2) in swine 23333 (Figure 3). The control defect treated with gel alone showed only rudimentary repair tissue in the defect (G). However, the quality of repair tissue in 23416 was poor in all defects, even those treated with dSRC (Figure 4). The range of results from these studies are presented in the histological figure showing H&E stained sections along with sections stained with toluidine blue and safranin O. Sections stained for types I, II, and III collagen are pending at the time of submission of this report.

Milestone #3 Outcomes of cartilage formation on joint surface and subchondral bone formation in swine 3-month study
Milestone #3 completed

Subtask 1.3.a Initiate 6-month study in swine with photochemically crosslinked collagen and PEG gels with bilayer of chondrocytes and osetoblasts
Subtask 1.3.b Evaluate cartilage and bone matrix formation in 6-month swine study
Eight swine were enrolled in the 6-month study evaluating the use of dSRC implanted with photochemically crosslinked collagen gels. In each swine three chondral defects were made in the patellar groove of the left knee joint. The sites of treatment and the type of treatment were randomized. Treatments were: 1) cells in photochemically crosslinked gels; 2) photochemically crosslinked gels not containing cells; and 3) empty defects. The surgery and results for swine 23412 are shown in Figure 5. Defects treated with cells (C1 and C2) in the gel showed regeneration of the cartilage surface. Those defects treated left empty (E) were filled with poorly regenerated tissue. The range of results from these studies are presented in the histological figure showing H&E stained sections along with sections stained with toluidine blue and safranin O. Sections stained for types I, II, and III collagen are pending at the time of submission of this report.

Milestone #4 Outcomes of cartilage formation on joint surface and subchondral bone formation in swine 6-month study
Milestone #4 completed

Subtask 1.4.a Initiate 12-month study in swine with photochemically crosslinked collagen and PEG gels with bilayer of chondrocytes and osetoblasts
Subtask 1.4.b Evaluate cartilage and bone matrix formation in 12-month swine study
Milestone #5 Outcomes of cartilage formation on joint surface and subchondral bone formation in swine 12-month study
Given the modest results of the 3 and 6-month swine studies in Subtasks 1.2 and 1.3, no 12 month animals were performed.

Specific Aim 2

Task 2 Stimulation of chondrogenesis by stem cells in photochemical gels

Subtask 2.1.a Perform initial study of collagen and PEG gels with stem cells implanted in mice

Subtask 2.1b Evaluate cartilage and bone matrix produced in vivo in mice with stem cells

Stage I: Bone marrow MSCs were harvested from donor swine and grown in culture using osteogeneic, chondrogenic and adipogenic differentiation media.

Results: BM-MSCs were isolated from swine bone marrow collected by aspiration from the iliac crest of swine. The MSC population was isolated by attachment to plastic culture dishes and propagated in high glucose DMEM. To test the multilineage potential of swine BM-MSCs, the cultured cells were placed into commercial differentiation media from Invitrogen to differentiate them into osteogenic, adipogenic and chondrogenic lineages. The assays for osteogenic and adipogenic assays were conducted on MSCs attached to culture plates. For osteogenic differentiation, the cells were assayed for the production of alkaline phosphatase shown in Figure 6a & b. Cells that were differentiated into an adipogenic lineage were assayed for the presence of lipid in the cells using Oil Red O staining (Figure 6c & d). For chondrogeneis, 250,000 cells were grown in pellet culture and treated with chondrogenic media. The pellets were evaluated histologically to assess the presence of cartilage-like matrix using stains for the presence of charged glycosaminoglycans (Figure 6e, f, & g). The results demonstrate that the isolated swine BM-MSCs were differentiated into the osteogenic lineage demonstrated by the increased production of alkaline phosphatase; into the adipogenic lineage with the formation intracellular lipid; and the chondrogenic lineage as demonstrated by the production of cartilage-specific extracellular matrix.

Another approach was employed using micromass culture of swine BMSCs and commercial differentiation medium (Lonza) to stimulate chondrogenesis. The results using rtPCR showed an increase in collagen type II (col2A1) by nearly 60-fold over nonstimulated BMSCs (Figure 7). Upregulation was also noted for col9A1, aggrecan, and cartilage oligomeric protein.

Milestone #6 Outcomes of cartilage and bone formed in test gels using stem cells stage I

Subtask 2.2.a Perform full study of implantation of collagen and PEG gels with stem cells
Subtask 2.2.b Evaluate cartilage matrix produced in vivo in mice with stem cells

Stage II: MSCs were placed into 3D alginate gels and stimulated with chondrogenic media from Invitrogen. After 2 weeks of culture, the gels were placed in vivo into nude mice for 5 weeks. Control gels were made with swine chondrocytes (positive control) and non-differentiated MSCs (negative control). The results are shown in Figure 8 showing that gels containing MSCs stimulated with chondrogenic factors produced new cartilage matrix, whereas MSCs in the gels that were not treated with chondrogenic factors failed to make cartilage matrix.

Milestone #7 Outcomes of cartilage and bone formed in test gels using stem cells stage II

Cartilage matrix formation was demonstrated in vivo by BMSC

Subtask 2.3.a Initiate 3-month pilot study in swine with collagen and PEG gels with stem cells
Subtask 2.3.b Evaluate cartilage and bone matrix formation in 3-month swine study
Milestone #8 Outcomes of cartilage and bone formation for joint surface restoration in swine 3-month study using photochemical gels and stem cells

Although we were able to detect small amounts of chondrogenesis from the in vitro stimulation studies and the in vivo mice studies, the results did not warrant proceeding to swine with a full scale study.

Subtask 1.3.a Initiate 6-month study in swine with collagen and PEG gels with stem cells
Subtask 1.3.b Evaluate cartilage and bone matrix formation in 6-month swine study

Milestone #9 Outcomes of cartilage and bone formation for joint surface restoration in swine 6-month study using photochemical gels and stem cells

Although we were able to detect small amounts of chondrogenesis from the in vitro stimulation studies and the in vivo mice studies, the results did not warrant proceeding to swine with a full scale study.

(b) Key research accomplishments

- Formulation of photochemically crosslinked gels:
  - Type I collagen solution using Rose Bengal as the photoinitiator and green light (532 nm)
  - Type I collagen solution using Riboflavin as the photoinitiator and blue light (458 nm)
  - Poly(ethylene) glycol thiol-ene gel using ultraviolet light (365nm nm)

- Modifications of photochemically crosslinked gels:
  - In vitro mechanical testing of photochemically crosslinked collagen hydrogels showing increased bulk modulus with addition of EDC treatment
  - Adding fibrin to the type I collagen solution and photochemically crosslinking the combination gel using Riboflavin as the photoinitiator and blue light (458 nm) increases the bulk modulus of the gels
  - Performing the photochemical crosslinking under hypoxic conditions may improve cell survival

- Confirmed cell viability in photochemically crosslinked gels
  - Cells are uniformly distributed throughout the crosslinked gels and the cells begin producing pericellular matrix by 2 weeks in vitro in the gels
  - High cell survival and matrix production was noted in the poly(ethylene) glycol thiol-ene gels
  - Cell tracking was verified in vivo with DiI labeled cells encapsulated in gels placed in nude mice for up to 8 weeks
  - Formation of new cartilage matrix was demonstrated in vivo in mice using photochemically crosslinked collagen gels and swine articular chondrocytes

- A degradable form of photochemically crosslinked PEG norbornene gel was formulated and growth factors tethered to the polymer.
  - Pericellular cartilage matrix was demonstrated around the encapsulated swine chondrocytes
  - Tethered TGF beta persisted longer than soluble growth factor

- In vitro preparation and testing of a cell-mediated degradable PEG hydrogel that promotes articular cartilage extracellular matrix production
  - A degradable form of photochemically crosslinked PEG norbornene gel was formulated and growth factors tethered to the polymer
  - Pericellular cartilage matrix was demonstrated around the encapsulated swine chondrocytes
  - The addition of MSCs aided in the degradation of the hydrogel

- Chondrocytes were encapsulated in photochemically crosslinked GelMA (gelatin methacrylamide) implanted in mice for matrix production in vivo
  - Cell viability of both chondrocytes and MSCs were >85% in the photopolymerized GelMA
  - The cells were capable of producing cartilage extracellular matrix when the gels were implanted into mice
  - The cells produced GAGs and collagen type II typical of hyaline cartilage in this gel

- Isolation of bone marrow-derived mesenchymal stem cells (BMSC) from swine and encapsulation of BMSCs using photochemically crosslinked hydrogels
  - Bone marrow-derived mesenchymal stem cells from swine were isolated and differentiated into osteogenic, adipogenic, and chondrogenic lineages with commercial differentiation media containing growth factors inducing differentiationCells populated the scaffold as shown with live-dead assays
  - Isolation of MSCs and stimulation towards osteogenesis in vitro on an octacalcium phosphate scaffold
    - Cells populated the scaffold as shown with live-dead assays
    - Calcium deposits demonstrated with von Kossa stains
  - Bone marrow-derived mesenchymal stem cells from swine were encapsulated in alginate, stimulated with chondrogenic growth factors, and placed in vivo in mice for new matrix formation

- MSCs were grown under dynamic culture to form cell aggregates in different conditions
  - Small aggregates of cells were formed under dynamic conditions and placed in cartilage rings with collagen gel
  - New tissue formed, but did not have the characteristics of cartilage matrix.

- Developed new technique to generate new cartilage matrix in vitro called dynamic Self-Regenerating Cartilage (dSRC)
  - dSRC capped with photochemically crosslinked collagen gels implanted in vivo in mice showed new cartilage matrix
  - dSRC were grown in vitro for 7, 14, or 21 days in vitro and were placed into rings of native cartilage and implanted into mice
  - dSRC were combined with fibrin, collagen crosslinked (collagen+hv), collagen non crosslinked (collagen-hv) and implanted in vivo in mice
  - Both studies showed reliable formation of contiguous cartilage inside the native cartilage ring
  - The new cartilage was predominantly collagen type II with small amounts of collagen type I on the periphery.

- Performed a pilot study where dSRC were encapsulated in photochemcially crosslinked GelMA (gelatin methacrylamide) and PEG thiol-ene gels and implanted in mice for matrix production in vivo
  - The dSRC formed new cartilage matrix, but gaps were present between individual aggregates

- dSRC were encapsulated in photochemcially crosslinked collagen and combined with Vitoss bone substrate and placed in vivo in mice
  - The dSRC formed cartilage matrix on the surface of the Vitoss
  - The new cartilage matrix appeared to integrate with the Vitoss

- In a pilot study, dSRC were encapsulated in photochemically crosslinked gels and implanted in swine to evaluate the survival of the cells in vivo in swine knee cartilage defects
  - The size of the defects was 2 mm in diameter

- Cartilage formed and filled the defect in specimens treated with chondrons and gel; not in the empty defects or those treated with gel alone
- Cartilage formed by the dSRC was high in type II collagen, whereas the control defects had high amounts of type I collagen

- dSRC were encapsulated in photochemically crosslinked gels and implanted in swine to evaluate the survival of the cells in vivo in swine knee cartilage defects for 3 and 6 months
  - Size of the defects was 5 mm in diameter
  - Cartilage formed and filled the defect in specimens treated with dSRC, but the results were variable
  - Defects filled with gel alone or left empty did not fill with cartilage

(c) Opportunities for training and professional development

Balaji V. Sridhar, B.S. received his Ph.D. from the University of Colorado, Boulder, CO, on December 19, 2015 for his thesis entitled "USE OF BIOFUNCTIONAL HYDROGEL MATRICES FOR CHONDROCYTE TRANSPLANTATION APPLICATIONS."

Xing Zhao, M.D. received his Ph. D. from the University of Utrecht, Netherlands on June 15, 2015 for his thesis entitled "BIOMATERIAL AND CELL BASED CARTILAGE REPAIR STRATEGIES."

Mark A. Randolph, M.A.S., was promoted to the rank of Assistant Professor of Surgery at Harvard Medical School in November 2016 in large part due to this funded project by the DoD, which added significantly to his eligibility for promotion.

(d) Dissemination of results to communities of interest

Five manuscripts have been published thus far in peer-reviewed journals as reported in section 6a and one is in draft form in section 6b (Appendices 1-6). Additionally, 10 abstracts have been presented at professional meetings on biomaterials and orthopedics.

(e) Plans for next reporting period

Nothing to report. This is the final project report.

4. IMPACT

(a) Impact on the development of the principal discipline(s) of the project

The challenges of joint surface cartilage repair cannot be underestimated. Cartilage is nonvascular and therefore does not undergo a normal inflammatory and healing response when injured. Bone marrow stimulation strategies such as microfracture through the subchondral bone does not promote normal, native cartilage repair. Rather, the tissue that forms following microfracture lacks the microarchitecture of native cartilage and is high in type I collagen that is more similar to scar tissue than articular cartilage, which has high amounts of type II collagen. Similar results have been reported when autologous chondrocyte implantation has been employed. Osteochondral transfer system replaces injured cartilage

with plugs of native cartilage harvested from uninjured areas of the joint. However, this can cause unwarranted morbidity in otherwise healthy areas of the joint. The goal of this project was to develop strategies to generate new cartilage matrix that possessed the microarchitecture, biochemical qualities, and biomechanical properties of native cartilage that could incorporate into articular cartilage defects and create a seamless repair by integrating with the surrounding native matrix.

Most proposed new approaches for generating articular cartilage involve placing cells in or on spongeous or fibrous matrices like collagen and encourage the cells to generate new matrix. The design is flawed in that the cells are expected to make new matrix that expands into the space between fibers and fill the defects. The use of hydrogels, as studied here, would fill the void space of the defects and new matrix would form as the gel scaffold degrades. Thus, our approach was to encapsulate chondrocyte or chondroprogenitor cells in hydrogels that could mimic the native microenvironment in which the cells normally exist and permit them to generate new matrix macromolecules. This project demonstrated that chondrocytes can be stabilized in hydrogels employing photochemical crosslinking. The gels permit temporal and spatial three-dimensional control of the cells, thus allowing them to fill in the intercellular spaces with new matrix generated by the cells. This is a novel approach to generating new cartilage for joint surface repair in the field of orthopedics.

The results demonstrated that these gels are successful in supporting chondrocyte viability and promoting new matrix formation. The in vitro studies and in vivo mice studies were successful in promoting cartilage formation. The more significant challenge is repairing defects in large animals with gels that have inferior mechanical properties at the time of initial crosslinking. Our studies demonstrated that the mechanical properties can be altered and improved by changing the crosslinking parameters, but these gels still cannot approximate the stiffness of native cartilage and, at the same time allow durable cartilage matrix to form. Nonetheless, the results from this project make significant contributions to the field of articular joint surface repair and regeneration. Further study is warranted to find the appropriate materials and crosslinking parameters to promote robust new cartilage matrix formation with the desirable biochemical and biomechanical properties to restore the joint surface.

(b) Impact on other disciplines

Nothing new to report

(c) Impact on technology transfer

Nothing new to report

(d) Impact on society beyond science and technology

Nothing new to report

5. CHANGES/PROBLEMS

(a) Changes in approach and reasons for change

Nothing new to report. The project followed the original SOW and the algorithm for testing cells placed into photochemical hydrogels (Figure 1). These have been reported in the annual reports and summarized above.

(b) Actual or anticipated problems or delays and action plans to resolve them

Nothing new to report. An extension was granted in 2014 due to the inability to obtain specially bred swine for this project. The swine were obtained in 2015-2016 and the project proceeded with implantation of cells in photochemically crosslinked hydrogels as proposed.

(c) Changes that had a significant impact on expenditures

Nothing new to report

(d) Significant changes in use or care of human subjects, vertebrate animals, biohazards and/or select agents

Nothing new to report

6. PRODUCTS

(a) Peer-reviewed publications

Appendix 1. Omobono MA, Zhao X, Furlong MA, Kwon CH, Gill TJ, Randolph MA, Redmond RW. Enhancing the stiffness of collagen hydrogels for delivery of encapsulated chondrocytes to articular lesions for cartilage regeneration. J Biomed Mater Res A. 2015 Apr;103(4):1332-8. doi: 10.1002/jbm.a.35266. PubMed PMID: 25044419.

Appendix 2. Sridhar BV, Doyle NR, Randolph MA, Anseth KS. Covalently tethered TGF-β1 with encapsulated chondrocytes in a PEG hydrogel system enhances extracellular matrix production. J Biomed Mater Res A. 2014 Dec;102(12):4464-72. doi:10.1002/jbm.a.35115. PubMed PMID: 24616326; PubMed Central PMCID: PMC4145048.

Appendix 3. Sridhar BV, Brock JL, Silver JS, Leight JL, Randolph MA, Anseth KS. Development of a cellularly degradable PEG hydrogel to promote articular cartilage extracellular matrix deposition. Adv Healthc Mater. 2015 Apr 2;4(5):702-13. doi: 10.1002/adhm.201400695. PubMed PMID: 25607633; PubMed Central PMCID: PMC4487633.

Appendix 4. Sridhar BV, Dailing EA, Brock JL, Stansbury JW, Randolph MA, Anseth KS. A Biosynthetic Scaffold that Facilitates Chondrocyte-Mediated Degradation and Promotes Articular Cartilage Extracellular Matrix Deposition. Regen Eng Transl Med. 2015 Dec;1(1-4):11-21. PubMed PMID: 26900597; PubMed Central PMCID:PMC4758520.

Appendix 5. Meppelink AM, Zhao X, Griffin DJ, Erali R, Gill TJ, Bonassar LJ, Redmond RW, Randolph MA. Hyaline Articular Matrix Formed by Dynamic Self-Regenerating Cartilage and Hydrogels. Tissue Eng Part A. 2016 Jul;22(13-14):962-70. doi:10.1089/ten.TEA.2015.0577. PubMed PMID: 27324118.

(b) Draft manuscript

Appendix 6. Griffin DJ, Meppelink AM, Randolph MA, Cohen I, Bonassar LJ. The characterization of local mechanics in an articular cartilage defect repair model

(c) Conference presentations

1. *Orthopedic Research Society,* San Antonio, TX, January 2013
   Photochemical Crosslinking Stabilizes Hydrogels for Cartilage Regeneration
   Omobono MA, Zhao X, Furlong MF, Kwong CH, Redmond RW, Randolph MA

2. *58th Annual Meeting of the Plastic Surgery Research Council,* Los Angeles, CA, June 2013
   Photochemical Crosslinking Stabilizes Protein Hydrogels for Cartilage Regeneration
   Zhao X; Omobono MA; Jang S; Randolph MA;Redmond RW; Gill TJ; Yaremchuk MJ

3. *11th World Congress of the International Cartilage Repair Society,* Izmir, Turkey, September 2013
   Photochemical Crosslinking Stabilizes Hydrogels for Cartilage Regeneration
   Omobono MA, Zhao X, Furlong MF, Kwong CH, Redmond RW, Randolph MA

4. *Orthopaedic Research Society*, Las Vegas, NV, March 2015
   Detection and Characterization of Local Interfacial Mechanics in a Cartilage Defect Repair Model
   Griffin D, Meppelink AM, Randolph MA, Cohen I, Bonassar LJ

5. *12th World Congress of the International Cartilage Repair Society*, Chicago, IL, May 2015
   Detection and Characterization of Local Interfacial Mechanics in a Cartilage Defect Repair Model
   Griffin D, Meppelink AM, Randolph MA, Cohen I, Bonassar LJ

6. *Orthopaedic Research Society*, Orlando, FL, March 2016
   Articular Cartilage Matrix Formation using Dynamic Self-Regenerating Cartilage and Photochemical Hydrogels
   Meppelink AM, Zhao X, Griffin D, Erali R, Bonassar LJ, Redmond RW, Randolph MA

7. *61st Annual Meeting of the Plastic Surgery Research Council*, New York, NY, May 2016
   Articular Cartilage Matrix Formation using Dynamic Self-Regenerating Cartilage and Photochemical Hydrogels
   Meppelink AM, Zhao X, Griffin D, Erali R, Bonassar LJ, Redmond RW, Randolph MA

8. *Military Health System Research Symposium*, Orlando, FL, August 2016
   Articular Cartilage Matrix Formation using Dynamic Self-Regenerating Cartilage and Photochemical Hydrogels
   Meppelink AM, Zhao X, Griffin D, Erali R, Bonassar LJ, Redmond RW, Randolph MA

9. *13th World Congress of the International Cartilage Repair Society*, Sorrento Italy, September 2016
   Articular Cartilage Matrix Formation using Dynamic Self-Regenerating Cartilage and Photochemical Hydrogels
   Meppelink AM, Zhao X, Griffin D, Erali R, Bonassar LJ, Redmond RW, Randolph MA

10. Biomedical Engineering Society 2016 Annual Meeting, Minneapolis, MN, October 2016
    Microscale Mechanics of the Interface Of Native And Repaired Articular Cartilage
    Irwin R, Griffin D, Meppelink AM, Cohen I, Randolph MA, Bonassar LJ

8) **SUPPORTING DATA**

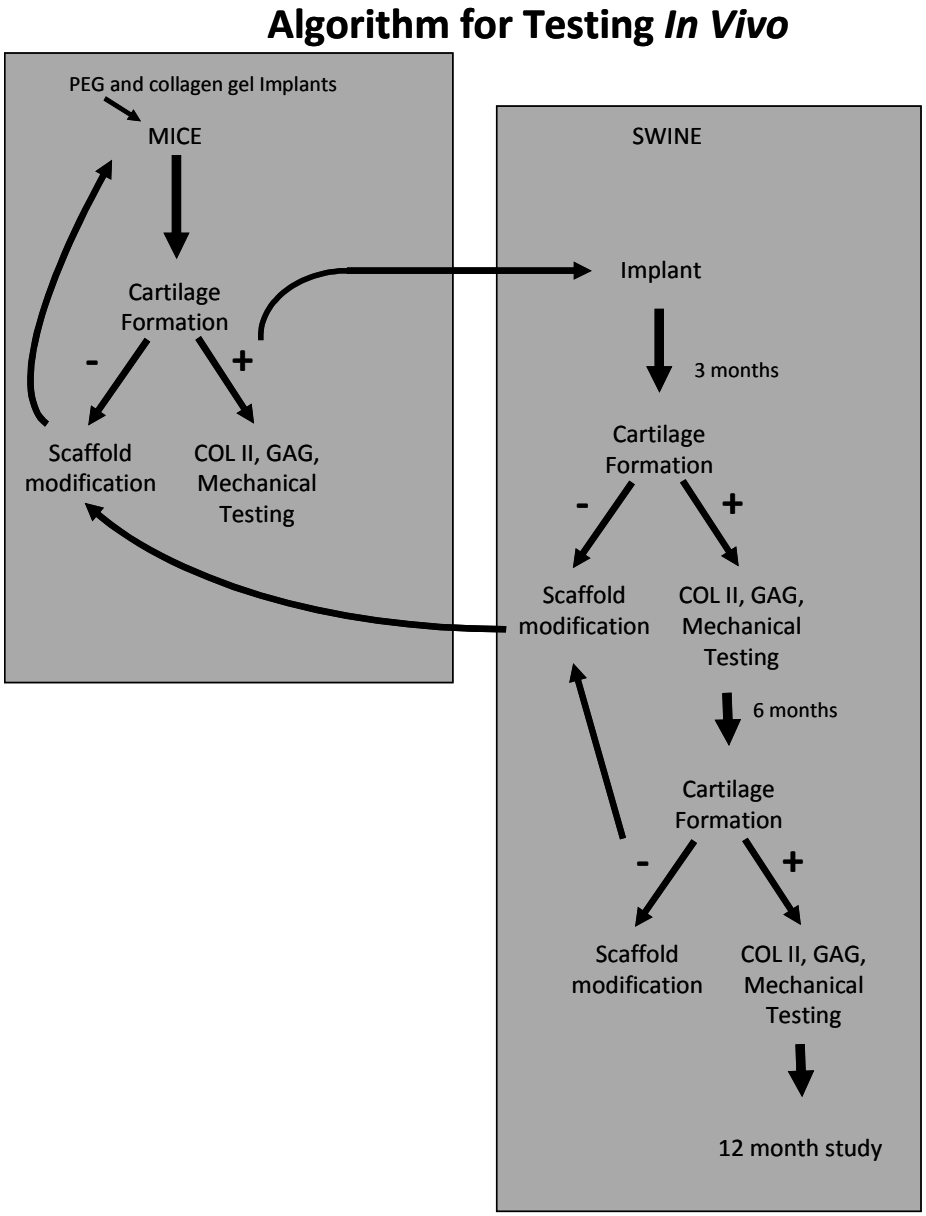

Figure 1. This is the testing paradigm proposed in the original grant application. The gels are made and tested in vitro and in vivo in mice (left box) prior to embarking on the large animal swine model (right box). If gels fail to perform in the mice they are not tested in swine. Additionally, if the gels should perform poorly in the early test phase in swine, the gels are reformulated and tested again in mice before re-embarking on the swine studies. Many changes outlined in this report describe changes to the gels and generating dynamic self-regenerating cartilage so that large animals are not used unnecessarily for gels that have not been optimized.

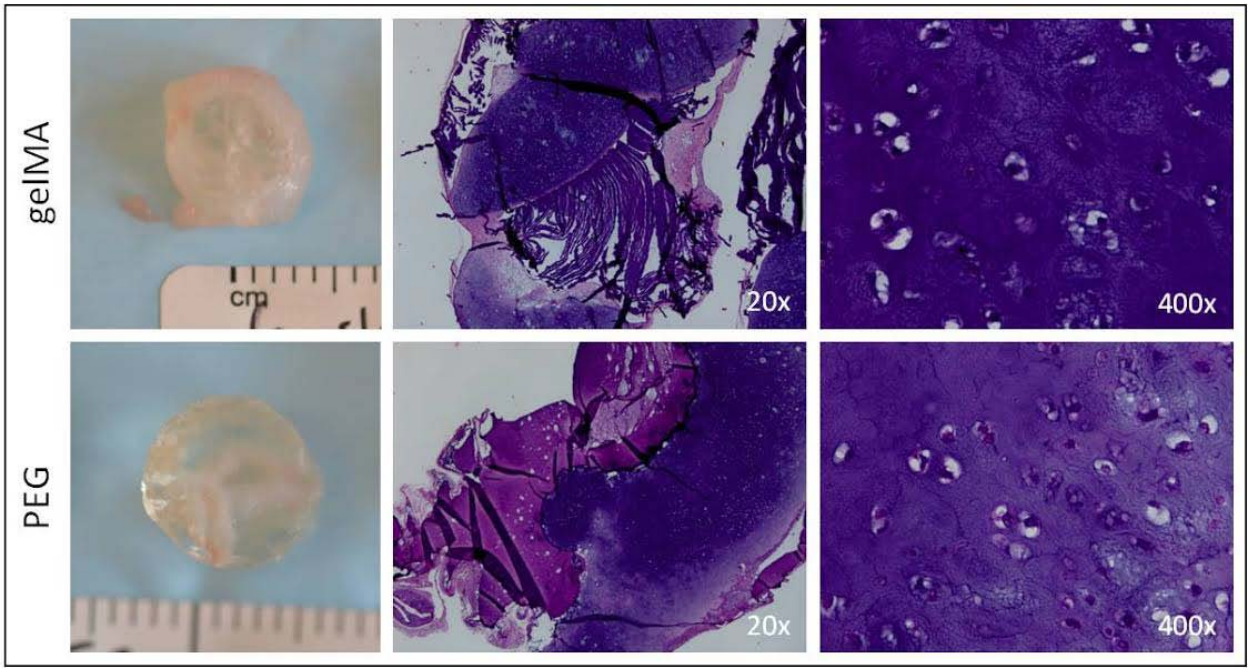

Figure 2. Encapsulation of dSRC in photochemically crosslinked GelMA (top row) and PEG (middle row). The dSRC were able to form nodules of new cartilage matrix. However, there are gaps between the cartilage nodules and residual polymer shown in pink stain.

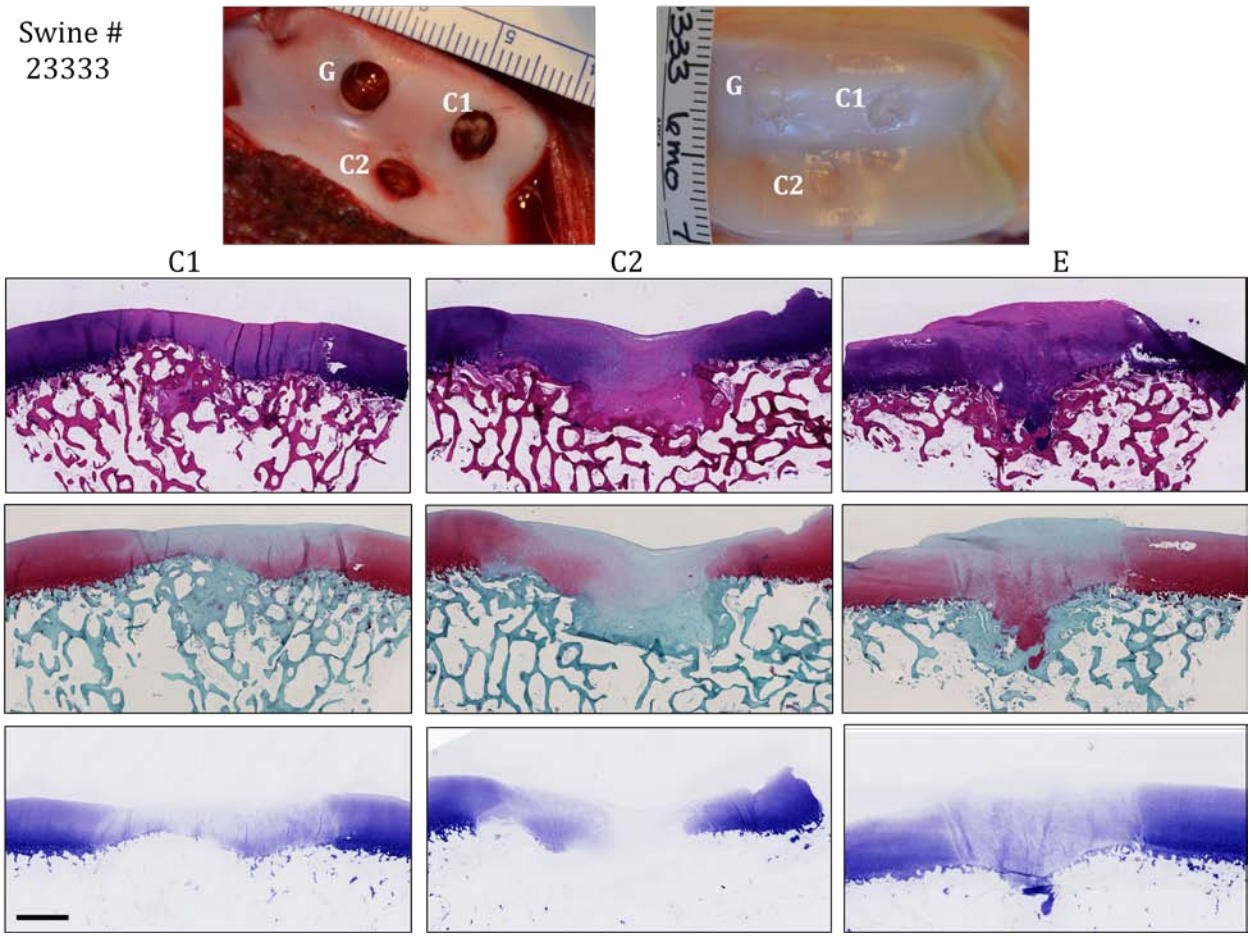

Figure 3. Surgery and harvest images from swine 23333 followed for 3 months. The surgical image (top left) shows the defects filled with cells (C1 and C2) and photochemically crosslinked collagen gel and the control defects filled with gel alone (G). The gross image of the joint at harvest is shown on the top right. The histology from each defect is shown the columns labeled by their respective defect site and stained with hematoxylin & eosin (top row), safranin O (middle row) and toluidine blue (bottom row). The defects treated with cells show early repair of the defect filled with new cartilage. (scale bar = 1mm)

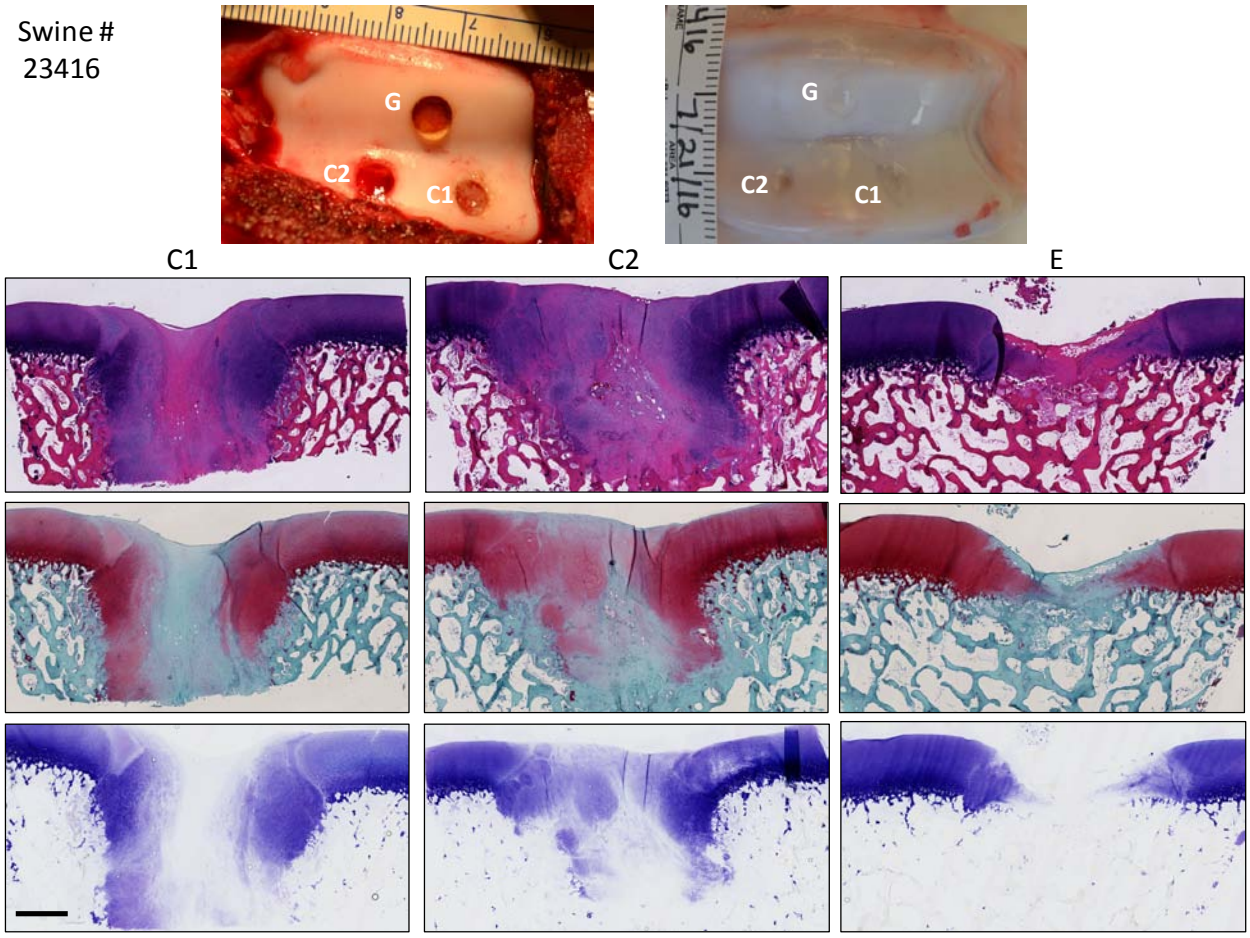

Figure 4. Surgery and harvest images from swine 23416 followed for 3 months. The surgical image (top left) shows the defects filled with cells (C1 and C2) and photochemically crosslinked collagen gel and the control defects filled with gel alone (G). The gross image of the joint at harvest is shown on the top right. The histology from each defect is shown the columns labeled by their respective defect site and stained with hematoxylin & eosin (top row), safranin O (middle row) and toluidine blue (bottom row). The repair tissue in defects filled with cells in this swine were of poor quality showing the variability of the repair technique. (scale bar = 1mm)

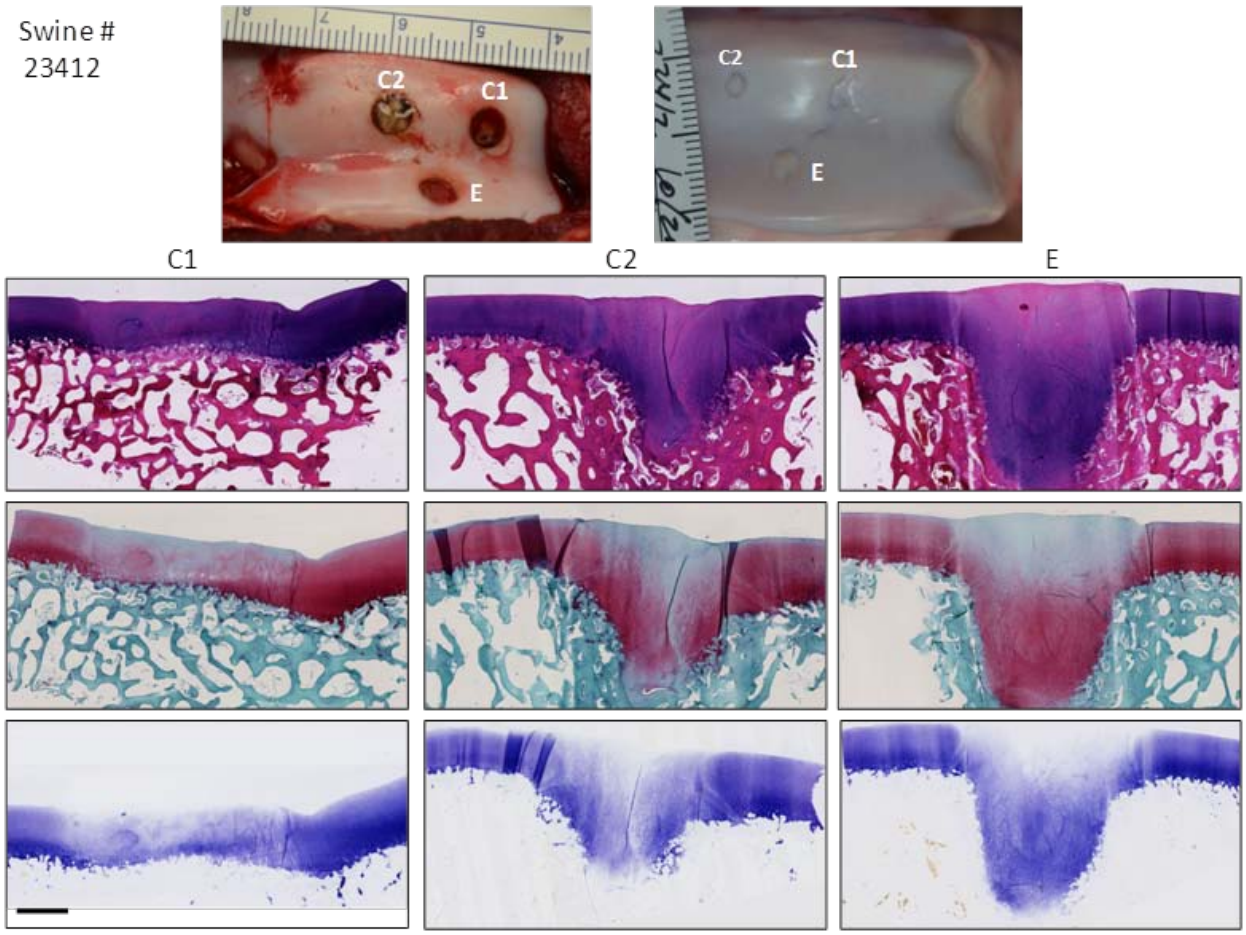

Figure 5. Surgery and harvest images from swine 23412 followed for 6 months. The surgical image (top left) shows the defects filled with cells (C1 and C2) and photochemically crosslinked collagen gel and the control empty defect (E). The gross image of the joint at harvest is shown on the top right. The histology from each defect is shown the columns labeled by their respective defect site and stained with hematoxylin & eosin (top row), safranin O (middle row) and toluidine blue (bottom row). The defects treated with cells show early repair of the defect filled with new cartilage. (scale bar = 1mm)

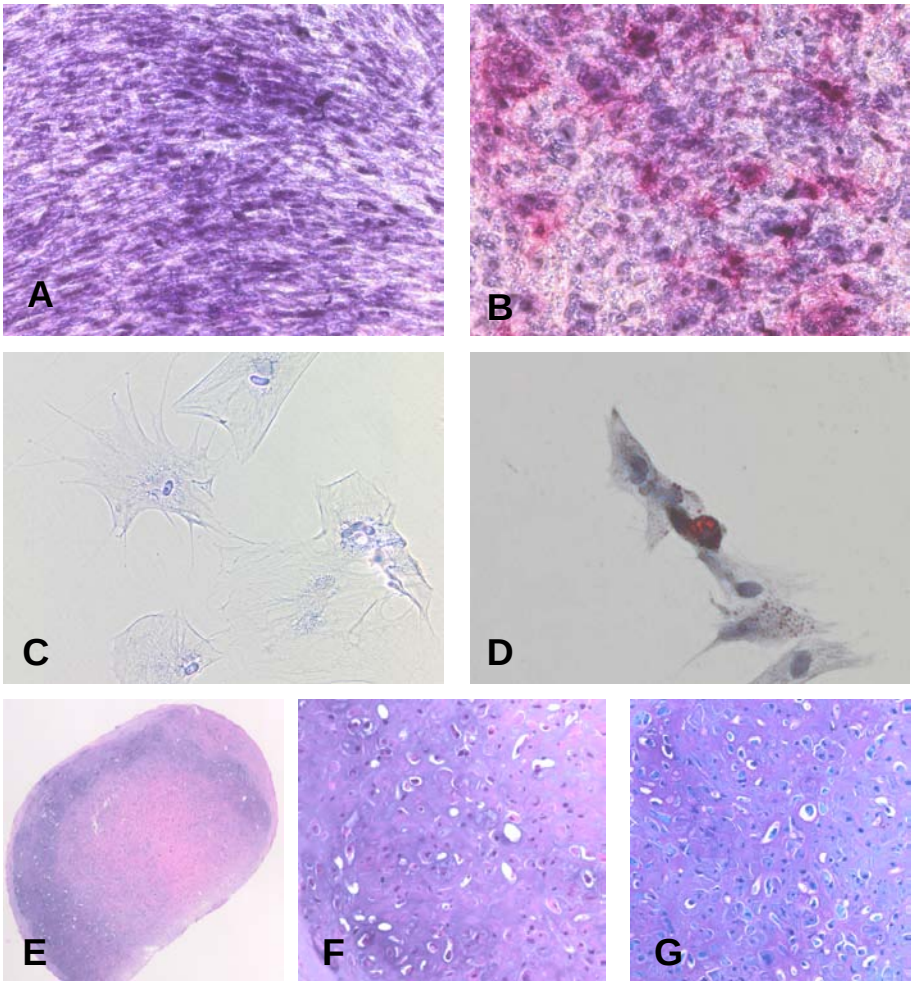

Figure 6. Differentiation of swine BM-MSCs in osteogenic (a&b), adipogenic (c&d), and chondrogenic lineages (e,f,&g). The cells grown in control media without osteogenic factors show no alkaline phosphatase activity (a; 100x), whereas cells treated with osteogenic factors show increased alkaline phosphatase as indicated by the red staining (b; 100x). Cells grown in control media do not have any evidence of intracellular lipid (c; 400x), but cells in the presence of adipogenic media show small red droplets of oil as evidenced with Oil Red O staining (d; 400x). Cell pellets treated with chondrogenic media show the coalescence of cells into a pellet and the presence of cartilage matrix formation (blue staining with H&E; c; 40x). High magnification of the blue-stained areas show chondrocytes encased in lacunae typical of cartilage (f; 400x). Sections from the same tissue block stained with toluidine blue shows GAG rich matrix indicative of cartilage formation (g; 400x).

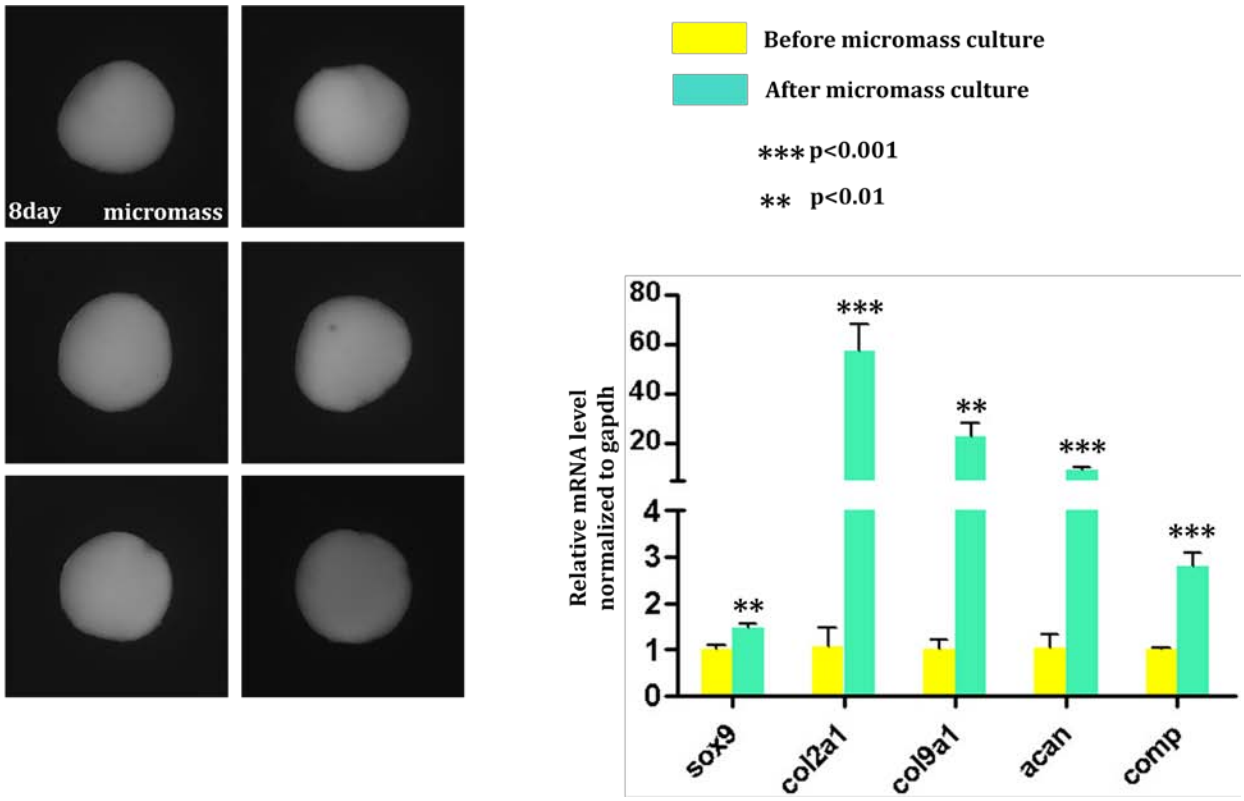

Figure 7. Image of micromass pellets generated from swine BMSCs (left) stimulated for chondrogenesis using differentiation reagents acquired from Lonza. These were compared to undifferentiated isolated BMSCs. Cells stimulated in micromass show upregulation of chondropgeneic genes in the micromass specimens compared to the individual undifferentiated cells.

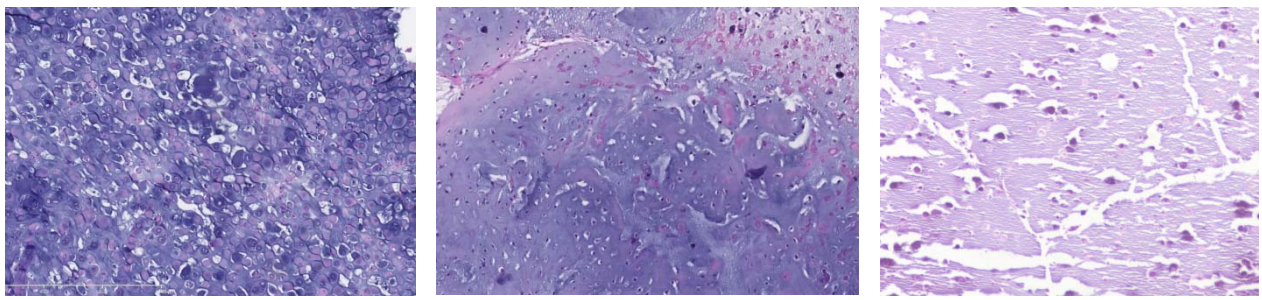

chondrocytes **differentiated MSCs** **undifferentiated MSCs**

Figure 8 . Swine chondrocytes (left) and MSCs (middle and right) were placed into alginate gels; cultured in vorto for 2 weeks, then placed in vivo into mice for 5 weeks. During the in vitro culture the gels containing MSCs were grown with or without chondrogenic factors provided by commercial Invitrogen mixture. MSCs exposed to the chondrogenic factors showed catrilage matrix formation (middle). Those gels with MSCs not exposed to the growth factors did not demonstrated matrix formation (right).

Society For Biomaterials

Enhancing the stiffness of collagen hydrogels for delivery of encapsulated chondrocytes to articular lesions for cartilage regeneration

Mark A. Omobono,[1,2] Xing Zhao,[3,4] Michael A. Furlong,[2] Chi-Heon Kwon,[2] Thomas J. Gill,[3] Mark A. Randolph,[1,3] Robert W. Redmond[2]

[1]Department of Surgery, Plastic Surgery Research Laboratory, Harvard Medical School, Massachusetts General Hospital, Boston, Massachusetts 02114
[2]Wellman Center for Photomedicine, Harvard Medical School, Massachusetts General Hospital, Boston, Massachusetts 02114
[3]Department of Orthopedics, Harvard Medical School, Massachusetts General Hospital, Boston, Massachusetts 02114
[4]Department of Orthopaedics, University Medical Center Utrecht, Utrecht, The Netherlands

Received 26 February 2014; revised 2 June 2014; accepted 24 June 2014
Published online 22 July 2014 in Wiley Online Library (wileyonlinelibrary.com). DOI: 10.1002/jbm.a.35266

Abstract: This study investigated a dual crosslinking paradigm, consisting of (a) photocrosslinking with Rose Bengal (RB) and green light followed by (b) chemical crosslinking with 1-ethyl-3-(3-dimethylaminopropyl)carbodiimide (EDC), and N-hydroxysuccinimide (NHS) to enhance collagen gel stiffness. In group 1, 50 μL collagen constructs of 2% (w/v) type I collagen containing 10 μ*M* RB were allowed to gel spontaneously at 37°C. In group 2, the spontaneous gels were exposed to green light (532 nm). In group 3, the photochemically crosslinked gels were subsequently treated with a 1-h exposure to 33 m*M* EDC/6 m*M* NHS. Samples ($n = 18$) were subjected to 0.08% (w/v) collagenase digestion, and the storage modulus of samples was measured by rheometry. Viability of encapsulated chondrocytes was measured by live/dead assay. Chondrocytes were ≥95% viable in all constructs at 10 days in vitro. Resistance to collagenase digestion increased as; spontaneous gels (2 h) < photochemical gels (3–4 h) < dual crosslinked gels (>24 h). The storage modulus of dual-crosslinked constructs was increased 5-fold over both photocrosslinked and spontaneous gels. As the dual crosslinking paradigm did not reduce encapsulated chondrocyte viability, these crosslinked collagen hydrogels could be a useful tool for the practical delivery of encapsulated chondrocytes to articular defects. © 2014 Wiley Periodicals, Inc. J Biomed Mater Res Part A: 103A: 1332–1338, 2015.

Key Words: collagen, cartilage tissue engineering, crosslinking, hydrogel, scaffold

How to cite this article: Omobono MA, Zhao X, Furlong MA, Kwon C-H, Gill TJ, Randolph MA, Redmond RW. 2015. Enhancing the stiffness of collagen hydrogels for delivery of encapsulated chondrocytes to articular lesions for cartilage regeneration. J Biomed Mater Res Part A 2015:103A:1332–1338.

INTRODUCTION

Articular cartilage has little innate ability to heal and presents significant clinical challenge for natural regeneration. It is populated exclusively by chondrocytes,[1] but is avascular and lacks the capacity for complete, spontaneous regeneration in response to any focal injury to the contiguous extra-cellular matrix (ECM). Any procedure aimed at restoring the articular surface is required to (a) create natural hyaline cartilage to fill the defect and (b) allow integration of the neocartilage with existing healthy cartilage.

Among many potential natural and synthetic matrices in tissue engineering, collagen has proven to be useful in hydrogel,[2,3] membrane,[4,5] and porous scaffold[6,7] forms. Collagen is naturally occurring in human tissue, including articular cartilage.[8] Collagen molecules self-assemble into a hydrogel matrix at physiological pH and temperature via hydrogen bonding but these spontaneous hydrogels are weak in mechanical integrity and are rapidly digested by enzymatic attack. In an attempt to overcome these drawbacks, we exposed collagen gels containing photoreactive dyes to visible light to induce crosslinking of adjacent collagen molecules. These photocrosslinked gels were protected from contraction due to cellular interaction with the matrix[9] and chondrocytes encapsulated in photocrosslinked collagen hydrogels formed hyaline-like cartilage.[10] However, these gels are relatively soft and difficult to handle, and the aim of this work was to modify the crosslinking process to provide a stiffer collagen hydrogel that would be more user-friendly in ultimate clinical use.

Any increase in gel stiffness must be achieved without affecting the viability of encapsulated chondrocytes or their

Correspondence to: R. W. Redmond; e-mail: redmond@helix.mgh.harvard.edu
Contract grant sponsor: AO/ASIF Foundation and the U.S. Department of Defense; contract grant number: W81XWH-10-1-0791

TABLE I. Group Designations for EDC/NHS Concentration and Time of Exposure Study

Dilution [EDC]/ [NHS] (m*M*)	15-Min Exposure	30-Min Exposure	45-Min Exposure	60-Min Exposure
33/6	1–15	1–30	1–45	1–60
16.5/3	2–15	2–30	2–45	2–60
6.6/1.2	5–15	5–30	5–45	5–60
3.3/0.6	10–15	10–30	10–45	10–60

This work was presented at the Annual Meeting of the Orthopedic Research Society, San Antonio, TX, in February 2013.

ability to remodel the existing type I collagen scaffold and generate neocartilage. The feasibility of implanting a collagen hydrogel in an articular surface defect hinges on the mechanical integrity of the hydrogel during implantation and early repair. During this early period chondrocytes must have a scaffold that supports viability and permits new cartilage formation. Photocrosslinked gels may lack the stiffness necessary to withstand extended mechanical loading and an enhancement in construct stiffness could be beneficial.

Chemical crosslinking using 1-ethyl-3-(3-dimethylaminopropyl)carbodiimide (EDC) and N-hydroxysuccinimide (NHS) is nontoxic and useful for crosslinking collagen in tissues.[11–15] EDC, in the presence of NHS, activates carboxyl groups of aspartic and glutamic acid residues of collagen to react with nucleophilles, such as primary amines (lysine and hydroxylysine) and hydroxyl groups, to create zero-length crosslinks.[16] Treating collagen hydrogels with EDC/NHS is a potential method for increasing crosslinking, and the combination of photo- and chemical crosslinking could yield a hydrogel with improved stiffness.[17]

In this study, we have used dual-crosslinking (photochemical + chemical) of type I collagen hydrogels to test whether the stiffness of collagen gels can be substantially increased to make them useful for articular cartilage defect repair. Effects on mechanical properties of the gel, encapsulated chondrocyte viability in vitro, and resistance to collagenase digestion were evaluated to determine the potential of this new crosslinking paradigm for articular cartilage regeneration.

MATERIALS AND METHODS

Materials

Rat tail type I collagen (11.4 mg/mL) was obtained from BD Biosciences, Bedford, MA. Ham F12, 10% fetal bovine serum. 1% antibiotic/antimycotic liquid and 1% MEM nonessential amino acids were all from Gibco (Carlsbad, CA). Sodium hydroxide (NaOH), Rose Bengal (RB), 1-ethyl-3-(3-dimethylaminopropyl)carbodiimide, N-hydroxysuccinimide and N-(2-hydroxyethyl)piperazine-*N*′-(2-ethanesulfonic acid) (HEPES) were purchased from Sigma-Aldrich (Natick, MA). Type II collagenase at 245 U/mg was purchased from Worthington Biochemical (Lakewood, NJ).

Preparation of collagen hydrogels

Rat tail type I collagen was mixed in an Eppendorf tube with chondrocyte media [Ham F12, 10% fetal bovine serum (Gibco), 1% antibiotic/antimycotic liquid, 1% MEM nonessential amino acids], 50 m*M* stock NaOH, and 90 μ*M* Rose Bengal diluted in chondrocyte media. The collagen solutions were adjusted to pH 7.2 ± 0.2 using 50 m*M* NaOH. The final concentrations were 10 μ*M* Rose Bengal and 2.54 mg collagen/mL.

Typically, 50 μL of the hydrogel mixture was aliquoted into cylindrical molds of 4.7 mm diameter and spontaneous gelation of the collagen solution was induced by incubation at 37°C for 1 h. Photochemically crosslinked gels were prepared by exposure to green light from a continuous wave KTP laser (LRS-0532-PFH-000500-05, Laserglow Technologies, Canada, 800 mW, 532 nm) at 20 J/cm^2 fluence from three different angles to assure equal illumination throughout the specimen. A group of photochemically crosslinked gels also underwent subsequent chemical crosslinking following ejection from the mold by immersion in a solution of 33 m*M* EDC, 6 m*M* NHS, in 50 m*M* HEPES buffer for 1 h. Another group of gels was prepared solely by exposure to EDC/NHS for 1 h without prior photochemical crosslinking.

To compare concentration and time of exposure to EDC/NHS solution, all collagen gels were prepared in a similar fashion through green laser exposure. Samples were then subjected to increasing dilutions and increasing times of exposure ($n = 3$ per group) according to Table I.

Collagenase digestion assay

Collagen hydrogel constructs were submerged in 10 mL of 0.08% w/v type II collagenase (in PBS) to determine the degree of protection from enzymatic degradation provided by crosslinking treatments in 15-mL conical tubes (BD Biosciences). Tubes were placed on a lab rocker at room temperature and checked every 15 min to determine the length of time for complete dissolution of the construct. Gels that were still intact after 24 h were recorded as "undigested". Three individual trials were conducted with $n = 6$ per trial for a total of $n = 18$ samples per group.

Mechanical testing

The viscoelastic storage modulus, G', of each collagen construct was measured using a rheometer (TA Instruments AR-G2, 8 mm Rough Steel Smart-Swap plate, part #511080.906). Samples were subjected to a frequency sweep from 1 to 10 radians/s with constant 2% strain rate and an 800-μm gap under continuous, room-temperature oscillation. Shear elastic moduli were calculated from the stress measured, using the equation;

$$G' = (\sigma_0/\varepsilon_0)\ \cos(\delta)$$

where σ_0 is the stress applied, ε_0 is the strain measured, and δ is the measured lag between phases. Three trials were conducted at $n = 6$ per group per trial for a total of $n = 18$ samples per group.

Chondrocyte viability

Knee joints were obtained from euthanized, 4-month-old Yorkshire swine and dissected under sterile conditions to expose the femoral condyles and the posterior face of the patella. The cartilage was dissected from the knee and

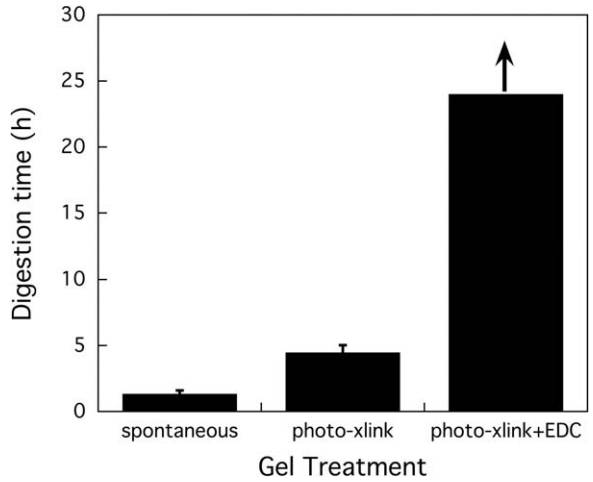

FIGURE 1. Times of degradation of 2% w/v collagen gels of various crosslinking treatments when exposed to 0.08% w/v collagenase enzyme at room temperature (n=6 per group). Photocrosslinked gels lasted significantly longer (3.46 ± 0.13 h) than spontaneous gels (1.32 ± 0.06 h) ($p < 0.0001$). Gels exposed to dual crosslinking were completely undigested after 24 hours.

digested in 0.1% w/v type II collagenase solution in Ham F-12 medium (Life Sciences, Grand Island, NY) containing 1% Anti-Anti (antibiotic, antimycotic, Life Sciences) overnight at 37°C. Digested cartilage solutions were passed through a 100-μm cell strainer and centrifuged at 250*g* for 10 min. The cell pellet was collected and washed twice with fresh chondrocyte media. Cells were counted on a hemacytometer and tested for initial viability using the trypan blue exclusion assay. Chondrocytes were plated in monolayer at a density of 2×10^6 cells/150 cm^2 and cultured at 37°C and 5% CO_2 until 80% confluent. Cultured plates were then exposed to 0.05% trypsin-EDTA (Invitrogen) and cells were collected in chondrocyte media, and washed twice with fresh media.

Cells were then suspended in collagen hydrogel mixture at 1.0×10^7 cells/mL hydrogel ($n = 4$). Gels were molded, incubated, and crosslinked using the dual-crosslinking approach. Photo-crosslinking was carried out as described above and the gels were then incubated in EDC/NHS (33/6 m*M*) in HEPES buffer for 1 h. After crosslinking treatment, gels were submerged in chondrocyte media for in vitro culture. After 10 days the gels were immersed in a solution of Live/Dead Viability Assay (Invitrogen, Grand Island, NY), containing 1.6 μ*M* calcein AM and 200 n*M* ethidium homodimer-1, for 1 h. The stained constructs were embedded in O.C.T. Compound (Tissue Tek), frozen at −20°C for 1 h, and sliced into 10-μm sections using a cryostat (Leica CM3050). These sections were then imaged using a Nikon Eclipse (TE2000U) fluorescence microscope using FITC (480ex/535em) and TRITC (535ex/610em) filters, and processed with NIH ImageJ software.

Statistics

Results of collagenase and mechanical testing data are reported as mean ± standard deviation. Significance was calculated using 1-way ANOVA analysis with Bonferroni's Multiple Comparison Test post-test with $p < 0.05$ considered significant. Percentage chondrocyte viability was calculated by counting dead (red) and live (green) cells from the fluorescent photographs. Samples were photographed in triplicate, capturing one central image and two boundary images per sample. Both live and dead cells were counted manually from which the viable fraction of cells was calculated. Manual counting was performed by five independent evaluators and results are presented as the mean of the five independent viability percentage for each gel ± standard deviation.

RESULTS

Resistance to collagenase digestion

Full degradation was defined as complete dissolution of the hydrogel by collagenase. The time to degradation (tdeg) of collagen hydrogels photocrosslinked with Rose Bengal and green laser exposure (3.5 ± 0.5 h) exhibited > 2-fold increase ($p < 0.0001$) in time of degradation from the spontaneous gels (1.3 ± 0.3 h). Dual-crosslinked constructs digested in collagenase solution exhibited no signs of degradation, even after 24 h (Fig. 1). Gels that were crosslinked with EDC/NHS alone for 60 min were soft but very resistant to degradation; after 24 h there were no signs of degradation. Exposure of constructs to different concentrations of EDC/NHS for different times showed varying degrees of resistance to digestion (Fig. 2). Within a treatment dilution group, t_{deg} increased with increasing time of exposure to EDC/NHS. Between treatment dilution groups, t_{deg} increased with increasing concentration of EDC/NHS.

Mechanical testing

Values for storage modulus in spontaneous control gels (25.8 ± 1.5 Pa) and storage modulus in photocrosslinked

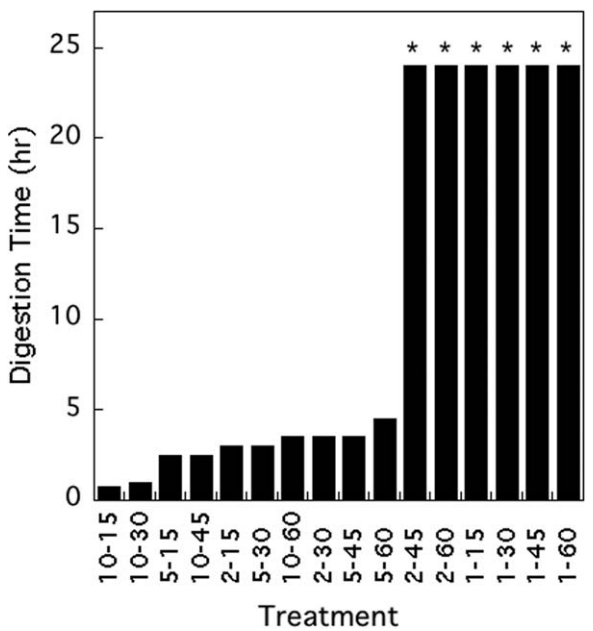

FIGURE 2. 0.08% w/v collagenase digestion of 2% w/v collagen gels treated with different dilutions and exposure times of EDC/NHS. Refer to Table I for group designations. Gels labeled with an asterisk (*) did not digest after 24 hours, when the study was capped.

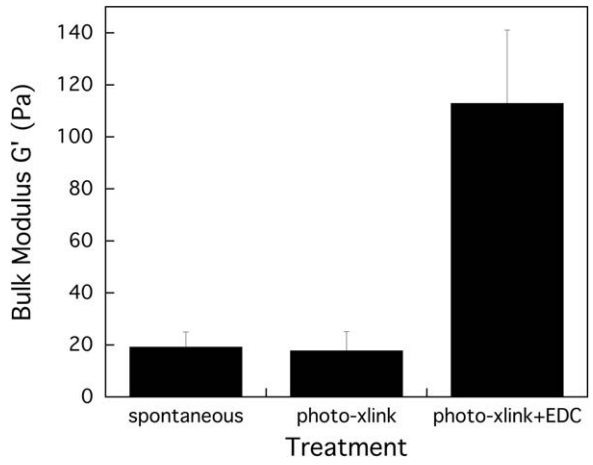

FIGURE 3. Storage modulus G′ as measured by a rheometer of 2% w/v collagen gels of various crosslinking treatments (n=6 per group). There was no significant difference between spontaneous gels (25.8 ± 1.5 Pa) and photocrosslinked gels (21.4 ± 1.8 Pa) ($p = 0.58$). There was a significant difference, up to a 5-fold increase in storage modulus when collagen gels were treated with dual crosslinking (117.6 ± 6.9 Pa) ($p < 0.0001$).

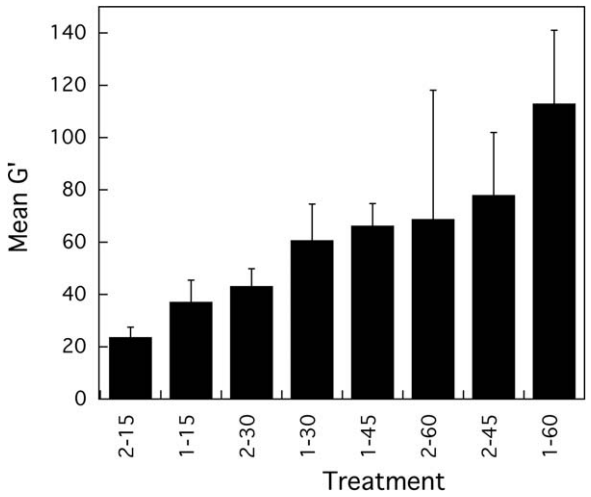

FIGURE 4. Storage modulus (G′) by rheometry of 2% w/v collagen gels treated with different dilutions and exposure times of EDC/NHS. Refer to Table I for group designations. There is no statistical significance between gels of groups exposed to lower concentrations of EDC/NHS. The first significant difference is noticed at group 2–30, with varying degrees of stiffness modulation between group 2–30 and maximum crosslinking treatment, group 1–60.

gels (21.4 ± 1.8 Pa) showed no statistically significant difference ($p = 0.07$). Storage modulus measurements for dual-crosslinked gels were 5-fold higher (117.6 ± 6.9 Pa) than both photocrosslinked and spontaneous gels ($p < 0.0001$, Fig. 3). Gels exposed to the most dilute concentrations of EDC/NHS (1 : 10, 1 : 5) did not show any significant difference in storage modulus from uncrosslinked and photocrosslinked groups but groups exposed to EDC/NHS diluted 1 : 2 for at least 15 min showed a trend of increasing storage modulus with increasing exposure time (Fig. 4).

Chondrocyte viability

Chondrocytes in six different gels treated with the dual-crosslinking approach exhibited $96.1 \pm 2.3\%$ viability in hydrogel implants after 10 days of in vitro culture (see Fig. 5 for an example). Cells residing in the peripheral regions of the constructs tended to have a lower viability than those in the central regions of the gels. Overall, the viability far exceeded our target viability of 90% for encapsulated chondrocytes to produce healthy ECM.

DISCUSSION

Articular cartilage regeneration is a challenging clinical problem. The newest tissue engineering-based therapy, autologous chondrocyte implantation (ACI), involves biopsy of healthy hyaline cartilage from a nonweight bearing area of the knee to harvest autologous chondrocytes for expansion in vitro followed by injection of cultured cells to the cartilage defect. The cells are typically suspended in saline and a periosteal flap is sutured to the cartilage surface. Not only does this repair require multiple surgeries to complete, but there is little data supporting the benefits of ACI versus microfracture[18] or OATS.[19] A common problem during this procedure is the leaking of cell-saline suspension from under the periosteal flap out of the target site due to compressive pressure despite sealing the surgical site with suture and fibrin glue.

Finding a suitable matrix to support cellular activity and ECM generation is a common problem in tissue engineering.[12,20–23] Native articular cartilage consists of different types of collagen fibrils, but is mostly type II collagen by dry weight.[8] Type I collagen is the main structural component in many native tissues in the body, therefore it is an attractive option as a nontoxic, biomimetic matrix to support natural ECM regeneration by chondrocytes. Collagen hydrogels can be formed at 37°C but these "spontaneous"

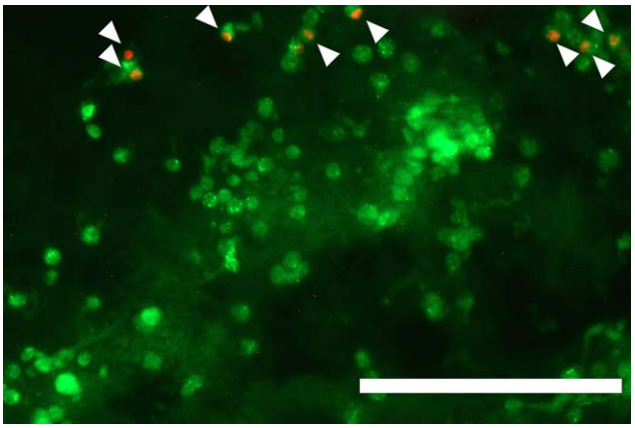

FIGURE 5. Live/Dead photographs of dual crosslinked construct after 10 days of in vitro culture. Pictures are taken at a height of $750\mu m \pm 50\mu m$ from the base of each construct in a $10\mu m$ cryotome slice. Dead cells are denoted by white arrows and scale bar is 300 μm. [Color figure can be viewed in the online issue, which is available at wileyonlinelibrary.com.]

gels are very soft and are unsuitable for implantation in focal articular cartilage defects.

Photocrosslinking of synthetic polymers typically is well-established and typically uses ultraviolet (UV) illumination of photoinitator compounds that react with synthetic monomers to cause chain reaction polymerization via radical reactions. However, for the purpose of cell encapsulation the UV illumination and the materials used would not be appropriate due to inherent cytotoxicity.[24] For this reason we have investigated visible light as the energy source for crosslinking along with nontoxic initiators. Under these milder conditions the initiating event can be electron transfer between excited initiator and monomer and/or energy transfer from photoinitator to dissolved oxygen to form singlet oxygen and its subsequent reactions (e.g., oxidation of histidine and reactions of photooxidized histidine with other amino-containing residues[25] to form a crosslink).[26]

We have previously shown that photochemical crosslinking of a collagen hydrogel provides a scaffold that supports encapsulated chondrocytes and stimulates cartilage-like ECM production.[9,10] Photochemical crosslinking certainly stabilizes the matrix and makes it more resistant to enzymatic degradation but provides little in the way of additional mechanical stiffness that would enhance practical handling of the gel and remove the need for a covering material to be affixed over the cartilage defect to prevent loss of unstable gel. Thus, we sought an improved crosslinking mechanism that enhances initial stiffness of these collagen-based hydrogels.

An obvious possibility would be to increase the fluence (photons/cm^2) incident on the gel. However, we have already shown in cell-free collagen gels that there is a plateau in the fluence dependence of crosslinking, suggesting a saturation of all sites that can be photochemically crosslinked, and further exposure does not equate to increased crosslinking. As an aside, this approach would also be complicated by side reactions of the photoinitiator that can generate reactive species that contribute to cell toxicity, as shown in previous studies. Thus, other methods are required and led to the investigation of chemical crosslinking of collagen-based matrices with a combination of EDC and NHS. This method has been shown to increase mechanical stiffness of materials,[11,12,16,20,27,28] including organized tissues, without cytotoxic effects.

We investigated this method alone and in combination with photocrosslinking as a method for increasing collagen hydrogel stiffness. Experiments using EDC/NHS crosslinking alone on collagen gels were disappointing. Constructs exposed to this treatment were only loosely organized and collapsed under their own weight after being ejected from the mold. These gels could not be subjected to storage modulus evaluation. Despite a lack of structural integrity, these gels proved highly resistant to collagenase digestion, showing that crosslinking did, in fact, occur. Since the clinical application requires implantation of snug-fitting gels with a defined geometry, crosslinking with EDC/NHS alone is not an option. However, when photocrosslinking was practiced prior to EDC/NHS treatment a stiffer gel construct was obtained that did retain its shape when extruded from the mold. Thus, a dual crosslinking paradigm has potential to provide a practical implant for focal defect repair.

Rheometry testing demonstrated that the stiffness (storage modulus) of the gels increased in dual crosslinked gels (117.6 ± 6.9) more than 5-fold from photochemically crosslinked gels (21.4 ± 1.8 Pa, Fig. 3). Previous results, showing the lack of significant difference between the storage modulus of noncrosslinked, spontaneous collagen gels (25.8 ± 1.5 Pa) and photochemically crosslinked gels, were also confirmed as a *t*-test results in $p = 0.58$ between these two groups.

We attribute the resulting increase in G' of dual-crosslinked hydrogels to the addition of new chemical crosslinks throughout the collagen matrix with a resulting increase in crosslinking density. The 5-fold increase in G' by EDC/NHS on prior photocrosslinked hydrogels, in comparison to the null effect of EDC/NHS on spontaneously formed collagen gels discussed earlier, is an interesting observation. A possible explanation is that photocrosslinking treatment provides a stabilizing effect to the hydrogel, aligning collagen molecules to make the EDC/NHS crosslinking more efficient. EDC/NHS crosslinking increases stiffness of structured tissues, such as amnion,[11] tendon,[28] and sheep dermis.[29] Therefore, forming a more organized collagen matrix by photocrosslinking before exposure to EDC/NHS can positively affect the G' of the hydrogel.

Any crosslinking paradigm for ultimate clinical use cannot be toxic to the encapsulated cells. It is clear that chondrocytes are viable after encapsulation in the dual-crosslinked matrix (Fig. 5). Encapsulation of chondrocytes in type I collagen hydrogels, both spontaneous and photocrosslinked, was shown to be nontoxic in previous studies. The dual-crosslinked constructs were shown to be $96 \pm 2\%$ viable, well above the threshold of 90% viability for good ECM generation capacity used in previous studies.[10] Dead cells were few in number and confined to the outer extremes of the construct. Cells also appeared to adhere well to the dual-crosslinked matrix.

The gels that underwent dual crosslinking also retarded degradation by collagenase digestion (Fig. 1). Protection from proteases is important for matrix stability during early-stage chondrocyte viability and ECM generation, but over time the initial matrix must be remodeled by natural enzymatic activity and deposition of new hyaline cartilage ECM. If not, the crosslinked type I collagen matrix will impede production of neocartilage. We anticipate that there will be an optimum crosslinking level that provides sufficient stiffness to the gel but also allows for gradual enzymatic digestion and remodeling *in vivo*. We have shown by using different concentrations of EDC/NHS or treatment times that we can fine-tune the stiffness and also the degradation rate. Although collagenase degradation is affected by exposing the hydrogel to even the most dilute EDC/NHS groups, there is no significant effect on storage modulus until the hydrogel is exposed to higher concentrations. Compared to full crosslinking (1 h exposure time and 33 m*M* EDC/6 m*M* NHS) the stiffness of the gel increased at lower

concentrations and lower times of exposure (Figs. 3 and 4). Further studies are planned to investigate the cartilage generation capacity of encapsulated chondrocytes in gels in these groups.

A major concern in articular cartilage engineering is the ability of a construct to withstand biocompressive forces in the knee, which can be up to 3.40 ± 0.18 times patient bodyweight during a normal walking gait.[30] The increase in storage modulus after dual-crosslinking treatment was a very positive result. Creating a construct that has a higher storage modulus, (stiffer) would be beneficial as long as the increased stiffness does not impede neocartilage deposition within the matrix. Using a construct similar to those tested here may lead to shorter patient immobilization periods, shorter post-operative physical therapy periods, and an overall faster recovery when compared with recovery periods after solution-based cartilage reparative procedures like ACI. The proven viability of encapsulated chondrocytes and the protection against rapid enzymatic degradation that is provided by this dual-crosslinking paradigm may offer a route to a new, matrix-assisted articular cartilage replacement system.

CONCLUSIONS

From these data we can conclude that photochemically crosslinking collagen gels increases their resistance to collagenase digestion 2-fold. Adding a chemical crosslinking step to the photochemical crosslinking makes them even more resistant to digestion with collagenase without compromising the cell viability. The storage modulus of dual-crosslinked constructs was increased 5-fold over that of both photocrosslinked and spontaneous gels. Thus, the photochemical crosslinking, with or without chemical crosslinking, could resist degradation *in vivo* and be used as a scaffold for delivery of chondrocytes into cartilage defects. Changing the crosslinking strategy can improve the stiffness of the gel to provide additional stability to the gels when used *in vivo*.

ACKNOWLEDGMENTS

The content of the article does not necessarily reflect the position or the policy of the Government, and no official endorsement should be inferred.

REFERENCES

1. Lin Z, Willers C, Xu J, Zheng MH. The chondrocyte: Biology and clinical application. Tissue Eng 2006;12:1971–1984. Review.
2. Yamamoto T, Katoh M, Fukushima R, Kurushima T, Ochi M. Effect of glycosaminoglycan production on hardness of cultured cartilage fabricated by the collagen-gel embedding method. Tissue Eng 2002;8:119–129.
3. Yuan T, Li K, Guo L, Fan H, Zhang X. Modulation of immunological properties of allogeneic mesenchymal stem cells by collagen scaffolds in cartilage tissue engineering. J Biomed Mater Res A 2011;98:332–341.
4. Caliari SR, Ramirez MA, Harley BA. The development of collagen-GAG scaffold-membrane composites for tendon tissue engineering. Biomaterials 2011;32:8990–8998.
5. Horch RE, Debus M, Wagner G, Stark GB. Cultured human keratinocytes on type I collagen membranes to reconstitute the epidermis. Tissue Eng 2000;6:53–67.
6. Ng KK, Thatte HS, Spector M. Chondrogenic differentiation of adult mesenchymal stem cells and embryonic cells in collagen scaffolds. J Biomed Mater Res A 2011;99:275–282.
7. Lin Z, Solomon KL, Zhang X, Pavlos NJ, Abel T, Willers C, Dai K, Xu J, Zheng Q, Zheng M. In vitro evaluation of natural marine sponge collagen as a scaffold for bone tissue engineering. Int J Biol Sci 2011;7:968–977.
8. Becerra J, Andrades JA, Guerado E, Zamora-Navas P, López-Puertas JM, Reddi AH. Articular cartilage: Structure and regeneration. Tissue Eng Part B Rev 2010;16:617–627.
9. Ibusuki S, Halbesma GJ, Randolph MA, Redmond RW, Kochevar IE, Gill TJ. Photochemically cross-linked collagen gels as three-dimensional scaffolds for tissue engineering. Tissue Eng 2007;13:1995–2001.
10. Ibusuki S, Papadopoulos A, Ranka MP, Halbesma GJ, Randolph MA, Redmond RW, Kochevar IE, Gill TJ. Engineering cartilage in a photochemically crosslinked collagen gel. J Knee Surg 2009;22:72–81.
11. Ma DH, Lai JY, Cheng HY, Tsai CC, Yeh LK. Carbodiimide cross-linked amniotic membranes for cultivation of limbal epithelial cells. Biomaterials 2010;31:6647–6658.
12. Rafat M, Li F, Fagerholm P, Lagali NS, Watsky MA, Munger R, Matsuura T, Griffith M. PEG-stabilized carbodiimide crosslinked collagen-chitosan hydrogels for corneal tissue engineering. Biomaterials 2008;29:3960–3972.
13. Sung HW, Chang Y, Chiu CT, Chen CN, Liang HC. Crosslinking characteristics and mechanical properties of a bovine pericardium fixed with a naturally occurring crosslinking agent. J Biomed Mater Res 1999;47:116–126.
14. Yao L, Billiar KL, Windebank AJ, Pandit A. Multichanneled collagen conduits for peripheral nerve regeneration: Design, fabrication, and characterization. Tissue Eng Part C Methods 2010;16:1585–1596.
15. Deng C, Li F, Hackett JM, Chaudhry SH, Toll FN, Toye B, Hodge W, Griffith M. Collagen and glycopolymer based hydrogel for potential corneal application. Acta Biomater 2010;6:187–194.
16. Everaerts F, Torrianni M, Hendriks M, Feijen J. Biomechanical properties of carbodiimide crosslinked collagen: Influence of the formation of ester crosslinks. J Biomed Mater Res A 2008;85:547–555.
17. Potta T, Chun C, Song SC. Injectable, dual cross-linkable polyphosphazene blend hydrogels. Biomaterials 2010;31:8107–8120.
18. Harris JD, Siston RA, Pan X, Flanigan DC. Autologous chondrocyte implantation: A systematic review. J Bone Joint Surg Am 2010;92:2220–2233.
19. Clar C, Cummins E, McIntyre L, Thomas S, Lamb J, Bain L, Jobanputra P, Waugh N. Clinical and cost-effectiveness of autologous chondrocyte implantation for cartilage defects in knee joints: Systematic review and economic evaluation. Health Technol Assess 2005;9:iii–iv, ix-x, 1–82. Review.
20. Burugapalli K, Chan JC, Naik H, Kelly JL, Pandit A. Tailoring the properties of cholecyst-derived extracellular matrix using carbodiimide cross-linking. J Biomater Sci Polym Ed 2009;20(7-8):1049–1063.
21. Coutinho DF, Sant SV, Shin H, Oliveira JT, Gomes ME, Neves NM, Khademhosseini A, Reis RL. Modified Gellan Gum hydrogels with tunable physical and mechanical properties. Biomaterials 2010;31:7494–7502.
22. Jeon O, Powell C, Ahmed SM, Alsberg E. Biodegradable, photocrosslinked alginate hydrogels with independently tailorable physical properties and cell adhesivity. Tissue Eng Part A 2010;16:2915–2925.
23. Passaretti D, Silverman RP, Huang W, Kirchhoff CH, Ashiku S, Randolph MA, Yaremchuk MJ. Cultured chondrocytes produce injectable tissue-engineered cartilage in hydrogel polymer. Tissue Eng 2001;7:805–815.
24. Rouillard AD, Berglund CM, Lee JY, Polacheck WJ, Tsui Y, Bonassar LJ, Kirby BJ. Methods for photocrosslinking alginate hydrogel scaffolds with high cell viability. Tissue Eng Part C Methods 2011;17:173–179.

25. Au V, Madison SA. Effects of singlet oxygen on the extracellular matrixprotein collagen: oxidation of the collagen crosslink histidinohydroxylysinonorleucine and histidine. Arch Biochem Biophys 2000;384:133–142.
26. Olde Damink LH, Dijkstra PJ, van Luyn MJ, van Wachem PB, Nieuwenhuis P, Feijen J. Cross-linking of dermal sheep collagen using a water-soluble carbodiimide. Biomaterials 1996;17:765–773.
27. Sung HW, Chang WH, Ma CY, Lee MH. Crosslinking of biological tissues using genipin and/or carbodiimide. J Biomed Mater Res A 2003;64:427–438.
28. Seto A, Gatt CJ Jr, Dunn MG. Radioprotection of tendon tissue via crosslinking and free radical scavenging. Clin Orthop Relat Res 2008;466:1788–1795.
29. Zeeman R, Dijkstra PJ, van Wachem PB, van Luyn MJ, Hendriks M, Cahalan PT, Feijen J. Successive epoxy and carbodiimide cross-linking of dermal sheep collagen. Biomaterials 1999;20:921–931.
30. Jensen SB, Henriksen M, Aaboe J, Hansen L, Simonsen EB, Alkjaer T. Is it possible to reduce the knee joint compression force during level walking with hiking poles? Scand J Med Sci Sports 2011;21:e195–e200.

Society For Biomaterials

Covalently tethered TGF-β1 with encapsulated chondrocytes in a PEG hydrogel system enhances extracellular matrix production

Balaji V. Sridhar,[1,2] Nicholas R. Doyle,[1,2] Mark A. Randolph,[3,4] Kristi S. Anseth[1,2,5]

[1]Department of Chemical and Biological Engineering, University of Colorado at Boulder, Boulder, Colorado
[2]Biofrontiers Institute, University of Colorado at Boulder, Boulder, Colorado
[3]Department of Orthopaedic Surgery, Laboratory for Musculoskeletal Tissue Engineering, Massachusetts General Hospital, Harvard Medical School, Boston, Massachusetts
[4]Division of Plastic Surgery, Plastic Surgery Research Laboratory, Massachusetts General Hospital, Harvard Medical School, Boston, Massachusetts
[5]Howard Hughes Medical Insitute, University of Colorado at Boulder

Received 16 September 2013; revised 24 January 2014; accepted 10 February 2014
Published online 26 February 2014 in Wiley Online Library (wileyonlinelibrary.com). DOI: 10.1002/jbm.a.35115

Abstract: Healing articular cartilage defects remains a significant clinical challenge because of its limited capacity for self-repair. While delivery of autologous chondrocytes to cartilage defects has received growing interest, combining cell-based therapies with growth factor delivery that can locally signal cells and promote their function is often advantageous. We have previously shown that PEG thiol-ene hydrogels permit covalent attachment of growth factors. However, it is not well known if embedded chondrocytes respond to tethered signals over a long period. Here, chondrocytes were encapsulated in PEG hydrogels functionalized with transforming growth factor-beta 1 (TGF-β1) with the goal of increasing proliferation and matrix production. Tethered TGF-β1 was found to be distributed homogenously throughout the gel, and its bioactivity was confirmed with a TGF-β1 responsive reporter cell line. Relative to solubly delivered TGF-β1, chondrocytes presented with immobilized TGF-β1 showed significantly increased DNA content, and GAG and collagen production over 28 days, while maintaining markers of articular cartilage. These results indicate the potential of thiol-ene chemistry to covalently conjugate TGF-β1 to PEG to locally influence chondrocyte function over 4 weeks. Scaffolds with other or multiple tethered growth factors may prove broadly useful in the design of chondrocyte delivery vehicles for cartilage tissue engineering applications. © 2014 The Authors. Journal of Biomedical Materials Research Part A Published by Wiley Periodicals, Inc.: 102A: 4464–4472, 2014.

Key Words: cartilage tissue engineering, chondrocytes, protein conjugation, hydrogels, transforming growth factor-β1

How to cite this article: Sridhar BV, Doyle NR, Randolph MA, Anseth KS. 2014. Covalently tethered TGF-β1 with encapsulated chondrocytes in a PEG hydrogel system enhances extracellular matrix production. J Biomed Mater Res Part A 2014:102A:4464–4472.

INTRODUCTION

Healing articular cartilage defects remains a significant clinical challenge because of its limited capacity for self-repair and mechanical properties that are difficult to emulate.[1] Articular cartilage is an avascular tissue with a sparse population of cells surrounded by an extracellular matrix (ECM) that is regulated by numerous growth factors.[2] Therefore, tissue engineering strategies involving chondrocytes and growth factor delivery may help to improve the treatment of articular cartilage lesions.[3,4]

There is growing interest in the regenerative medicine community in methods to sequester and present bioactive therapeutic proteins to chondrocytes immobilized in three-dimensional matrices.[5] Cytokines are attractive targets for tissue engineering since, at low concentrations, they can regulate cellular functions, such as proliferation and matrix production.[6] Many of these proteins are commonly introduced as soluble factors in culture media during *in vitro* experiments; however, *in vivo*, growth factors tend to be sequestered in the extracellular matrix, allowing local presentation to cells.[5]

A variety of natural and synthetic materials have been examined as potential cell carriers or as therapeutic agents for cartilage repair.[7–9] Hydrogel scaffolds appear to be one promising class of materials, due to their high water content which mimics native tissue microenvironments.[10] Furthermore, poly-(ethylene glycol) (PEG) hydrogels have been used to improve micofracture cartilage regeneration outcomes in human trials.[11]

Hydrogel systems permit sequestration of growth factors via covalent tethering, which can provide advantages

Additional Supporting Information may be found in the online version of this article.
Correspondence to: B. V. Sridhar; e-mail: balaji.sridhar@colorado.edu
Contract grant sponsor: Howard Hughes Medical Institute and Department of Defense; contract grant number: W81XWH-10-1-0791
Contract grant sponsor: The US Army Medical Research Acquisition Activity

compared with other forms of protein delivery. In particular, growth factors are typically cross-reactive with multiple cell types and can have short serum half-lives *in vivo*, limitations that often necessitate localized presentation.[12] Since diffusion of lower molecular weight proteins in hydrogels can be quite rapid, some researchers have used microparticles for controlled release presentation of growth factors to encapsulated chondrocytes.[13] While this approach is quite useful, the process can increase the complexity of scaffold preparation and design. Variability can result from differences in protein loading, release kinetics, as well as the size distribution of loaded microparticles. Therefore, strategies to immobilize growth factors in a bioactive, physiologically relevant context are a complementary and important step towards directing cells to regenerate cartilage tissue.

As one robust method to create protein-functionalized materials, we used thiol-ene chemistry to incorporate thiolated proteins in PEG hydrogels. Previously, PEG systems have been broadly explored for cell delivery applications.[14–17] Specifically, we formed PEG hydrogels through a photoinitiated step-growth polymerization, by reacting norbornene-terminated PEG macromolecules with a dithiol PEG crosslinker.[18] This photopolymerizable system allows for precise spatial and temporal control over polymer formation, as well as facile encapsulation of cells and biologics. The resulting crosslinked PEG hydrogel has been employed to encapsulate numerous primary cells with high survival rates following photoencapsulation.[10,19]

Previously, our group has successfully incorporated thiolated TGF-β1 in a chain-growth polymerized PEG diacrylate system and showed enhanced chondrogenesis of human mesenchymal stem cells (MSC).[20] Here, we encapsulated chondrocytes in step-growth polymerized PEG thiol-ene hydrogels, and we hypothesized that local presentation of TGF-β1 would influence chondrocyte secretory properties and improve the system's application for cartilage regeneration. Step-growth polymerization leads to more ideal network structures than chain-growth polymerization, and the thiol-ene chemistry has also been shown to be more compatible for coupling proteins and maintaining their activity.[21] In contrast to other cell types, primary chondrocytes are a versatile cell source since they deposit a matrix more similar to articular cartilage. For example, MSC derived fibrocartilage is biomechanically inferior.[22] Additionally, a recent comparison study revealed that encapsulating chondrocytes in a PEG thiol-ene system yielded more hyaline-like cartilage than cells encapsulated in a PEG diacrylate system.[23]

In this work TGF-β1 was thiolated and incorporated into a PEG thiol-ene hydrogel. We selected TGF-β1 because it has been shown to increase chondrocyte proliferation and cartilage ECM production in both three-dimensional[13] and two-dimensional studies.[24] We confirmed the presence of tethered TGF-β1 in the gel by ELISA and investigated its bioactivity using a PE-25 cell reporter assay for SMAD2 signaling.[25] We also found that tethering growth factors to a scaffold results in increased cell proliferation and ECM production *in vitro*. These results suggest that a step-growth PEG hydrogel system is capable of tunable control of local bioactive signals. Chondrocytes encapsulated in this system are presented with a local and sustained delivery of TGF-β1, resulting in enhanced cartilage tissue regeneration.

MATERIALS AND METHODS

PEG monomer synthesis

Polyethylene glycol (PEG) (8-arm) amine norbornene M_n 10,000 was synthesized as previously described.[16] Briefly, 5-norbornene-2-carboxylic acid (predominantly endo isomer, Sigma Aldrich) was first converted to a dinorbornene anhydride using *N,N'*-dicyclohexylcarbodiimide (0.5 molar eq. to norbornene, Sigma Aldrich) in dichloromethane. The 8-arm PEG monomer (JenKem Technology) was then reacted overnight with the norbornene anhydride (5 molar eq. to PEG hydroxyls) in dichloromethane. Pyridine (5 molar eq. to PEG hydroxyls) and 4-dimethylamino pyridine (0.05 molar eq. to PEG hydroxyls) were also included. The reaction was conducted at room temperature under argon. End group functionalization was verified by ^{1}H NMR to be >90%. ^{1}H NMR (500 MHz,$CDCl_3$) δ 6.30–5.80 (m,16H), 4.0–3.0 (m,1010H), 2.5–1.2 (m,100H). The photoinitiator lithium phenyl-2,4,6-trimethylbenzoylphosphinate (LAP) was synthesized as described.[19] The 3.5 kDa PEG dithiol linker was purchased from JenKem Technology.

Cell harvest and expansion

Primary chondrocytes were isolated from articular cartilage of the femoral-patellar groove of 6-month-old Yorkshire swine as detailed previously.[26] Cells were grown in a culture flask in media as previously described.[27] Briefly, cells were grown in DMEM growth medium (phenol red, high glucose DMEM supplemented with ITS + Premix 1% v/v (BD Biosciences), 50 μg/mL L-ascorbic acid 2-phosphate, 40 μg/mL L-proline, 0.1 μ*M* dexamethasone, 110 μg/mL pyruvate, and 1% penicillin-streptomycin-fungizone with the addition of 10 ng/mL IGF-1 (Peprotech) to maintain cells in de-differentiated state. ITS promotes formation of hyaline cartilage over serum.[28] Cultures were maintained at 5% CO_2 and 37°C.

Mink lung epithelial PE-25 cells containing a stably transfected luciferase reporter gene for TGF-β1 were cultured in low glucose DMEM supplemented with 10% fetal bovine serum, and 1% penicillin-streptomycin-fungizone. Cells that were passaged three times were used in encapsulation experiments.

PEG hydrogel polymerization and growth factor incorporation

Human TGF-β1 (Peprotech) was thiolated using 2-iminothiolane (Pierce). Briefly, 2-iminothiolane was reacted at a 4:1 molar ratio to TGF-β for 1 h at RT. Thiolated TGF-β was prereacted at various concentrations with PEG norbornene monomer solution before cross-linking via photoinitiated polymerization with UV light (I_o ~3.5 mW/cm^2 at $\lambda = 365$ nm) and 0.05 wt% LAP for 30 s. The monomer solution was then crosslinked with a 3.5 kDa PEG dithiol at a stoichiometric ratio of [40 m*M* dithiol]: [80 m*M*

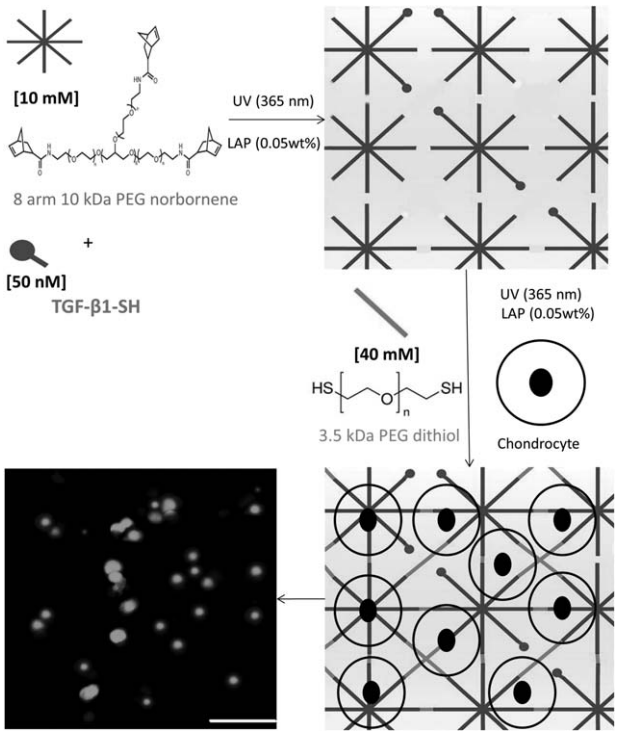

SCHEME 1. Pre-polymerization scheme with thiolated TGF-β1. Initially thiolated TGF-β1 is phototethered into the 8 arm 10 kDa PEG norbornene network, then the 3.5 kDa dithiol crosslinker is added in with chondrocytes to complete the encapsulation process. Growth factor is not drawn to scale. In featured experiments, there is a lower amount of growth factor attached to the monomer end. Chondrocytes seeded at 40 million cells/mL retain a rounded morphology similar to cells in native tissue. Scale bar represents 50 μm.

Norbornene] in a 10 wt% PEG solution using longwave ultraviolet light (I_o ~3.5 mW/cm^2 at $\lambda = 365$ nm) for 30 s (Scheme 1).

Quantifying growth factor incorporation

Hydrogels (10 wt%) were synthesized with tethered TGF-β1 at 0, 10, 50, or 90 n*M* and prepared for cryosectioning as previously described.[29] Briefly, hydrogels were flash frozen in liquid nitrogen and placed in HistoPrep (Fisher Scientific) in cryomolds. 20 μm cross-sections along the plane of the construct were collected on SuperFrost® Plus Gold slides (Fisher Scientific).

Disc-shaped gels (40 μL) (O.D. ~5 mm, thickness ~ 2 mm) without encapsulated cells and with varying concentrations of tethered growth factor were also prepared and sectioned. Sections (20 μm) were collected from the top, middle, and bottom of gel. To quantify the TGF-β concentration in each section, a modified ELISA was used as previously described.[14] Briefly, sections were blocked for 1 h at RT in 5% bovine serum albumin (BSA). Sections were washed 3× in ELISA buffer (0.01% BSA, and 0.05% Tween-20 in PBS) before incubation with a mouse anti-human TGF-β1 antibody (Peprotech) at 1:100 dilution overnight at 4°C. Sections were washed again, then incubated with goat anti mouse–HRP (eBioscience) for 1 h at RT and washed again. Sections were incubated with 100 μL of peroxidase and 3,3',5,5' tetramethylbenzidine substrate until color developed then the reaction was stopped using 100 μL 2*N* sulfuric acid. The absorbance was measured at 450 nm using a Bio-Tek H1 spectrophotometer.

To calculate the theoretical loading of growth factor in each section, the volume was determined assuming the section was a thin disc with a 5 mm diameter and 20 μm height. Using $V = \pi r^2 h$ and the molecular weight of TGF-β1 ($M_n = 25{,}000$ g/mol), the amount of growth factor per section was calculated in nanograms. For instance, a 50 n*M* 40 μL gel section is expected to have 0.5 ng of TGF-β1 per 20 μm section assuming ideal conditions.

Finally, a standard curve was made simultaneously by prepping 96-well high binding clear plates with known amounts of TGF-β1. The 0 n*M* value at 450 nm absorbance was subtracted out from all values in the curve.

TGF-β1 bioactivity and cellular signaling

PE-25 cells were encapsulated in 10 wt% gels functionalized with a 1 m*M* Cys-Arg-Gly-Asp-Ser (CRGDS) peptide to promote survival. Thiolated TGF-β1 was incorporated into the gel at 0, 12.5, 25, 50, or 100 n*M*. Additionally, cells encapsulated in PEG gels without tethered growth factor were exposed to soluble TGF-β1 at concentrations of 0, 0.2, 0.3, 1, or 2 n*M*. Cells were photo-encapsulated at a density of 40 million cells/mL, and cell-laden hydrogels were formed in syringe tips at a volume of 40 μL. Following encapsulation, hydrogels were placed into DMEM growth medium in 48 well plates and incubated overnight at 37°C, 5% CO_2. Afterwards, hydrogels were incubated in Glo-Lysis buffer (Promega) for 10 min at 37°C; the samples were centrifuged for 10 min (13,400 rpm, 4°C), and the lysate was transferred to white 96-well plates (50 μL per well). 50 μL luciferase substrate (Promega) was added to the lysate for 5 min and luminescence was quantified between 300 and 700 nm.

Chondrocyte encapsulation in PEG thiol-ene hydrogels

Chondrocytes were encapsulated at 40 million cells/mL in 10 wt% monomer solution and thiolated TGF-β1 at concentrations of 0 or 50 n*M*. 40 μL of cell-laden gels were immediately placed in 1 mL DMEM growth medium (without phenol red) in 48-well nontreated tissue culture plates. As a positive control, a subset group of gels without tethered growth factor was exposed to 0.3 n*M* (7.5 ng/mL) soluble TGF-β1. Media was changed every 3 days. Samples were collected at days 1, 14, and 28 for analysis of ECM production and chondrocyte proliferation. At day 1 and 28 cell viability was assessed using a LIVE/DEAD® membrane integrity assay and confocal microscopy.

Biochemical analysis of cell-hydrogel constructs

Cell-laden hydrogels were collected at specified time points, snap frozen in LN_2, and stored at −70°C until analysis. Hydrogels were digested in enzyme buffer (125 μg/mL papain [Worthington Biochemical], and 10 m*M* cysteine) and

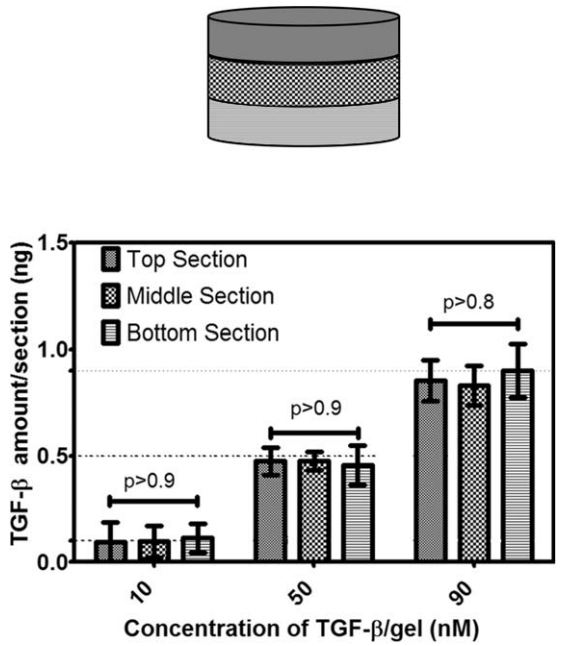

FIGURE 1. TGF-β1 is homogenously distributed throughout the PEG hydrogel. Section ELISA of tethered gels without cells show detection of TGF-β at similar levels to theoretical values with graphic on top depicting slice areas. Each section ~20 μm thickness. Theoretical values indicated by dashed lines (0.1 ng for 10 n*M*, 0.5 ng for 50 n*M*, and 0.9 ng for 90 n*M* gels). 0 n*M* value is subtracted out of all conditions. Results are presented as mean activity ± SD ($n = 2$). Solid lines indicate p values with one way ANOVA analysis to confirm sections of each gel are not statistically different from each other.

homogenized using 5 mm steel beads in a TissueLyser (Qiagen). Homogenized samples were digested overnight at 60°C.

DNA content was measured using a Picogreen assay (Invitrogen). Cell number was determined by assuming each cell produced 7.7 pg DNA per chondrocyte.[30] Sulfated glycosaminoglycan (GAG) content was assessed using a dimethyl methylene blue assay as previously described with results presented in equivalents of chondroitin sulfate.[31] Collagen content in the gels was measured using a hydroxyproline assay, where hydroxyproline is assumed to make up 10% of collagen.[32] DNA content was normalized per gel while GAG and collagen content were normalized per cell.

Histological and immunohistochemical analysis

On day 28, constructs ($n = 2$) were fixed in 10% formalin for 30 min at RT, then snap frozen and cryosectioned. Sections were stained for safranin-O or masson's trichrome on a Leica autostainer XL and imaged in bright field (40× objective) on a Nikon inverted microscope.

For immunostaining, sections were blocked with 10% goat serum, then analyzed by anti-collagen type II (1:50, US Biologicals) and anti-collagen type I (1:50, Abcam). Sections were treated with appropriate enzymes for 1 h at 37°C: hyaluronidase (2080 U) for collagen II, and pepsin A (4000 U) with Retrievagen A (BD Biosciences) treatment for collagen I to help expose the antigen. Sections were probed with Alexa-Fluor 568-conjugated secondary antibodies and counter-stained with DAPI for cell nuclei. All samples were processed at the same time to minimize sample-to-sample variation. Images were collected on a Zeiss LSM710 scanning confocal microscope with a 20× objective using the same settings and post-processing for all images. The background gain was set to negative controls on blank sections that received the same treatment. Positive controls were performed on porcine hyaline cartilage for collagen type II and porcine meniscus for collagen type I (Supporting Information Fig. 1).

Statistical analyses

Data are shown as mean ± standard deviation. Two-way analysis of variance (ANOVA) with Bonferroni post-test for pairwise comparisons was used to evaluate the statistical significance of data. One-way ANOVA was used to assess differences within specific conditions. $p < 0.05$ was considered to be statistically significant.

RESULTS

Distribution of thiolated TGF-β1 in PEG hydrogels

We confirmed that TGF-β1 was homogenously distributed within the gel after the thiol-ene tethering process, using a

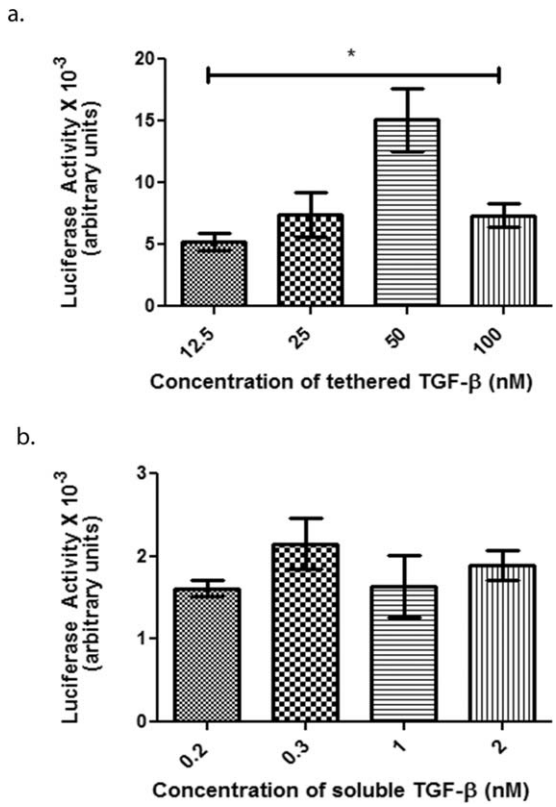

FIGURE 2. Determining TGF-β1 concentration that yields maximal response. (a) PE-25s were encapsulated at 40 million cells/mL with varying concentrations of tethered TGF-β and 50 n*M* yielded a maximal response. * indicates statistically significant difference between 50 n*M* and the other concentrations with $p < 0.001$. Results are presented as mean activity ± SD ($n = 4$). (b) PE-25 cells encapsulated at 40 million cells/mL were transiently exposed to varying concentrations of TGF-β in the media. The 0.3 n*M* output is higher on average than the other concentrations. Results are presented as mean activity ± SD ($n = 4$).

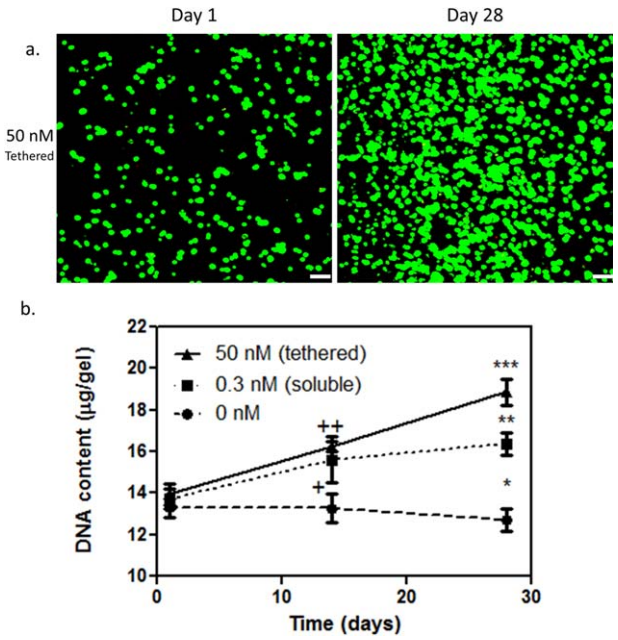

FIGURE 3. Increased proliferation of chondrocytes exposed to TGF-β1. (a) Live/dead staining of 50 n*M* gels seeded at 40 million cells/mL on day 1 and day 28 shows chondrocytes retain a spherical morphology, have high viability, and increase in number. Scale bars represent 50 μm. (b) DNA content of chondrocytes encapsulated at 40 million cells/mL that were exposed to 0 n*M*, 0.3 n*M* which was delivered through the media, or 50 n*M* which was tethered into the gel. Over a 28-day period, the cells in the 50 n*M* condition show a steady rate of increase of DNA content. + indicates significant difference between the 0.3 n*M* and 0 n*M* case ($p < 0.001$), ++ indicates significant difference between 50 n*M* and 0 n*M* case ($p < 0.001$), * indicates significant difference between 0.3 n*M* and 0 n*M* ($p < 0.001$), ** indicates significant difference between 50 n*M* and 0.3 n*M* case at day 28 ($p < 0.001$), and *** indicates significant difference between 50 n*M* and 0 n*M* for day 28 ($p < 0.001$). Results are presented as mean ± SD ($n = 3$). [Color figure can be viewed in the online issue, which is available at wileyonlinelibrary.com.]

modified section ELISA.[14] The results presented in Figure 1 show TGF-β1 incorporation throughout the gel, and its relatively homogeneous distribution among gel regions. We further showed that experimentally measured values were similar to theoretically calculated levels (0.1 ng for 10 n*M*, 0.5 ng for 50 n*M*, and 0.9 ng for 90 n*M*).

Bioactivity and concentration of tethered TGF-β1 in three-dimensional culture

We investigated the bioactivity of tethered TGF-β1 in three-dimensional culture using a reporter cell line. Briefly, it was shown that tethered proteins typically maintain high levels of bioactivity when conjugated using thiol-ene reactions.[20] We further determined concentrations of soluble and tethered TGF-β1 that yielded a maximal response in PE-25 cells at a seeding density of 40 million cells/mL. In Figure 2(a), there was a significant difference in luciferase output of 50 n*M* gels compared with other conditions. In Figure 2(b), 0.3 n*M* via soluble delivery elicited a maximal cellular response. Interestingly, when we dosed 50 n*M* of soluble TGF β-1 to encapsulated PE-25s at 40 million cells/mL, the average luciferase response was ~6510 arbitrary units ($n = 4$), which is a threefold lower response than for the same concentration of tethered TGF-β1. Based on these results, we elected to dose soluble TGF-β1 at the magnitude of 0.3 n*M*. Overall, these results suggest that tethered TGF-β1 is bioactive, and at 40 million cells/mL, the conditions that elicited the highest response to TGF-β1 were 0.3 n*M* (soluble) and 50 n*M* (tethered).

Proliferation of chondrocytes exposed to TGF-β1

Cell viability for all encapsulation and culture conditions was between 80%-90% assessed by live/dead membrane integrity assay at both days 1 and 28. Figure 3(a) shows the rounded shape of encapsulated cells; there was significant increase in number of cells in the 50 n*M* TGF-β1 tethered gels. To further quantify this proliferation, we harvested samples at day 1, 14, and 28 and assayed for DNA content [Fig. 3(b)]. There was a statistically significant increase in DNA content, at day 28, for cells encapsulated in 50 n*M* TGF-β1 containing gels. Further, there was significantly more DNA in the day 28 50 n*M* condition than either the 0.3 n*M* or 0 n*M* gel condition ($p < 0.001$). Combined with the viability results, these data suggest an increase in chondrocyte proliferation in response to tethered growth factor presentation.

Matrix deposition as a function of TGF-β1 presentation and culture time

We assessed glycosaminoglycan (GAG) and total collagen content of gels at day 1, 14, and 28. Encapsulated chondrocytes were either exposed to 0 n*M*, 0.3 n*M* solubly or 50 n*M* tethered TGF-β1. Measured quantities were normalized to cell content in the respective hydrogel formulations.

In Figure 4(a), GAG production per cell on day 28 for the tethered construct was significantly higher than non-treated groups ($p < 0.001$). There was also a significant difference at day 28 between constructs that presented tethered TGF-β1 compared with solubly delivered TGF-β1 ($p < 0.05$), suggesting that the tethered growth factor enhanced ECM production over soluble growth factor delivered in the media.

In Figure 4(b), total collagen production per cell was highest at day 28 from the construct with tethered TGF-β1. Further, there was a significant difference between the tethered and soluble TGF-β1 conditions ($p < 0.01$) at day 28, and the tethered group was significantly increased from the 0 n*M* group ($p < 0.001$), indicating that collagen content is highest in the tethered protein constructs.

Matrix organization

We examined the distribution and deposition of extracellular matrix molecules by histological and immunofluorescence techniques. Masson's trichrome staining [Fig. 5(a,c,e)] revealed collagen deposition increased in the pericellular space of encapsulated chondrocytes with both tethered and soluble TGF-β1 gels on day 28 compared with 0 n*M* gels. Overall, it appears that most of the pericellular collagen deposition occurs in the 50 n*M* gels at day 28. In a similar

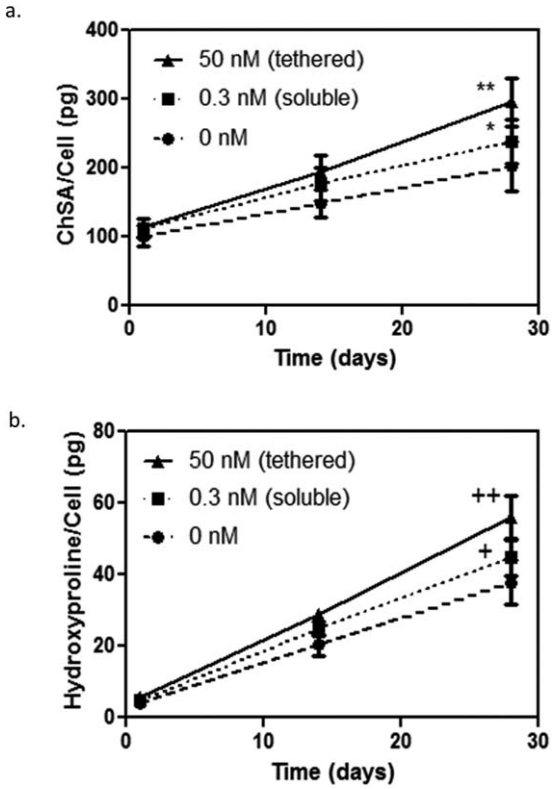

FIGURE 4. Enhanced matrix production of encapsulated chondrocytes exposed to TGF-β. (a) GAG production was normalized per cell. * indicates significant difference between 50 n*M* and 0.3 n*M* condition at day 28 ($p < 0.05$), ** indicates significant difference between 50 n*M* and 0 n*M* at day 28 ($p < 0.001$). Data presented as mean ± SD ($n = 3$). (b) Collagen production was normalized per cell. + indicates significant difference between 50 n*M* and 0.3 n*M* at day 28 ($p < 0.01$) and ++ indicates significant difference between 50 n*M* and 0 n*M* at day 28 ($p < 0.001$). Data presented as mean ± SD ($n = 3$).

fashion, safranin-O [Fig. 5(b,d,f)] staining revealed that GAG deposition localized in the pericellular region with increased deposition per cell in the presence of TGF-β1. These results support the data that tethered TGF-β increases ECM secretion.

Immunofluorescence staining revealed that by day 28, there was a scarce amount of collagen I throughout all samples [Fig. 6(a,c,e)] and that collagen II was prevalent in the growth factor treated samples [Fig. 6(d,f)] compared with the 0 n*M* sample [Fig. 6(b)]. A high collagen II and low collagen I signal is indicative of articular cartilage, and the constructs maintained that phenotype over 28 days of culture.[33]

DISCUSSION

Engineering a clinically viable scaffold for chondrocyte delivery and promotion of cartilage regeneration is challenging, partly because of the time required for chondrocytes to generate a robust matrix. By encapsulating chondrocytes in a PEG thiol-ene system with localized presentation of a growth factor, we have shown quantitatively and qualitatively, *in vitro,* that cells survive, proliferate, and generate cartilage specific ECM molecules at a higher rate than without the growth factor. Tethering growth factors into a synthetic material scaffold integrates the promoting effects of a protein cross-linked gel without gel to gel variability. A cell delivery system with such properties can provide certain advantages for clinical applications in techniques such as matrix assisted autologous chondrocyte transplantation (MACT).

There are many advantages to tethering growth factors into a gel system for tissue engineering purposes. Localized presentation precludes growth factors from activating unnecessary cell targets in an *in vivo* setting. Additionally, it requires a lower amount of growth factor. In this 28-day study, TGF-β1 is dosed in 1 mL media every 3 days at 0.3 n*M* that results in ~70 ng of protein delivered to the cell-laden gel. For the same time period and experimental conditions, a 50 n*M* tethered gel corresponds to ~50 ng of TGF-β1/gel, yet led to higher matrix production and DNA content at day 28. When using an expensive and/or potent growth factor to promote tissue regeneration, a tethered system can potentially provide a more efficient and effective delivery system for long time periods appropriate for clinical settings.

In these studies, we chose to look specifically at chondrocytes encapsulated at 40 million cells/mL, since this cell density has been previously shown to be an optimal choice for *in vivo* studies with hydrogel delivery systems.[34–36] We used a cellular assay, based on PE-25 cells as a reporter system with a luciferase output, to determine that an effective concentration of growth factor to deliver to cells was 50 n*M* [Fig. 2(a)] for tethered TGF-β1 and 0.3 n*M* for soluble TGF-β1 [Fig. 2(b)]. We chose the initial concentrations of TGF-β1 for the PE-25 experiments based on previous work for promoting chondrogenesis of hMSCs.[20] We hypothesized that encapsulated cells may not respond as well to higher concentrations of soluble TGF-β1 than tethered TGF-β1, because PE-25s may internalize the factor, and seeding at high density may reduce the cellular response. Related studies with Mv1Lu cells showed that they internalized TGF-β1, so it is reasonable to consider this explanation for the PE-25 experiments.[37]

We speculate that for gels presenting 100 n*M* of tethered TGF-β1, the PE-25s encapsulated at 40 million cells/mL showed less activity compared with 50 n*M* gels [Fig. 2(a)] because growth factors can have pleiotropic effects that may lead to a negative feedback loop. Additionally, since TGF-β binds to a dimer receptor, which requires two receptor subtypes to join to initiate the signaling cascade, it is possible that the orientation of growth factors around the cell prevents complete binding since both subtype receptors may be occupied by separate ligands when only one is required for signaling activation.[38]

We chose to use human TGF-β1 with porcine chondrocytes because the PE-25 system has already been established with human TGF-β1,[25] and porcine chondrocytes will be used in future pre-clinical animal studies. We believe that this is unlikely to affect the outcomes of our studies, since mature TGF-β1 is known to be highly conserved (>99% amino acid sequence identity) throughout mammalian species.[39]

The data presented in this study suggest that the PEG thiol-ene platform with tethered TGF-β represents a bioactive

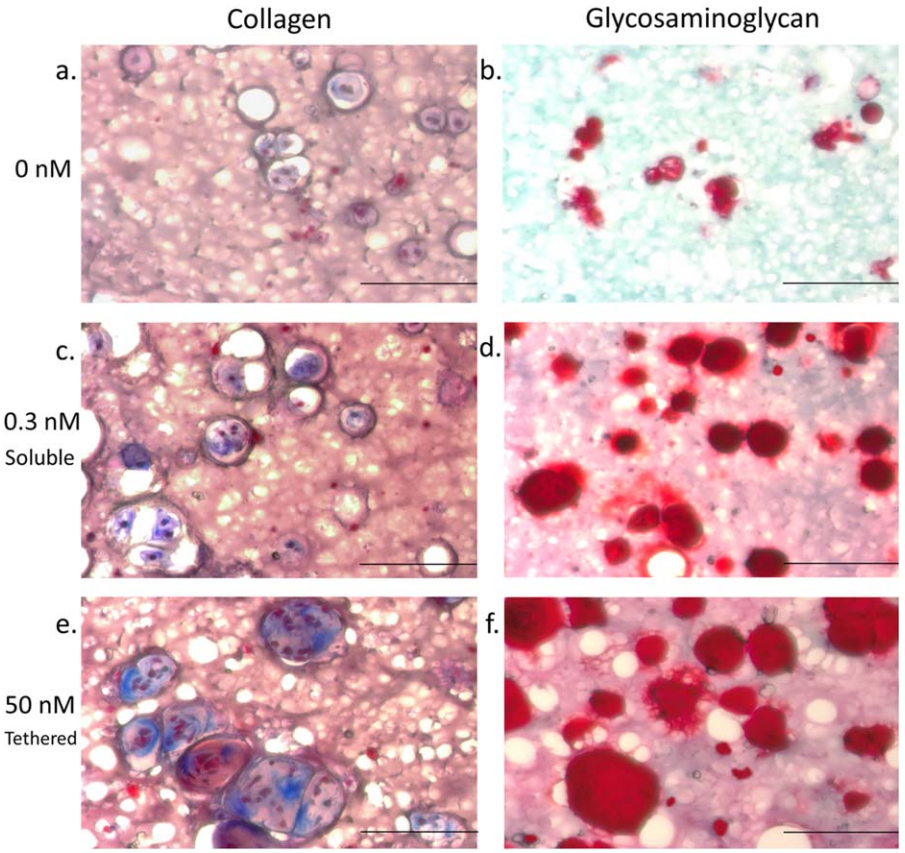

FIGURE 5. Matrix protein distribution in gels. At day 28, gels seeded with chondrocytes at 40 million cells/mL were sectioned and stained for matrix distribution. (a) 0 n*M* gel stained for collagen, (b) 0 n*M* gel stained for GAG, (c) 0.3 n*M* (soluble) gel stained for collagen, (d) 0.3 n*M* (soluble) gel stained for GAG, (e) 50 n*M* (tethered) gel stained for collagen, (f) 50 n*M* (tethered) gel stained for GAG. Blue indicates collagen and red indicates GAG. Scale bars represent 100 μm.

scaffold with potential tissue engineering applications for chondrocyte delivery. Chondrocytes maintained a spherical morphology, similar to native chondrocytes, in the gel over a 28-day period, as shown in Figure 3(a), which suggests the cells are less likely to de-differentiate and generate hyaline-like cartilage.[40] Chondrocytes also increased in cell number when cultured in PEG thiol-ene gels as shown in Figure 3(b), and especially when TGF-β1 is presented, which is known to induce proliferation.[24] Porcine chondrocyte doubling time in two-dimensional culture is around 6.4 ± 0.3 days in serum-containing media.[41] We speculate that part of the reason the cells did not double at a similar rate when encapsulated in the PEG gels is that the selected gel formulations are non-degradable. Thus, the polymer network limited the amount of space available for chondrocytes to grow, and the media did not contain serum. This result was confirmed by a study with rat chondrocytes grown in a nondegradable three-dimensional scaffold which had a longer doubling time (10.04 ± 0.9 days) than cells grown in 2D (2.94 ± 0.3 days).[42]

Extracellular matrix production data revealed that over 28 days, the tethered-protein gel stimulated chondrocytes to produce more GAGs and collagen, as quantified in Figure 4. The cells maintained a high rate of ECM production even though matrix proteins accumulate around the cell after 28 days. This phenomenon implies that TGF-β1 may maintain activity and interact with the chondrocytes, despite the increased pericellular matrix. Furthermore, when compared with a tethered TGF-β study investigating MSC chondrogenesis,[20] chondrocytes maintained a similar level of GAG production and also express collagen type II on a similar time scale.

A study with juvenile and adult chondrocytes encapsulated in degradable gels had higher GAG and collagen outputs per cell over a 28-day period compared with the ones in this study.[43] We expected that a degradable gel allows for greater ECM deposition as posited by various groups.[44,45] Additionally, histology and immunofluorescence staining confirmed that matrix was primarily deposited pericellularly in all conditions, but at a higher level in gels with tethered TGF-β1. While the secreted matrix was primarily confined to the pericellular region, there were some areas where the ECM molecules, especially GAGs, were more dispersed between cells (Fig. 5). These data suggest the need for tethering TGF-β1 to a degradable PEG thiol-ene system to enhance ECM production and elaboration, with the potential to better capture biochemical and biomechanical properties of native hyaline tissue.

CONCLUSION

We confirmed that thiol-ene reactions allow conjugation of TGF-β1 into PEG gels, while maintaining bioactivity and

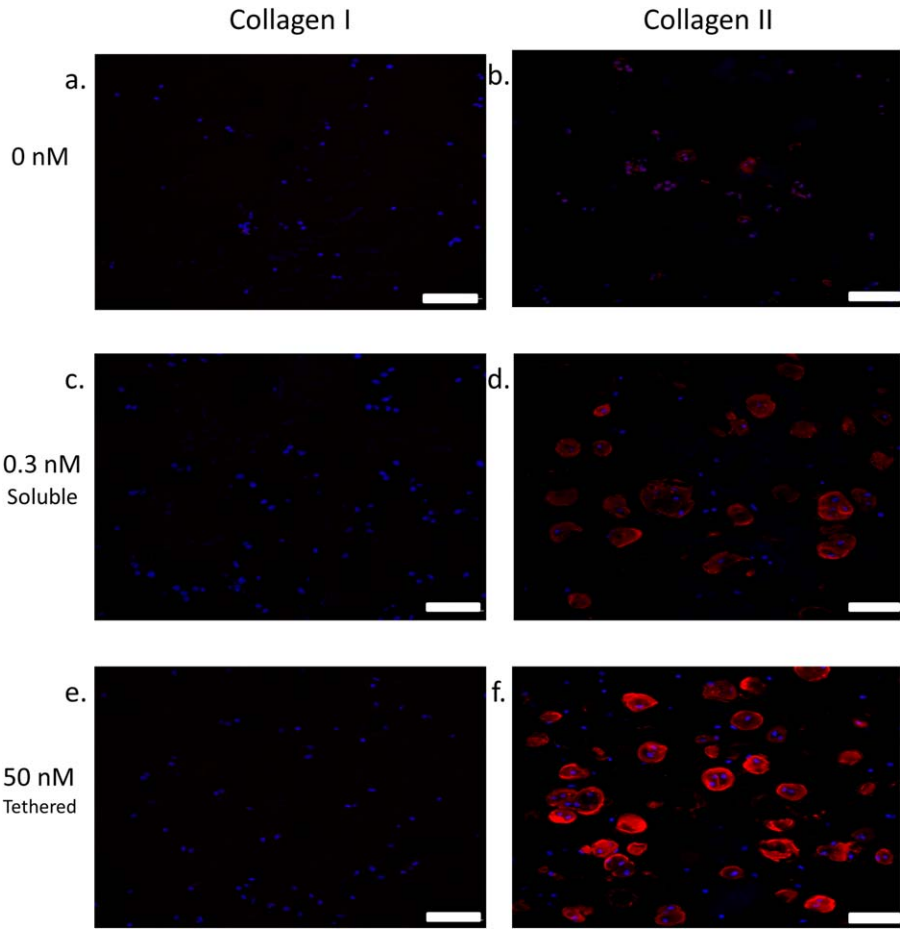

FIGURE 6. Collagen I *versus* collagen II distribution in constructs. Gels seeded with chondrocytes at 40 million cells/mL were cryosectioned at day 28. Immunohistochemistry analysis reveals collagen type distribution in scaffolds. (a) 0 n*M* with collagen I, (b) 0 n*M* with collagen II, (c) 0.3 n*M* (soluble) with collagen I, (d) 0.3 n*M* (soluble) with collagen II, (e) 50 n*M* (tethered) with collagen I, (f) 50 n*M* (tethered) with collagen II. Sections were stained red for both anti-collagen I and anti-collagen II antibodies and were counterstained with DAPI (blue) for cell nuclei. Scale bars represent 50 μm.

signaling to encapsulated cells. We showed that tethered TGF-β1 increased the proliferation rate and ECM production of chondrocytes over a 28-day period, at levels exceeding that of cells in gels where TGF-β1 was dosed in the culture medium or those that were untreated. The tethered TGF-β hydrogels utilized a lower total protein dosage while still promoting high levels of proliferation and matrix production of chondrocytes. Furthermore, chondrocytes maintained a spherical morphology in the thiol-ene PEG gels with high viability and a phenotype that resembles articular cartilage (i.e. high collagen II and low collagen I levels). Collectively, these results demonstrate the feasibility of delivering bioactive protein signals in a 3D culture platform to enhance matrix production of chondrocytes. This platform may have further applications as a scaffold for *in vivo* cartilage regeneration.

ACKNOWLEDGMENTS

The authors acknowledge Dr. Xuedong Liu for the PE-25 cells. The authors also acknowledge Dr. William Wan, Dr. Huan Wang, Dr. Justine Roberts, and Stacey Skaalure for assistance on experimental design, as well as Dr. Malar Azagarsamy for help with NMR characterization of the macromolecules.

REFERENCES

1. Hunziker EB. Articular cartilage repair: basic science and clinical progress. A review of the current status and prospects. Osteoarthritis Cartilage 2002;10:432–63.
2. Holland TA, Mikos AG. Advances in drug delivery for articular cartilage. J. Controlled Release 2003;86:1–14.
3. Chen FH, Rousche KT, Tuan RS. Technology Insight: adult stem cells in cartilage regeneration and tissue engineering. Nat Clin Pract Rheumatol 2006;2:373–382.
4. Jackson DW, Simon TM. Tissue engineering principles in orthopaedic surgery. Clin Orthop Relat Res 1999;(367 Suppl): S31–S45.
5. Masters KS. Covalent growth factor immobilization strategies for tissue repair and regeneration. Macromol Biosci 2011;11: 1149–1163.
6. Tayalia P, Mooney DJ. Controlled growth factor delivery for tissue engineering. Adv Mater 2009;21:3269–3285.
7. Zhao W, Jin X, Cong Y, Liu Y, Fu J. Degradable natural polymer hydrogels for articular cartilage tissue engineering. J Chem Technol Biotechnol 2012;88:327–339.
8. Kock L, van Donkelaar CC, Ito K. Tissue engineering of functional articular cartilage: The current status. Cell Tissue Res 2012;347: 613–627.

9. Spiller KL, Maher SA, Lowman AM. Hydrogels for the repair of articular cartilage defects. Tissue Eng Part B 2011;17:281–299.
10. Bryant SJ, Anseth KS. Hydrogel properties influence ECM production by chondrocytes photoencapsulated in poly(ethylene glycol) hydrogels. J Biomed Mater Res 2002;59:63–72.
11. Sharma B, Fermanian S, Gibson M, Unterman S, Herzka D, Cascio B, Coburn J, Hui A, Marcus N, Gold G, Elisseeff J. Human cartilage repair with a photoreactive adhesive-hydrogel composite. Sci Transl Med 2013;5:167–173.
12. Lee SJ. Cytokine delivery and tissue engineering. Yonsei Med J 2000;41:704–719.
13. Park H, Temenoff JS, Holland TA, Tabata Y, Mikos AG. Delivery of TGF-beta1 and chondrocytes via injectable, biodegradable hydrogels for cartilage tissue engineering applications. Biomaterials 2005;26:7095–103.
14. Hume PS, He J, Haskins K, Anseth KS. Strategies to reduce dendritic cell activation through functional biomaterial design. Biomaterials 2012;33:3615–3625.
15. Deforest CA, Anseth KS. Photoreversible patterning of biomolecules within click-based hydrogels. Angew Chem Int Ed Engl 2012;51:1816–1819.
16. Aimetti AA, Machen AJ, Anseth KS. Poly(ethylene glycol) hydrogels formed by thiol-ene photopolymerization for enzyme-responsive protein delivery. Biomaterials 2009;30:6048–6054.
17. Benton JA, Fairbanks BD, Anseth KS. Characterization of valvular interstitial cell function in three dimensional matrix metalloproteinase degradable PEG hydrogels. Biomaterials 2009;30:6593–6603.
18. Fairbanks BD, Schwartz MP, Halevi AE, Nuttelman CR, Bowman CN, Anseth KS. A versatile synthetic extracellular matrix mimic via thiol-norbornene photopolymerization. Adv Mater 2009;21: 5005–5010.
19. Fairbanks BD, Schwartz MP, Bowman CN, Anseth KS. Photoinitiated polymerization of PEG-diacrylate with lithium phenyl-2,4,6-trimethylbenzoylphosphinate: polymerization rate and cytocompatibility. Biomaterials 2009;30:6702–6707.
20. McCall JD, Luoma JE, Anseth KS. Covalently tethered transforming growth factor beta in PEG hydrogels promotes chondrogenic differentiation of encapsulated human mesenchymal stem cells. Drug Deliv Transl Res 2012;2:305–312.
21. McCall JD, Anseth KS. Thiol-ene photopolymerizations provide a facile method to encapsulate proteins and maintain their bioactivity. Biomacromolecules 2012;13:2410–2417.
22. Huey D, Hu J, Athanasiou K. Unlike bone, cartilage regeneration remains elusive. Science 2012;6933:917–921.
23. Roberts JJ, Bryant SJ. Comparison of photopolymerizable thiol-ene PEG and acrylate-based PEG hydrogels for cartilage development. Biomaterials 2013;34:9969–9979.
24. Li T, O'Keefe R, Chen D. TGF-β signaling in chondrocytes. Front Biosci 2005;10:681–688.
25. Clarke DC, Brown ML, Erickson RA, Shi Y, Liu X. Transforming growth factor beta depletion is the primary determinant of Smad signaling kinetics. Mol Cell Biol 2009;29:2443–2455.
26. Yoo JJ, Bichara DA, Zhao X, Randolph MA, Gill TJ. Implant-assisted meniscal repair in vivo using a chondrocyte-seeded flexible PLGA scaffold. J Biomed Mater Res A 2011;99:102–108.
27. Byers BA, Mauck RL, Chiang IE, Tuan RS. Transient exposure to transforming growth factor beta 3 under serum-free conditions enhances the biomechanical and biochemical maturation of tissue-engineered cartilage. Tissue Eng Part A 2008;14:1821–1834.
28. Chua KH, Aminuddin BS, Fuzina NH, Ruszymah BHI. Insulin-transferrin-selenium prevent human chondrocyte dedifferentiation and promote the formation of high quality tissue engineered human hyaline cartilage. Eur Cell Mater 2005;9:58–67.
29. Ruan J-L, Tulloch NL, Muskheli V, Genova E, Mariner PD, Anseth KS, Murry CE. An improved cryosection method for polyethylene glycol hydrogels used in tissue engineering. Tissue Eng. Part C. Methods 2013;19:794–801.
30. Kim Y-J, Sah RLY, Doong J-YH, Grodzinsky AJ. Fluorometric assay of DNA in cartilage explants using Hoechst 33258. Anal Biochem 1988;174:168–176.
31. Farndale RW, Sayers CA, Barrett AJ. A direct spectrophotometric microassay for sulfated glycosaminoglycans in cartilage cultures. Connect Tissue Res 1982;9:247–248.
32. Woessner JF. The determination of hydroxyproline in tissue and protein samples containing small proportions of this imino acid. Arch Biochem Biophys 1961;93:440–447.
33. Ballock RT, O'Keefe RJ. The biology of the growth plate. J Bone Joint Surg 2003;85:715–726.
34. Passaretti D, Silverman RP, Huang W, Kirchhoff CH, Ashiku S, Randolph MA, Yaremchuk MJ. Cultured chondrocytes produce injectable tissue-engineered cartilage in hydrogel polymer. Tissue Eng 2001;7:805–815.
35. Burdick JA, Chung C, Jia X, Randolph MA, Langer R. Controlled degradation and mechanical behavior of photopolymerized hyaluronic acid networks. Biomacromolecules 2005;6:386–391.
36. Ibusuki S, Papadopoulos A, Ranka M, Halbesma G, Randolph MA, Redmond R, Kochevar I, Gill T. Engineering Cartilage in a Photochemically Crosslinked Collagen Gel. J. Knee Surg. 2010;22:72–81.
37. Zwaagstra JC, El-Alfy M, O'Connor-McCourt MD. Transforming growth factor (TGF)-beta 1 internalization: modulation by ligand interaction with TGF-beta receptors types I and II and a mechanism that is distinct from clathrin-mediated endocytosis. J Biol Chem 2001;276, 27237–27245.
38. Shi Y, Massagué J. Mechanisms of TGF-beta signaling from cell membrane to the nucleus. Cell 2003;113:685–700.
39. Derynck R, Jarrett JA, Chen EY, Eaton DH, Bell JR, Assoian RK, Roberts AB, Sporn MB, Goeddel DV. Human transforming growth factor-beta complementary DNA sequence and expression in normal and transformed cells. Nature 1985;316:701–705.
40. Lin Z, Willers C, Xu J, Zheng M-H. The chondrocyte: Biology and clinical application. Tissue Eng 2006;12:1971–1984.
41. Jin RL, Park SR, Choi BH, Min B-H. Scaffold-free cartilage fabrication system using passaged porcine chondrocytes and basic fibroblast growth factor. Tissue Eng. Part A 2009;15: 1887–1895.
42. Baghaban Eslaminejad M, Taghiyar L, Falahi F. Quantitative analysis of the proliferation and differentiation of rat articular chondrocytes in alginate 3D culture. Iran Biomed J 2009;13: 153–160.
43. Skaalure SC, Milligan IL, Bryant SJ. Age impacts extracellular matrix metabolism in chondrocytes encapsulated in degradable hydrogels. Biomed Mater 2012;7:1–13.
44. Park Y, Lutolf MP, Hubbell JA, Hunziker EB, Wong M. Bovine primary chondrocyte culture in synthetic matrix hydrogels as a scaffold for cartilage repair. Tissue Eng 2004;10:515–522.
45. Roberts JJ, Nicodemus GD, Greenwald EC, Bryant SJ. Degradation improves tissue formation in (un)loaded chondrocyte-laden hydrogels. Clin Orthop Relat Res 2011;469:2725–2734.

Materials Views
www.MaterialsViews.com

ADVANCED HEALTHCARE MATERIALS
www.advhealthmat.de

Development of a Cellularly Degradable PEG Hydrogel to Promote Articular Cartilage Extracellular Matrix Deposition

Balaji V. Sridhar, John L. Brock, Jason S. Silver, Jennifer L. Leight, Mark A. Randolph, and Kristi S. Anseth**

Healing articular cartilage remains a significant clinical challenge because of its limited self-healing capacity. While delivery of autologous chondrocytes to cartilage defects has received growing interest, combining cell-based therapies with scaffolds that capture aspects of native tissue and promote cell-mediated remodeling could improve outcomes. Currently, scaffold-based therapies with encapsulated chondrocytes permit matrix production; however, resorption of the scaffold does not match the rate of production by cells leading to generally low extracellular matrix outputs. Here, a poly (ethylene glycol) (PEG) norbornene hydrogel is functionalized with thiolated transforming growth factor (TGF-β1) and cross-linked by an MMP-degradable peptide. Chondrocytes are co-encapsulated with a smaller population of mesenchymal stem cells, with the goal of stimulating matrix production and increasing bulk mechanical properties of the scaffold. The co-encapsulated cells cleave the MMP-degradable target sequence more readily than either cell population alone. Relative to non-degradable gels, cellularly degraded materials show significantly increased glycosaminoglycan and collagen deposition over just 14 d of culture, while maintaining high levels of viability and producing a more widely-distributed matrix. These results indicate the potential of an enzymatically degradable, peptide-functionalized PEG hydrogel to locally influence and promote cartilage matrix production over a short period. Scaffolds that permit cell-mediated remodeling may be useful in designing treatment options for cartilage tissue engineering applications.

1. Introduction

Articular cartilage has limited self-healing properties, in part due to its lack of innervation and vascularization, and cartilage repair remains a significant clinical challenge. Cartilage is composed primarily of specialized extracellular matrix (ECM) components that absorb water and maintain the structure of the tissue. Chondrocytes are the sole, differentiated resident cells found in mature articular cartilage and are responsible for the generation and maintenance of this ECM.[1]

As a result of its low cellularity and absence of stimulating growth factors provided by vasculature, cartilage exhibits a low rate of regeneration; hence, focal lesions caused by trauma or joint disorders can lead to debilitating osteoarthritis.[2] Matrix-assisted autologous chondrocyte transplantation (MACT) involves encapsulating autologous chondrocytes into a tunable scaffold to promote increased matrix synthesis, which is then implanted into a cartilage defect of a patient.[3] A variety of natural and synthetic materials have been examined as potential cell carriers and as therapeutic agents for cartilage repair.[4–7]

Despite advances in MACT, a limitation with many of the scaffold carriers is that their resorption rates do not necessarily match the rate of matrix deposition by encapsulated cells (i.e., what is observed in healthy native tissue).[8] In the case of hydrogel carriers, synthetic materials often limit deposition of chondrocyte-secreted matrix molecules to the space around the cell, also known as the pericellular space.[9] In order to

B. V. Sridhar, J. L. Brock, J. S. Silver, Prof. J. L. Leight, Prof. K. S. Anseth
Department of Chemical and Biological Engineering
and the Biofrontiers Institute
University of Colorado
596 UCB, Boulder, CO 80303–0596, USA
E-mail: kristi.anseth@colorado.edu
Prof. J. L. Leight
Department of Biomedical Engineering and Comprehensive Cancer Center
The Ohio State University
291 Bevis Hall, Columbus, OH 43210, USA
Prof. J. L. Leight, Prof. K. S. Anseth
The Howard Hughes Medical Institute
University of Colorado
596 UCB, Boulder, CO 80303–1904, USA
M. A. Randolph
Department of Orthopaedic Surgery
Laboratory for Musculoskeletal Tissue Engineering
Massachusetts General Hospital
Harvard Medical School
55 Fruit St., WAC 435, Boston, MA 02114, USA
E-mail: randolph.mark@mgh.harvard.edu
M. A. Randolph
Division of Plastic Surgery
Plastic Surgery Research Laboratory
Massachusetts General Hospital
Harvard Medical School
15 Parkman St., WACC 453, Boston, MA 02114, USA

DOI: 10.1002/adhm.201400695

overcome this issue, current synthetic hydrogels are engineered to hydrolytically degrade at physiologic pH, and while bulk degradation is readily engineered and controlled, numerous material properties are highly coupled to this degradation. For example, high extents of degradation must occur before collagen can assemble throughout hydrogel scaffolds, but this often coincides with a precipitous drop in gel mechanics.[9,10] Alternatively, hydrogels derived from native matrix components (e.g., collagen, hyaluronan) can be degraded by cells, and this leads to a local degradation mechanism where the rate is dictated by the cells. However, it is often more challenging to control the degradation and mechanical properties of these materials, which can necessitate synthetic modification to these materials to control their time varying properties.[11,12] As a result, recent efforts in the field have focused on hybrid synthetic ECM-mimics that can capture the tunability of synthetic scaffolds while integrating the properties of a cell-dictated local degradation.

In this work, we explored the application of a peptide- and protein-functionalized poly (ethylene glycol) (PEG) hydrogel for chondrocyte encapsulation and cartilage regeneration. PEG is a hydrophilic polymer that has been broadly explored for cell delivery applications.[13–16] We formed biologically active PEG hydrogels through a photoinitiated step-growth polymerization scheme, by reacting four-arm norbornene-terminated PEG macromolecules with a non-degradable PEG dithiol linker or a bis-cysteine collagenase-sensitive peptide cross-linker, KCGPQG↓IWGQCK (where the arrow indicates cleavage site).[17] This thiolene photopolymerization allows for precise spatial and temporal control over polymer formation, as well as facile encapsulation of cells and biologics.[18] Multiple studies have shown the resulting cross-linked PEG hydrogel can encapsulate numerous primary cells with high survival rates (>90%) following photoencapsulation.[19,20]

Previous work in our group further demonstrated that chondrocyte ECM production is enhanced in the presence of locally tethered transforming growth factor (TGF-β1) in a non-degradable PEG network; however, matrix deposition was limited to the pericellular space.[21] These results motivated the experiments reported here, where we study how tethered TGF-β1 in concert with a cellullarly degradable peptide cross-linker influences cartilage ECM production and its distribution. Since degradation of collagen is a rate-limiting step in cartilage remodeling, as it is the most abundant component of the ECM,[22] we selected a peptide linker derived from collagen, KCGPQG↓IWGQCK. Previously, Lutolf and Hubbell [23] encapsulated chondrocytes in a PEG gel linked with this peptide and found increased gene expression of cartilage matrix molecules compared to non-degradable gels; however, matrix deposition was pericellularly restricted,[24] suggesting that proper degradation did not occur to permit wide-spread ECM deposition. As chondrocytes release both MMP-8[25] and MMP-13,[26] which are known to cleave this sequence, they are not highly metabolically active.[27] We hypothesize that when these primary cells differentiate from their stem cell origin, their low metabolic activity translates to very slow degradation of MMP-cleavable scaffolds.

To catalyze this pericellular degradation process, we examine the MMP activity of chondrocytes and explore the co-encapsulation of chondrocytes with mesenchymal stem cells (MSCs) to aid in scaffold remodeling. In complementary migration experiments, MSCs have been shown to readily degrade the KCGPQG↓IWGQCK sequence when encapsulated in similar PEG gels.[28] Furthermore, Bahney et al.[29] incorporated a collagen-derived peptide linker into PEG hydrogels to encourage chondrogenesis of MSCs. In addition to catalyzing degradation of the target peptide linker, MSCs co-encapsulated with chondrocytes can also stimulate matrix deposition and reduce hypertrophy of chondrocytes.[30] Furthermore, in clinical settings, a low density of MSCs has the potential to migrate into a PEG MACT scaffold when combined with a procedure like microfracture surgery, which stimulates MSC migration.[31]

In this work, we report the development of a MMP-sensitive PEG-based hydrogel that employs co-culture of MSCs and chondrocytes to suggest that local degradation facilitates diffuse ECM deposition. This multifunctional scaffold is further engineered to present TGF-β1 to encourage matrix deposition by both chondrocytes[21] and MSCs.[32] MSCs are seeded at a low density to facilitate degradation of the linker, while allowing us to design experiments focused on ECM secretion by co-encapsulated chondrocytes. Other common co-culture studies utilize much higher ratios of MSCs to chondrocytes.[30,33] Additionally, we demonstrate in situ degradation by encapsulated cells utilizing a fluorogenic peptide, assess construct matrix deposition both qualitatively and quantitatively, and show increased scaffold mechanical integrity over 14 d.

2. Results

2.1. Chondrocyte Cleavage of the MMP-Degradable Sequence in 3D Monoculture

We confirmed in situ degradation of the peptide linker sequence (KCGPQG↓IWGQCK) utilizing a fluorogenic peptide sensor (Dab-GGPQG↓IWGQK-Fl-AhxC)[34] that was covalently tethered to the gel network. **Figure 1**a shows a four-arm PEG-NB hydrogel formulation, which includes tethered TGF-β1 (50×10^{-9} M), and fluorogenic peptide sensor (0.5×10^{-3} M), for experiments used to determine the amount of cleavage of the MMP-sensitive sequence. We chose the chondrocyte seeding density of 40 million cells mL^{-1}, because chondrocytes have been studied at this density and shown to produce native-like tissue at this concentration in 3D experiments.[35–37] Over a 3 d period, we found that chondrocytes seeded at this density degrade the MMP-degradable sequence at a higher rate than either a chondrocyte-laden non-degradable or acellular gel of the same formulation as shown in Figure 1b. However, when chondrocytes were encapsulated and cultured long term in this formulation, glycosaminoglycan (GAG) (Figure 1c) and collagen (Figure 1d) distribution was limited to the pericellular space in degradable, cell-laden constructs, even after 28 d. Even at a shorter culture time of 7 d, the chondrocytes alone do not significantly degrade the surrounding network, which restricts matrix deposition to the pericellular spaces (Figure S2, Supporting Information).

DOI: 10.1002/adhm.201400695

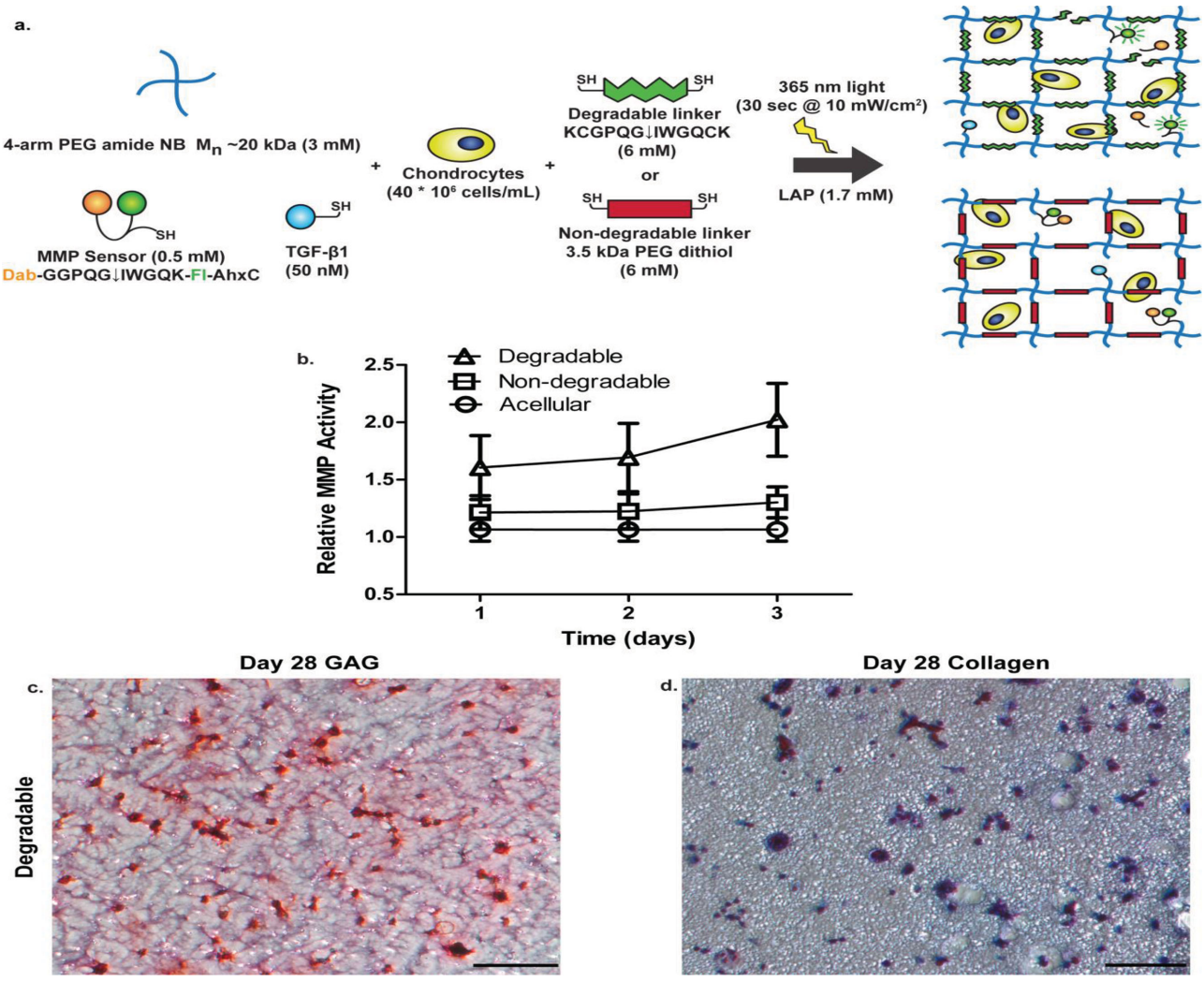

Figure 1. Effect of chondrocytes encapsulated in an MMP-degradable gel. a) Schematic of four-arm 20 kDa PEG norbornene network with tethered MMP fluorescent sensor (Dab- GGPQG↓IWGQK-Fl-AhxC), and TGF-β1. The macromer solution, containing tethered growth factor, is combined with chondrocytes at 40 million cells mL^{-1}. Resultant networks are either cross-linked by an MMP-degradable peptide sequence (KCGPQG↓IWGQCK) or non-degradable (3.5 kDa PEG dithiol) linker for in situ cleavage experiments. b) Measurement of in situ cleavage of fluorescent sensor by chondrocytes. Over 3 d, acellular and chondrocyte-laden nondegradable gels had similar normalized fluorescent activity, but in a degradable gel, chondrocytes had higher fluorescent activity (where A.U. stands for arbitrary units) suggesting cleavage of the sequence. Results are presented as mean ± SD (n = 3). c) GAG staining of sections obtained at day 28 with chondrocytes seeded in degradable gels at 40 million cells mL^{-1} with nuclei stained black and GAGs stained red. d) Collagen staining of sections obtained at day 28 with chondrocytes seeded in degradable gels at 40 million cell mL^{-1} with nuclei stained black and collagen stained blue. Scale bars represent 100 μm.

2.2. Utilization of Co-culture to Aid in Degradation of the MMP-Sensitive Sequence

Since chondrocytes alone could not cleave this particular MMP-degradable sequence at a rate that permitted diffuse matrix production, we investigated the use of co-culture with MSCs, as we had previous experience with high levels of degradation of this sequence over shorter time scales.[28,38] **Figure 2**a shows a four-arm PEG-NB hydrogel formulation, which includes tethered TGF-β1 (50×10^{-9} M), RGD (1×10^{-3} M), and the fluorogenic peptide sensor (0.5×10^{-3} M) with varying amounts of encapsulated MSCs and a fixed density of chondrocytes, for experiments used to determine cleavage of the MMP-sensitive sequence. Using the same hydrogel formulation over a 3 d period, we found that not only do MSCs seeded at a lower density than chondrocytes degrade the sequence at a faster rate, but there also seems to be a synergistic effect between MSCs and chondrocytes to degrade the sequence at a significantly higher rate. As shown in Figure 2b, MSCs seeded at 5 million cells mL^{-1} cleaved the target sequence faster than chondrocytes seeded at 40 million cells mL^{-1} with increasing relative fluorescent activity. Interestingly, when encapsulated in co-culture with a 24:1 chondrocyte: MSC ratio, with chondrocytes held constant at a density of 40 million cells mL^{-1}, the cells increased the amount of cleavage of the target sequence compared to either cell type alone. At each time point, the co-culture (8:1) gel (40 million

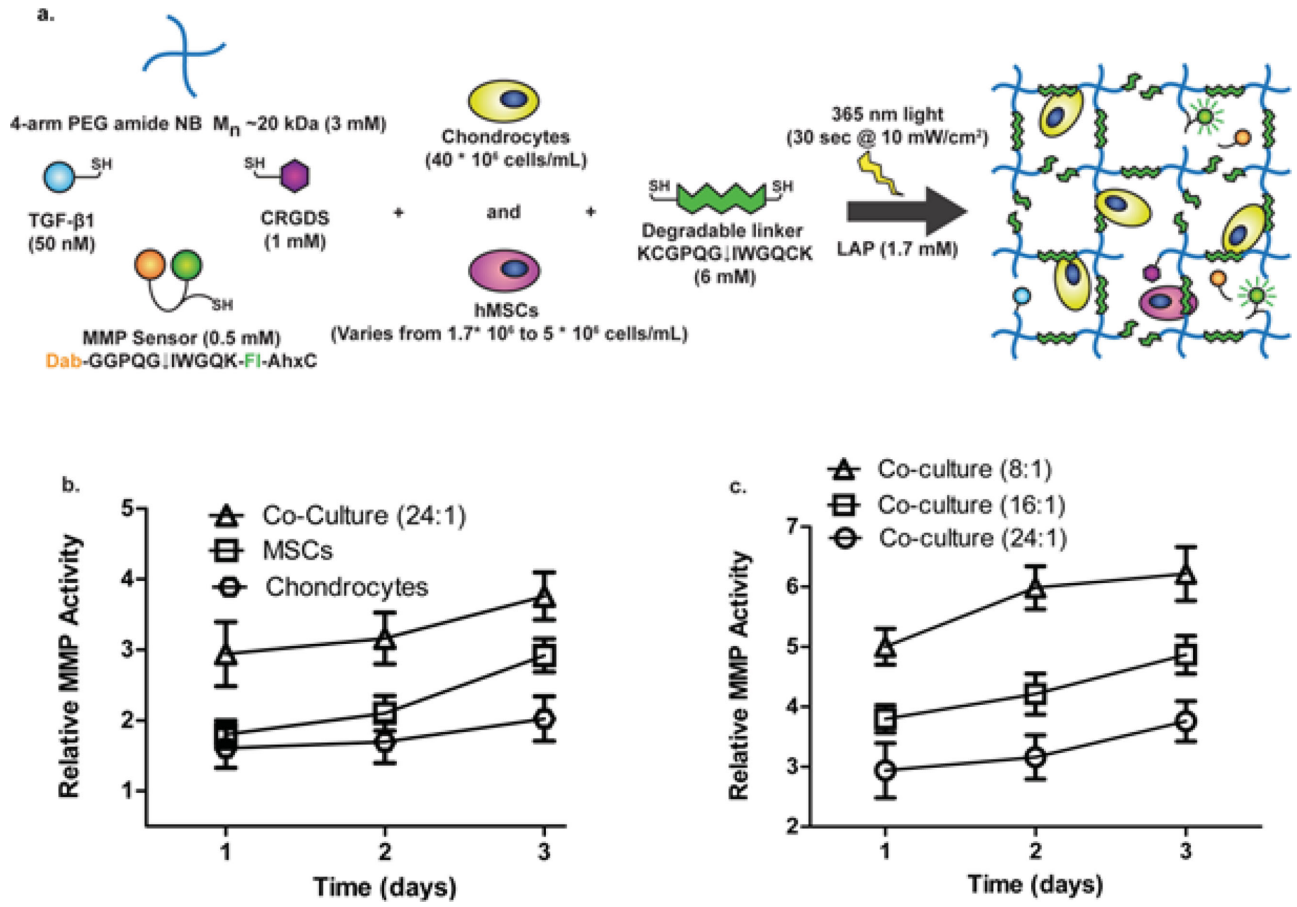

Figure 2. Effect of co-culture of chondrocytes and MSCs on degradation of MMP-sensitive sequence. a) Schematic of four-arm 20 kDa PEG norbornene network with tethered TGF-β1, RGD, and MMP fluorescent sensor (Dab-G GPQG↓IWGQK-Fl-AhxC) cross-linked by an MMP degradable peptide sequence (KCGPQG↓IWGQCK). Chondrocytes were encapsulated at a fixed seeding density of 40 million cell mL^{-1}, and the density of MSCs varied from 1.7 to 5 million cells mL^{-1} during the co-encapsulation process for in situ cleavage experiments to measure the effect of co-culture on local degradation. b) After 3 d, chondrocytes, at 40 million cells mL^{-1}, have a lower fluorescent signal than MSCs, at 5 million cells mL^{-1}, in degradable gels. Fluorescent signal is highest from day 1 to 3 when cells are co-encapsulated at a ratio of 24:1 chondrocytes: MSCs (40×10^6 chondrocytes mL^{-1} + 1.67×10^6 MSCs mL^{-1}). c) By varying the ratio of chondrocytes to MSCs, and keeping the chondrocyte seeding density constant at 40 million cells mL^{-1}, it was found after 3 d, 8:1 yielded the highest amount of degradation out of the tested conditions and was used for subsequent matrix deposition experiments. The MMP activity of each group is significantly different from each other at each timepoint ($p < 0.05$) with the 8:1 condition generating the highest MMP activity. Results are presented as mean ± SD ($n = 3$).

chondrocytes mL^{-1} + 5 million MSCs mL^{-1}) MMP activity value was significantly higher than a simple additive effect (from the single-cell cultures), suggesting there is indeed a synergistic effect of the co-culture on MMP activity.

In order to determine an appropriate seeding density of MSCs to use in co-culture with chondrocytes in the matrix deposition experiments, we varied the encapsulation ratio of chondrocytes to MSCs. In Figure 2c, we show that when chondrocytes are held constant at 40 million cells mL^{-1} and the concentration of MSCs is increased in the scaffold incrementally, there is a resultant increase in cleavage of the target sequence. There is a statistically significant difference between each of the co-culture groups in Figure 2c at each time point ($p < 0.05$) with the 8:1 gel generating the highest MMP activity. Since the lowest ratio of 8:1 chondrocyte:MSC condition yielded the highest fluorescent signal over 3 d, we decided to use this cell ratio for all subsequent experiments.

2.3. Viability of Cells and Morphology of MSCs in Co-culture Scaffolds

Cell viability for both non-degradable and degradable co-culture gel conditions was assessed by a live/dead membrane integrity assay at both day 1 (**Figure 3**a) and 14 (Figure S3, Supporting Information). Nondegradable gels had a viability of 92 ± 2% at day 1 and 95 ± 4% at day 14. Degradable gels had a viability of 93 ± 3% at day 1 and 96 ± 2% at day 14 as determined by image quantification where results are presented as mean ± SD ($n = 3$). Since both conditions looked very similar, only the viability results of the degradable condition are shown in this article. In addition to assessing viability, we observed the morphology of MSCs present in the scaffold to see if they maintained a rounded shape to suggest a more chondrogenic phenotype[27] as opposed to an osteogenic phenotype with a more fibroblastic appearance.[38] As shown in Figure 3a,

DOI: 10.1002/adhm.201400695

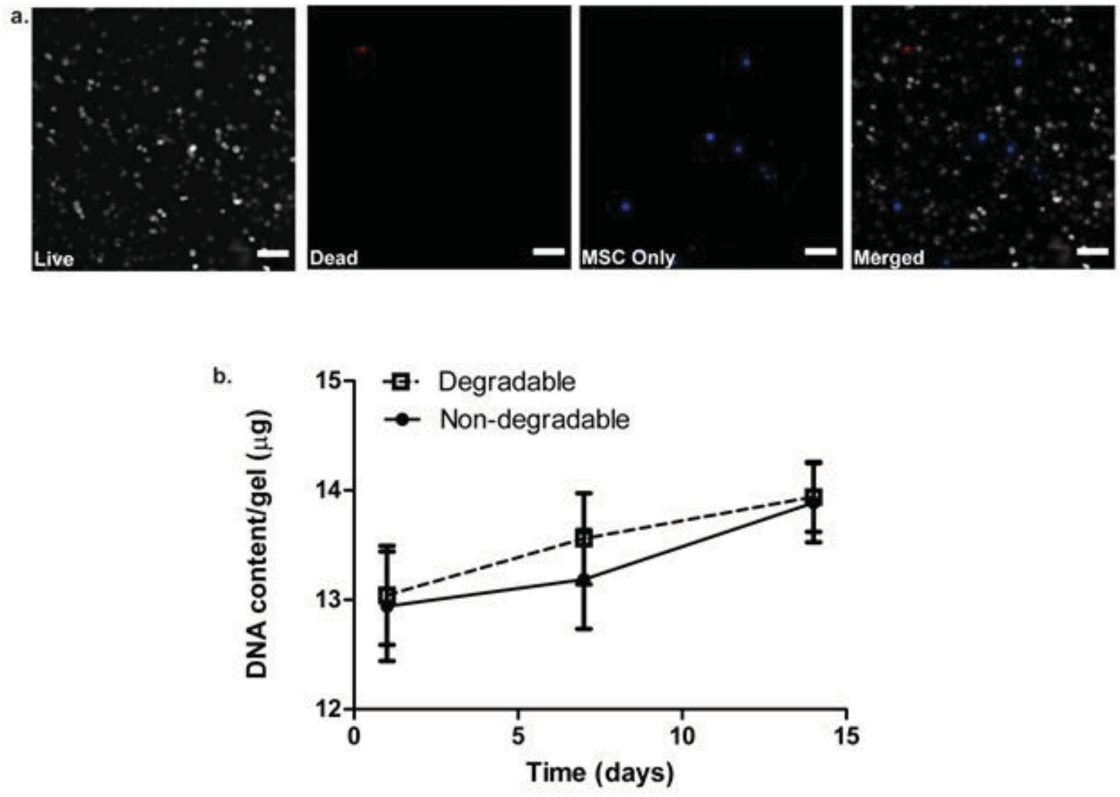

Figure 3. Viability, morphology, and cellularity of co-culture system. a) Viability at day 1 with degradable 8:1 co-culture gels with live cells (gray), dead cells (red), MSCs labeled with CellTracker Violet (blue), and all three images merged together. Viability was quantified at 93 ± 3%. Scale bars represent 100 μm. b) DNA content of degradable and non-degradable 8:1 co-culture gels assessed at day 1, 7, and 14. Both degradable and non-degradable conditions show similar DNA content at each time point, but they increase over the 14 d period. Results are presented as mean ± SD ($n = 3$).

viability of both chondrocytes and MSCs was high on day 1. Furthermore, MSCs, which have been labeled with Cell Tracker Violet prior to encapsulation (blue), retained a spherical morphology in spite of being in a degradable system with integrin-binding epitopes. Moreover, DNA content was assessed at day 1, 7, and 14 (Figure 3b). There was no statistically significant difference in cellularity between degradable and non-degradable conditions, as measured by the amount of DNA present, but there was a steady increase in DNA content from day 1 to 14 in both conditions.

2.4. Effect of Local Degradation on Cartilage-Specific Matrix Production and Distribution

We assessed GAG and total collagen content of gels at day 1, 7, and 14 and further examined the distribution of these molecules throughout the network by staining sections with safranin-O (GAG) and Masson's trichrome (collagen). Measured quantities of either non-degradable or degradable co-culture scaffolds were normalized to the wet weight (wet weight values shown in Figure S4a, Supporting Information) of the respective hydrogel formulations. In **Figure 4**a and **Figure 5**a, at day 14, GAG and collagen distribution were restricted to the pericelluar space in nondegradable gels. On the other hand, in Figure 4b and Figure 5b, at day 14, GAG and collagen were widely distributed throughout the gel and connected with other molecules generated by nearby cells. Not only is the visual difference in distribution striking, but it was further confirmed by quantitative analysis. In Figure 4c and Figure 5c, the sGAG and total collagen production as a percentage of the wet weight of the gel on day 7 and 14 for the degradable construct was significantly higher than the nondegradable gel ($p < 0.01$). While cartilage-specific ECM production increases in both conditions over 14 d, it does so at a significantly higher amount in a locally degradable system.

2.5. Effect of Cell-Mediated, Local Degradation on the Mechanical Properties of the Scaffold

To confirm that our degradable system produced functional, cartilage-specific matrix molecules and increased its mechanical properties over time while permitting ECM expansion, we assessed the bulk compressive modulus of cell-laden non-degradable and degradable gels at day 1, 7, and 14. In **Figure 6**, at day 7, and 14, the value of the compressive modulus of the degradable construct was significantly higher than of the non-degradable gel ($p < 0.001$). Furthermore, there was a significant increase ($p < 0.001$) between day 1 and 14 of the compressive modulus in degradable scaffolds while the values between day 1 and 14 were not statistically different

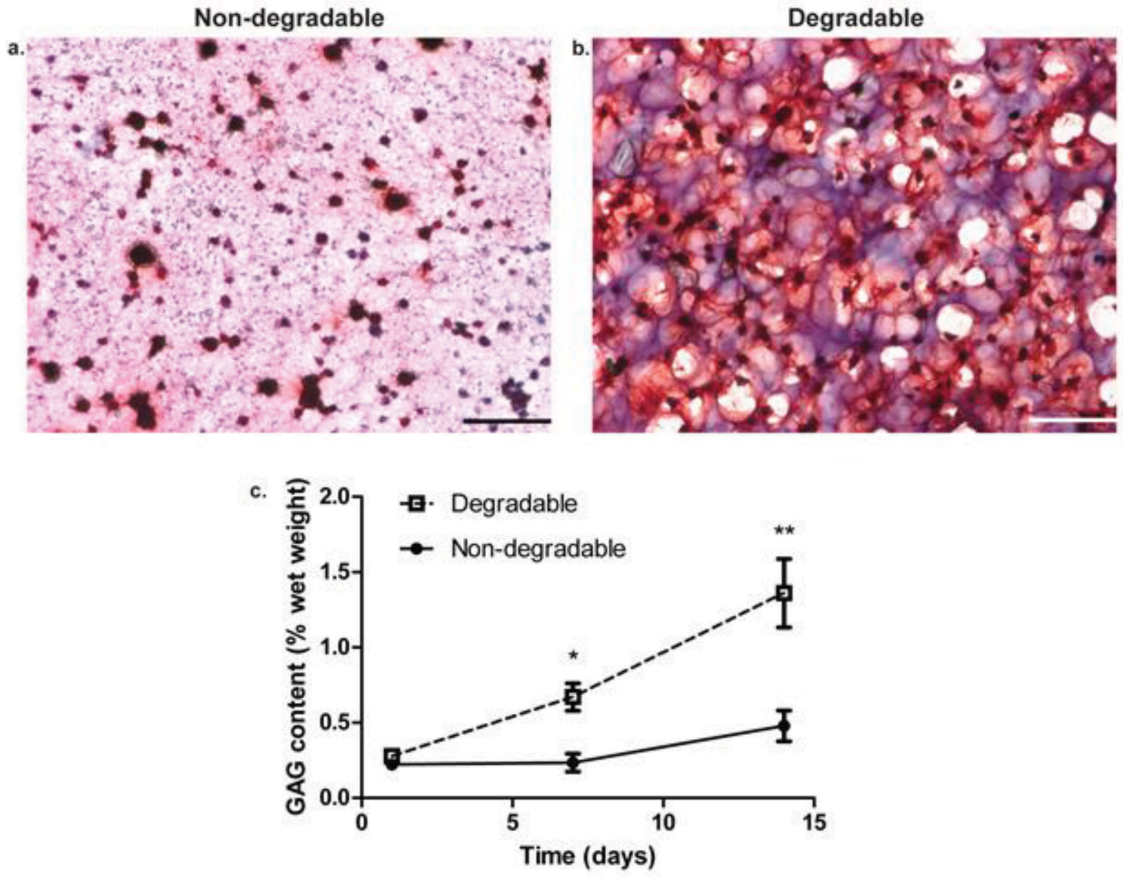

Figure 4. Glycosaminoglycan distribution and production in non-degradable and degradable 8:1 co-culture constructs. a) Non-degradable gel section stained for GAGs at day 14. b) Degradable gel stained for GAGs at day 14 with nuclei stained black and GAGs stained red. Scale bars represent 100 μm. c) GAG content expressed as a percentage of the respective construct wet weight assessed at day 1, 7, and 14. * indicates a statistically significant difference in GAG content at day 7 between degradable and non-degradable gels ($p < 0.01$), and ** indicates a statistically significant difference in GAG content at day 14 between degradable and non-degradable gels ($p < 0.001$). Results are presented as mean ± SD ($n = 3$).

($p > 0.75$) with non-degradable gels even though both conditions have similar values of compressive elastic modulus initially.

2.6. Quality of Composition of ECM in Co-culture Scaffolds

To verify that the ECM produced had an articular cartilage phenotype, we qualitatively assessed the qualitative ratio of type II collagen to type I collagen on gel immunostained sections. Images revealed that at day 14 there was a scarce amount of type I collagen throughout all samples (**Figure 7**a,c). In contrast, type II collagen was more diffusely distributed in the degradable construct (Figure 7d) than in the nondegradable sample, where it was pericellularly restricted and less prevalent (Figure 7b). Quantification of the amount of cells that stained positive for type I and type II collagen with image analysis revealed similar conclusions. As shown in **Table 1**, more cells stained positive for type II collagen in the degradable than the nondegradable sample, and the number of cells staining positive for type II collagen was dramatically higher than type I positive cells for both.

2.7. Effect of Inhibition of MMP Activity on Cartilage-Specific Matrix Production and Distribution

We sought to test the effect of inhibiting MMP secretion by encapsulated cells and observe if the resulting matrix production was similar to non-degradable gels. Figure S1a, Supporting Information shows how the addition of the MMP inhibitor to a co-culture system led to a fluorescent activity level similar to non-degradable gels. Live/Dead staining of gels at day 1 and 14 showed viability greater than 90% (data not shown). Histology staining at day 14 revealed that the co-culture degradable gels treated with the MMP inhibitor had a similar appearance to non-degradable gels with pericellularly limited matrix distribution (Figure S1b,c, Supporting Information). These data show how MMP secretion specifically plays a major role in matrix deposition and remodeling within this system, even more so than TGF-β1 or the co-culture synergistic effects.

3. Discussion

Engineering a clinically viable scaffold for promotion of cartilage regeneration is challenging, partly because of the time

Adv. Healthcare Mater. **2015**,
DOI: 10.1002/adhm.201400695

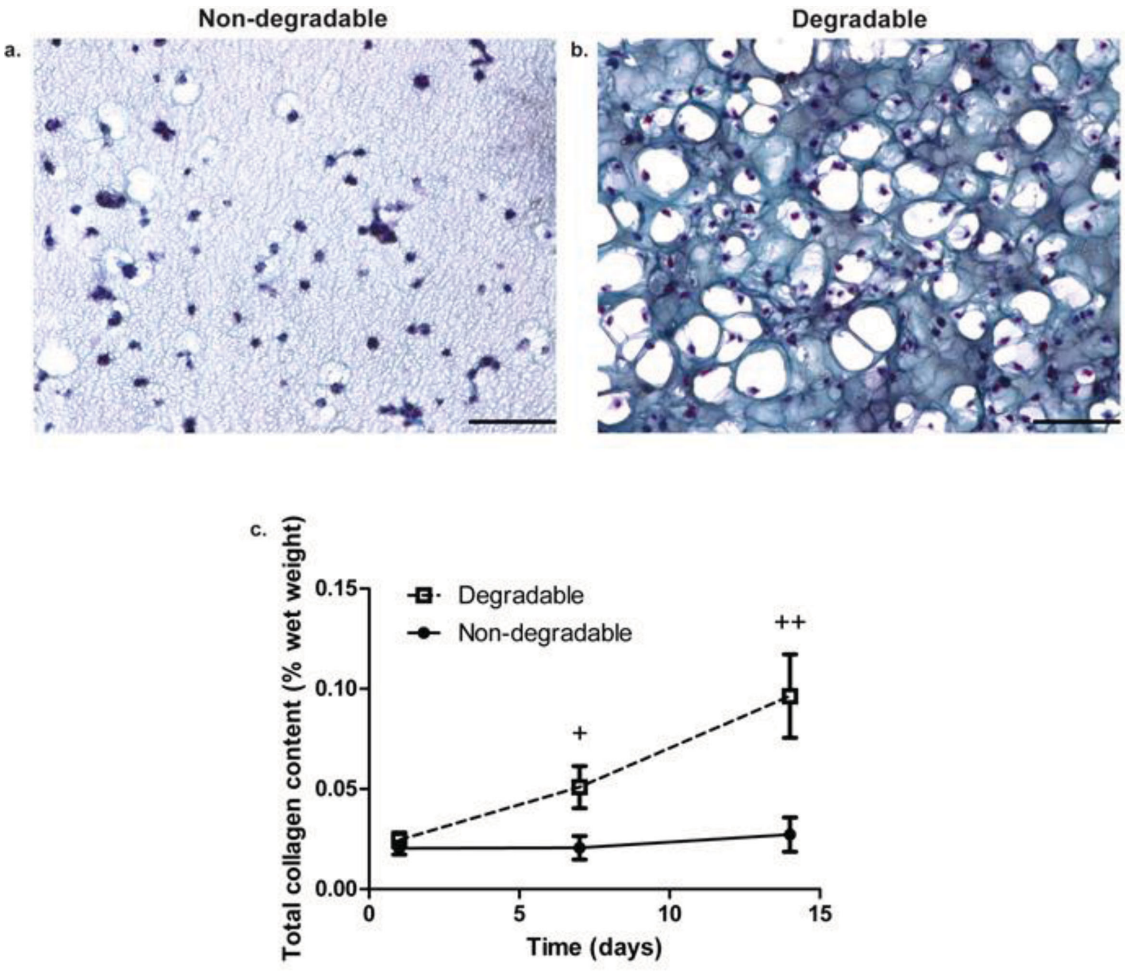

Figure 5. Collagen distribution and production in non-degradable and degradable 8:1 co-culture constructs. a) Non-degradable gel section stained for collagen at day 14. b) Degradable gel stained for collagen at day 14 with nuclei stained black or violet and collagen stained blue. Scale bars represent 100 μm. c) Total collagen content expressed as a percentage of the respective construct wet weight assessed at day 1, 7, and 14. + indicates a statistically significant difference in collagen content at day 7 between degradable and non-degradable gels ($p < 0.05$), and ++ indicates a statistically significant difference in collagen content at day 14 between degradable and non-degradable gels ($p < 0.001$). Results are presented as mean ± SD ($n = 3$).

required to generate a robust matrix by encapsulated cells, especially chondrocytes in monoculture. By utilizing an enzymatically degradable PEG-peptide system with localized presentation of TGF-β1 and co-culture of chondrocytes with MSCs, we have shown quantitatively and qualitatively, in vitro, that encapsulated cells generate highly distributed and elaborate cartilage-specific ECM molecules at a higher rate than in a non-degradable scaffold. This system that responds to cell-mediated cues permits cells to secrete and distribute large matrix molecules that pervade throughout the scaffold and ultimately, should lead to mechanically robust constructs. Furthermore, since the construct utilized the synergistic effects of co-culture (to promote scaffold remodeling) along with the benefits of a tethered growth factor, it expedited ECM generation by encapsulated cells relative to other common cartilage tissue engineering scaffolds.[39,40]

When chondrocytes were encapsulated in PEG gels linked with an MMP-cleavable peptide at 40 million cells mL^{-1}, they produced cartilage tissue that was limited to the pericellular space (Figure 1b,c). This suggests that chondrocytes alone may not sufficiently degrade this particular peptide linker. Chondrocytes have relatively low metabolic activity since they reside in a hypoxic and hyperosmotic environment.[41] This may be part of the reason that the chondrocytes were not observed to secrete MMPs at an appreciable rate in 3D culture.

On the other hand, when encapsulated alone, even at a lower seeding density of 5 million cells mL^{-1}, MSCs degraded the sequence at a higher rate than chondrocytes at 40 million cells mL^{-1}. This is likely because MSCs are more metabolically active than chondrocytes, as MSCs remodel their environments more frequently during development. There appears to be a synergistic effect between encapsulated MSCs and chondrocytes to degrade the sequence as shown in Figure 2b,c. The enhancing effect may be from paracrine signaling between cells to boost each other's activity.[42] This may be more reflective of the native, developing cartilaginous environment, where MSCs and chondrocytes co-exist before all the MSCs differentiate into chondrocytes.[43] Furthermore, MSCs may play a role in cell number in the system, as they are known to drive chondrocyte proliferation in co-culture.[30] Future experiments

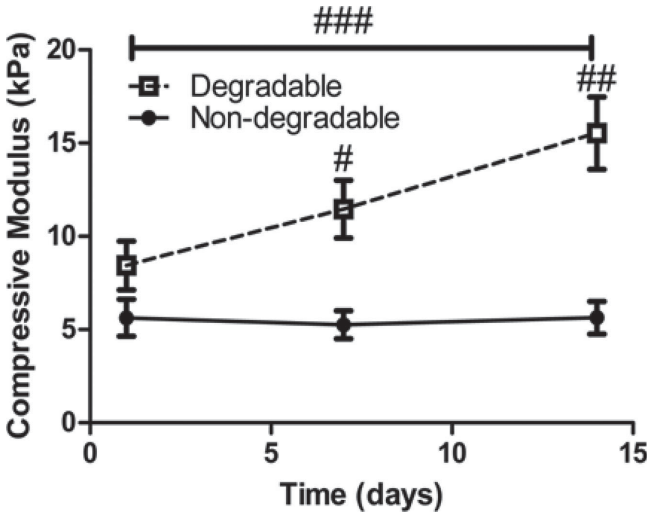

Figure 6. Compressive modulus of constructs assessed at day 1, 7, and 14. # indicates a statistically significant difference in modulus value at day 7 between degradable and non-degradable gels ($p < 0.05$) and ## indicates a statistically significant difference in modulus value at day 14 between degradable and non-degradable gels ($p < 0.001$). The line with ### indicates a statistically significant difference between day 1 and day 14 in moduli values for degradable gels only ($p < 0.001$). Results are presented as mean ± SD ($n = 3$).

could delve deeper into the signaling effects as to why there is increased MMP activity in co-culture between MSCs and chondrocytes. Additionally, studies could look for alternate ways to permit cell-mediated local degradation, which include investigating other peptide-linker sequences that are more amenable to cleavage by chondrocyte-secreted enzymes.

In these experiments, a four-arm 20 kDa PEG backbone at 6 wt% was used for co-culture experiments, since this formulation was studied in the aforementioned MSC experiments to assist in degradation of the peptide linker.[28,38] Other studies investigating the gel cross-link density on matrix production by encapsulated cells found that scaffolds with a lower cross-linking density, like our monomer formulation, best supported ECM deposition in hydrogels.[10,44]

Extracellular matrix production data revealed that over just 14 d, the cell-mediated degradable gels permitted greater and widely distributed matrix production than non-degradable gels as revealed in Figure 4–6. Furthermore, compressive modulus measurements confirmed that degradable constructs had superior mechanical properties relative to non-degradable gels as shown in Figure 6. There is a steadily increasing trend in modulus values over a short period of time, which suggests that the matrix macromolecules generated in the degradable construct assemble in an appropriate fashion to stiffen the mechanical properties of the scaffold.[45] It is interesting to note that there are pockets of space around the cells in the degradable gel histology images, while only a few are present in non-degradable histology images. These pockets have a similar appearance to lacunae found in cartilage and could be due to pericellular degradation of the network. It is evident that cartilage ECM molecule distribution is widespread throughout the degradable scaffold, which likely led to the superior functional mechanical properties of the gel while the pericellularly restricted matrix in the non-degradable gels did not lead to an increased modulus.

The rate at which cartilage matrix molecules are produced and assembled in the locally degradable constructs is substantial. Compared to the bulk degradation mechanism of hydrolytically cleavable PEG-PLA gels that use chondrocytes at 75 million cells mL^{-1},[11] our system produces greater than 2.5 fold increase in GAGs (% wet weight) after 2 weeks while also increasing modulus over time. Furthermore, when compared to a PEG/Chondroitin sulfate copolymer gel with encapsulated chondrocytes at 75 million cells mL^{-1},[40] our system produces greater than sixfold increase in total collagen content (% wet weight) over 2 weeks. Since matrix production is relatively rapid in these constructs, long culture times may not be necessary like they are in conventional cartilage tissue engineering experiments.

There was a concern that encapsulated MSCs in the co-culture system could lead to fibrocartilage formation as they do in monoculture in scaffolds.[46] However, past studies of co-culture scaffolds with higher amounts of MSCs have confirmed that the neotissue generated is not of fibrocartilagenous nature.[33] Furthermore, after a day, MSCs maintain a spherical morphology in co-culture, which could indicate a chondrogenic phenotype as shown in Figure 3a. Additionally, collagen typing (high type II: type I collagen ratio by immunofluorescence) revealed an articular cartilage phenotype with type II collagen being diffusely distributed in degradable gels (Figure 7). Future studies could track the long-term fate of the MSCs in this co-culture system to ensure they maintain a chondrogenic phenotype and do not revert to generating fibrocartilage or bone.

In a potential clinical application as an MACT scaffold, this system could be advantageous due to the low amount of MSCs needed for co-culture. The subchondral bone under the cartilage defect could be stimulated by a technique like microfracture to recruit MSCs into the environment. The chondrocyte-laden PEG construct could then be implanted into the defect and the MSCs could migrate into the gel. Because only a small quantity of MSCs is required to initiate degradation of the target sequence, there is clinical potential with this technique. Furthermore, it is known that increased age of encapsulated chondrocytes can lead to increased MMP activity of the cells.[8] Future studies should focus on optimizing the chondrocyte: MSC seeding ratio and the monomer formulation to further tune the local degradation and enhance ECM production. Additional studies could confirm whether older chondrocytes might degrade this system without the aid of MSCs, and one could test the influence of various localized growth factors (e.g., TGF-β, insulin-like growth factor) on promoting the secretory properties and ECM deposition by aged cells. It would also be interesting to see how matrix production is affected as the length of culture time is extended, especially in an in vivo environment.

4. Conclusion

A cell-mediated degradable hydrogel system based on peptide- and protein-functionalized PEG hydrogels was designed to allow local cell degradation in a manner that promotes wide-spread cartilage ECM production, which ultimately leads

DOI: 10.1002/adhm.201400695

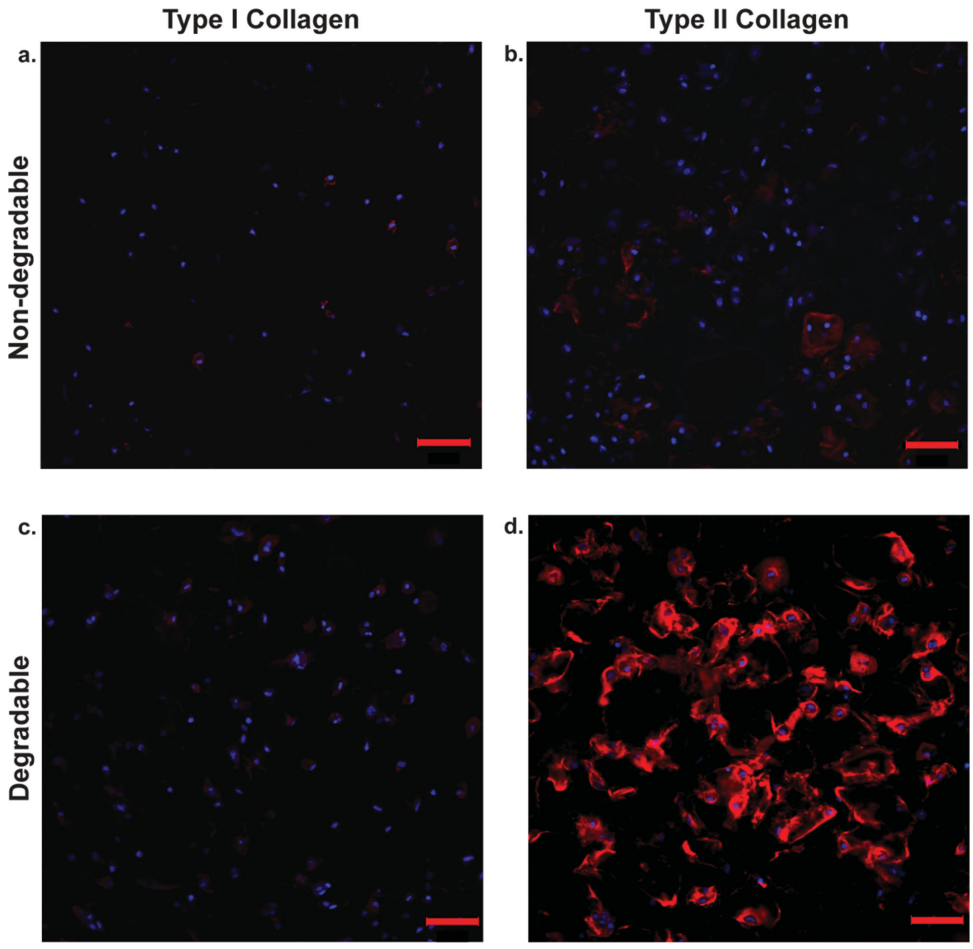

Figure 7. Type I collagen versus type II collagen distribution assessed by immunofluorescence in non-degradable and degradable 8:1 co-culture constructs. a) Non-degradable gel section stained for type I collagen at day 14, b) non-degradable gel section stained for type II collagen at day 14, c) degradable gel section stained for type I collagen at day 14, d) degradable gel stained for type II collagen at day 14. Sections were stained for both anti-collagen type I and anti-collagen type II antibodies (red) and were counterstained with DAPI (blue) for cell nuclei. Scale bars represent 50 μm.

to constructs with improved mechanical properties over just 14 d. The approach exploited the synergistic effects of co-culture between MSCs and chondrocytes to facilitate degradation of a collagen-derived, MMP-degradable peptide sequence (KCGPQG↓IWGQCK) as well as to promote cartilage ECM production in the presence of tethered TGF-β1. Results confirmed that both encapsulated cell types maintained a high viability and a spherical morphology in the gels. Furthermore, the generated ECM resembles articular cartilage with respect to collagen typing by immunofluorescent staining (high type II collagen: type I collagen ratio). Local degradation seems to play a critical role in matrix elaboration with tissue engineering constructs, and non-degradable constructs of the same formulation had significantly less ECM production and lower moduli values over 14 d. This PEG hydrogel system may prove useful in applications as a scaffold for in vivo cartilage regeneration.

5. Experimental Section

PEG Monomer Synthesis: Four-arm PEG amine ($M_n \approx 20\,000$) was modified with norbornene end groups as previously described.[15] Briefly, 5-norbornene-2-carboxylic acid (predominantly endo isomer;

Table 1. Percentage of cells that stained positive for different types of collagen. There is a higher amount of cells that stained positive for type II collagen than type I collagen in both systems. In the degradable system, there is a significantly higher amount of cells that stained positive for type II collagen than there is in the non-degradable system ($p < 0.01$). Results are presented as mean ± SD ($n = 3$).

Percentage of cells that stain positive for type I or type II collagen in gels at day 14			
Non-degradable		Degradable	
Type I collagen	Type II collagen	Type I collagen	Type II collagen
26 ± 6%	53 ± 7%	48 ± 6%	84 ± 4%

Sigma Aldrich) was first converted to a dinorbornene anhydride using *N,N′*-dicyclohexylcarbodiimide (0.5 molar eq. to norbornene; Sigma Aldrich) in dichloromethane. Four-arm PEG amine (JenKem Technology) was then reacted overnight with the norbornene anhydride (5 molar eq. to PEG amines) in dichloromethane. Pyridine (5 molar eq. to PEG amines) and 4-dimethylamino pyridine (0.05 molar eq. to PEG amines) were also included. The reaction was conducted at room temperature under argon. End-group functionalization was verified by ^{1}H NMR (Varian 400 MHz) to be >90%. The photoinitiator lithium phenyl-2,4,6-trimethylbenzoylphosphinate (LAP) was synthesized as described.[20] Peptides were purchased from American Peptide Company, Inc., which included an MMP-degradable cross-linker (KCGPQG↓IWGQCK) and a pendant adhesion peptide sequence derived from fibronectin (CRGDS). The non-degradable 3.5 kDa PEG dithiol linker was purchased from JenKem Technology.

Cell Harvest and Expansion: Primary chondrocytes were isolated from articular cartilage of the femoral-patellar groove of 6-month-old Yorkshire swine as detailed previously.[47] Cells were grown in a T-75 culture flask with media as previously described.[48] Briefly, chondrocytes were grown in growth medium (high-glucose Dulbecco's Modified Eagle's Medium (DMEM) supplemented with ITS+ Premix 1%, v/v (BD Biosciences), 50 mg mL^{-1} L-ascorbic acid 2-phosphate, 40 μg mL^{-1} L-proline, 0.1 × 10^{-6} M dexamethasone, 110 μg mL^{-1} pyruvate, and 1% penicillin-streptomycin-fungizone) with the addition of 10 ng mL^{-1} IGF-1 (Peprotech) to maintain cells in a de-differentiated state. ITS was used because it promotes formation of articular cartilage over serum.[49] Cultures were maintained at 5% CO_2 and 37 °C. Human mesenchymal stem cells (hMSCs) were isolated from bone marrow aspirates (Lonza) as previously described.[28] Cells were grown in low-glucose DMEM supplemented with 10% fetal bovine serum (FBS), 1% penicillin-streptomycin-fungizone, and 1 ng mL^{-1} recombinant human fibroblast growth factor (FGF-2, Peprotech). MSCs that were passaged two times were used for encapsulation experiments.

Hydrogel Formulation and Cell Encapsulation: Human TGF-β1 (Peprotech) was thiolated using 2-iminothiolane (Pierce) as previously described.[32] Briefly 2-iminothiolane was reacted at a 4:1 molar ratio of TGF-β1 for 1 h at RT. Thiolated TGF-β1 was pre-reacted with a PEG norbornene monomer solution prior to cross-linking in the hydrogel formulations at a pre-determined concentration of 50 × 10^{-9} M. This concentration was selected based on previous work, demonstrating a maximal response from chondrocytes seeded at 40 million cells mL^{-1}.[21] Additionally, 1 × 10^{-3} M CRGDS was added to promote survival of the encapsulated MSCs.[50] RGD was not added to the chondrocyte-only system as it has previously been shown to have no impact on chondrocyte metabolic activity.[51] Both growth factors were coupled to PEG norbornene via photoinitiated thiolene polymerization with 1.7 × 10^{-3} M LAP and light (I_0 ≈ 3.5 mW cm^{-2} at λ = 365 nm,ThorLabs M365L2-C2) for 30 s. Subsequently, the monomer solution was cross-linked using a degradable MMP linker (KCGPQG↓IWGQCK, MW ≈ 1800 kDa) or 3.5 kDa PEG dithiol at a 1:1 (thiol:ene) stoichiometric ratio of (12 × 10^{-3} M thiol in either bis-cysteine peptide, or dithiol): (12 × 10^{-3} M norbornene) in a 6 wt% PEG solution using additional light (I_0 ≈ 3.5 mW cm^{-2} at λ = 365 nm, ThorLabs M365L2-C2) for 30 s. For all experiments, 40 μL cylindrical gels (O.D. ≈ 5 mm, height ≈ 2 mm) were formed in the cut end of a 1 mL syringe. Since the degradable MMP linker is synthesized in an acidic solution, the pH of the final solution was adjusted to 7, so as to not interfere with the bioactivity of the tethered TGF-β or the viability of encapsulated cells. Unless otherwise specified, chondrocytes were co-encapsulated at 40 million cells mL^{-1} along with MSCs at 5 million cells mL^{-1} at an 8:1 chondrocyte: MSC ratio in 6 wt% monomer solution with tethered TGF-β and RGD. After gel formation, the cell-laden constructs were immediately placed in 48-well nontreated tissue culture plates with 1 mL DMEM growth medium (without phenol red). Media were changed every 3 d. For viability and morphology studies, MSCs were labeled with CellTracker Violet BMQC dye (Life Technologies) prior to encapsulation. At day 1 and 14, cell viability was assessed using a LIVE/DEAD (Life Technologies) membrane integrity assay and confocal microscopy. Cell viability was quantified by image analysis using ImageJ software.

In Situ Confirmation of MMP Cleavage in a 3D Microenvironment: To determine whether the specific variant of the collagen-derived MMP degradable linker sequence used in the experiments (KCGPQG↓IWGQCK) was being cleaved by encapsulated cells, a fluorescently labeled peptide sensor of the same sequence was tethered in the gel. Leight et al. developed the fluorogenic peptide substrate Dab-GGPQG↓IWGQK-Fl-AhxC using solid-phase peptide synthesis (Tribute Peptide Synthesizer, Protein Technologies, Inc.) as previously described.[34] When the MMP-sensitive sequence is cleaved, it separates the quencher dabycl (Dab) from the fluorophore, fluorescin (Fl), permitting excitation. This fluorescent peptide was tethered into the gel at 0.5 × 10^{-3} M along with TGF-β1 (50 × 10^{-9} M) and RGD (1 × 10^{-3} M) prior to cross-linking as depicted in Figure 2a. Various ratios of co-culture seeding densities were used to determine which formulation degraded the sequence at an appreciable rate. As a control, the fluorescence of an acellular gel was measured over 4 d. For chondrocytes in monoculture, cells were encapsulated at 40 million cells mL^{-1}, and for MSCs in monoculture, cells were seeded at 5 million cells mL^{-1}. For co-culture experiments, cells were seeded at 8:1, 16:1, and 24:1 (chondrocyte:MSC) where the chondrocyte cell seeding density was held constant at 40 million cells mL^{-1}. For MMP inhibitor experiments, the inhibitor GM 6001 (Millipore) was added at a concentration of 100 × 10^{-6} M to the media with co-culture gels every 3 d, and viability was tested at day 1 and 14. All values were normalized to the fluorescence value obtained immediately after gel formation (labeled day 0). Fluorescence measurements were conducted using a Synergy H1 microplate reader (BioTek) at 494 nm excitation/521 nm emission. An area scan was performed using a 48-well plate format with a 7 × 7 matrix, and the average fluorescent intensity was calculated for the entire matrix.

Wet Weight, Compressive Modulus, and Biochemical Analysis: On days 1, 7, and 14, hydrogels were removed from culture (n = 3), weighed directly on a Mettler Toledo scale to determine the wet weight, and assessed for compressive modulus. Cell-laden constructs were subjected to unconfined compression to 15% strain at a strain rate of 0.5 mm min^{-1} to obtain stress–strain curves (MTS Synergie 100, 10 N using TestWorks 4 software). The modulus was estimated as the slope of the linear region of the stress–strain curves. Immediately afterwards, gels were snap frozen in LN_2 and stored at −70 °C till biochemical analysis. Hydrogels were digested in 500 μL enzyme buffer (125 μg mL^{-1} papain (Worthington Biochemical) and 10 × 10^{-3} M cysteine) and homogenized using 5 mm steel beads in a TissueLyser (Qiagen) that vibrates at 30 Hz for 10 min. Homogenized samples were digested overnight at 60 °C. Digested constructs were analyzed for biochemical content. DNA content was measured using a Picogreen assay (Life Technologies). Sulfated glycosaminoglycan (sGAG) content was assessed using a dimethylmethylene blue assay as previously described with results presented in equivalents of chondroitin sulfate.[52] Collagen content in the gels was measured using a hydroxyproline assay where hydroxyproline is assumed to make up 10% of collagen.[53] Additionally, digested acellular gels of either non-degradable or degradable formulations with tethered TGF-β1 and RGD were assessed by the colorimetric assays using the Synergy H1 microplate reader (BioTek), and the resulting values were subtracted from their respective cell-laden sample values. GAG and collagen content were expressed as a percentage of the wet weight of the respective gels.

Histology and Immunofluorescent Analysis: On day 14, constructs (n = 3) were fixed in 10% formalin for 30 min at RT, then snap frozen and cryo-sectioned as previously described.[54] Sections were stained for safranin-O and Masson's trichrome on a Leica autostainer XL and imaged in brightfield (20X objective) on a Nikon (TE-2000) inverted microscope. For immunostaining, on day 14, sections were blocked with 5% BSA, then analyzed by anti-collagen type II (1:50, US Biologicals) and anti-collagen type I (1:50, Abcam). Sections were pretreated with appropriate enzymes for 1 h at 37 °C: hyaluronidase (2080 U) for collagen II, and pepsin A (4000 U) with Retrievagen A (BD Biosciences) treatment for collagen I to help expose the antigen. Sections were probed with AlexaFluor 555-conjugated secondary antibodies and counterstained with DAPI to reveal cell nuclei. All samples were processed at the

same time to minimize sample-to-sample variation. Images were collected on a Zeiss LSM710 scanning confocal microscope with a 20× objective using the same settings and post-processing for all images. The background gain was set to negative controls on blank sections that received the same treatment. Positive controls were performed on porcine hyaline cartilage for collagen type II and porcine meniscus for collagen type I (Figure S5, Supporting Information). The amount of cells that stained positive for each type of collagen was quantified by image analysis using Image J software.

Statistical Analysis: Data are shown as mean ± standard deviation. Two-way analysis of variance (ANOVA) with Bonferonni post-test for pairwise comparisons was used to evaluate the statistical significance of the data where the factors were culture time and hydrogel condition. One-way ANOVA was used to assess differences between conditions at specific time points for cases with two and three different groups. A value of $p < 0.05$ was considered to be statistically significant.

Supporting Information

Supporting Information is available from the Wiley Online Library or from the author.

Acknowledgements

The authors acknowledge Kyle Kyburz and Chun Yang for providing MSCs, as well as Amanda Meppelink and Richard Erali for providing knees on which chondrocyte isolations were performed. The authors would also like to acknowledge Emi Tokuda for helping purify the fluorescent peptide sensor as well as Dr. William Wan, Dr. Huan Wang for assistance on experimental design, and Russell Chagolla for help with image analysis. Funding for these studies was provided by the Howard Hughes Medical Institute and Department of Defense award number W81XWH-10–1–0791. The US Army Medical Research Acquisition Activity, 820 Chandler Street, Fort Detrick MD 21702–5014 is the awarding and administering acquisition office.

Received: November 9, 2014
Revised: December 19, 2014
Published online:

[1] M. Adolphe, *Biological Regulation of the Chondrocytes*, CRC Press, Boca Raton **1992**.
[2] M. Falah, G. Nierenberg, M. Soudry, M. Hayden, G. Volpin, *Int. Orthop.* **2010**, *34*, 621.
[3] E. Kon, P. Verdonk, V. Condello, M. Delcogliano, A. Dhollander, G. Filardo, E. Pignotti, M. Marcacci, *Am. J. Sports Med.* **2009**, *37*, 1565.
[4] I. L. Kim, R. L. Mauck, J. A. Burdick, *Biomaterials* **2011**, *32*, 8771.
[5] C. B. Hutson, J. W. Nichol, H. Aubin, H. Bae, S. Yamanlar, S. Al-Haque, S. T. Koshy, A. Khademhosseini, *Tissue Eng. Part A* **2011**, *17*, 1713.
[6] L. Kock, C. C. van Donkelaar, K. Ito, *Cell Tissue Res.* **2012**, *347*, 613.
[7] K. L. Spiller, S. A. Maher, A. M. Lowman, *Tissue Eng. Part B* **2011**, *17*, 281.
[8] C. B. Forsyth, A. Cole, G. Murphy, J. L. Bienias, H.-J. Im, R. F. Loeser, *J. Gerontol. A. Biol. Sci. Med. Sci.* **2005**, *60*, 1118.
[9] G. D. Nicodemus, S. C. Skaalure, S. J. Bryant, *Acta Biomater.* **2011**, *7*, 492.
[10] S. J. Bryant, K. S. Anseth, *J. Biomed. Mater. Res.* **2002**, *59*, 63.
[11] S. J. Bryant, K. S. Anseth, *J. Biomed. Mater. Res. A* **2003**, *64*, 70.
[12] W. Zhao, X. Jin, Y. Cong, Y. Liu, J. Fu, *J. Chem. Technol. Biotechnol.* **2013**, *88*, 327.
[13] P. S. Hume, J. He, K. Haskins, K. S. Anseth, *Biomaterials* **2012**, *33*, 3615.
[14] C. A. Deforest, K. S. Anseth, *Angew. Chem. Int. Ed.* **2012**, *124*, 1852.
[15] A. A. Aimetti, A. J. Machen, K. S. Anseth, *Biomaterials* **2009**, *30*, 6048.
[16] J. A. Benton, B. D. Fairbanks, K. S. Anseth, *Biomaterials* **2009**, *30*, 6593.
[17] B. D. Fairbanks, M. P. Schwartz, A. E. Halevi, C. R. Nuttelman, C. N. Bowman, K. S. Anseth, *Adv. Mater.* **2009**, *21*, 5005.
[18] C. E. Hoyle, C. N. Bowman, *Angew. Chem. Int. Ed.* **2010**, *49*, 1540.
[19] M. P. Schwartz, B. D. Fairbanks, R. E. Rogers, R. Rangarajan, M. H. Zaman, K. S. Anseth, *Integr. Biol.* **2010**, *2*, 32.
[20] B. D. Fairbanks, M. P. Schwartz, C. N. Bowman, K. S. Anseth, *Biomaterials* **2009**, *30*, 6702.
[21] B. V Sridhar, N. R. Doyle, M. A. Randolph, K. S. Anseth, *J. Biomed. Mater. Res. A* **2014**, *102*, 4464.
[22] D. H. Manicourt, J. P. Devogelaer, E. J. Thonar, in *Dynamics of Bone and Cartilage Metabolism*, (Eds: M. Seibel, S. P. Robins, J. P. Bilezikian), Elsevier Science, Burlington **2006**, p 421.
[23] M. P. Lutolf, J. A. Hubbell, *Nat. Biotechnol.* **2005**, *23*, 47.
[24] Y. Park, M. P. Lutolf, J. A. Hubbell, E. B. Hunziker, M. Wong, *Tissue Eng.* **2004**, *10*, 515.
[25] S. Chubinskaya, *J. Biol. Chem.* **1996**, *271*, 11023.
[26] P. Wu, E. DeLassus, D. Patra, W. Liao, L. J. Sandell, *Tissue Eng. Part A* **2013**, *19*, 1199.
[27] Z. Lin, C. Willers, J. Xu, M.-H. Zheng, *Tissue Eng.* **2006**, *12*, 1971.
[28] K. A. Kyburz, K. S. Anseth, *Acta Biomater.* **2013**, *9*, 6381.
[29] C. S. Bahney, C.-W. Hsu, J. U. Yoo, J. L. West, B. Johnstone, *FASEB J.* **2011**, *25*, 1486.
[30] L. Bian, D. Y. Zhai, R. L. Mauck, J. A. Burdick, *Tissue Eng. Part A* **2011**, *17*, 1137.
[31] J. R. Steadman, K. K. Briggs, J. J. Rodrigo, M. S. Kocher, T. J. Gill, W. G. Rodkey, *Arthroscopy* **2003**, *19*, 477.
[32] J. D. McCall, J. E. Luoma, K. S. Anseth, *Drug Delivery Transl. Res.* **2012**, *2*, 305.
[33] R. L. Dahlin, L. A. Kinard, J. Lam, C. J. Needham, S. Lu, F. K. Kasper, A. G. Mikos, *Biomaterials* **2014**, *35*, 7460.
[34] J. L. Leight, D. L. Alge, A. J. Maier, K. S. Anseth, *Biomaterials* **2013**, *34*, 7344.
[35] R. P. Silverman, D. Passaretti, W. Huang, M. A. Randolph, M. J. Yaremchuk, *Plast. Reconstr. Surg.* **1999**, *103*, 1809.
[36] D. Passaretti, M. J. Silverman, R. P. Huang, W Kirchhoff, C. H. Ashiku, S. Randolph, M. A. Yaremchuk, *Tissue Eng.* **2001**, *7*, 805.
[37] S. Ibusuki, A. Papadopoulos, M. Ranka, G. Halbesma, M. Randolph, R. Redmond, I. Kochevar, T. Gill, *J. Knee Surg.* **2010**, *22*, 72.
[38] S. B. Anderson, C.-C. Lin, D. V Kuntzler, K. S. Anseth, *Biomaterials* **2011**, *32*, 3564.
[39] S. J. Bryant, R. J. Bender, K. L. Durand, K. S. Anseth, *Biotechnol. Bioeng.* **2004**, *86*, 747.
[40] S. J. Bryant, J. A. Arthur, K. S. Anseth, *Acta Biomater.* **2005**, *1*, 243.
[41] I. B. Coimbra, S. A. Jimenez, D. F. Hawkins, S. Piera-Velazquez, D. G. Stokes, *Osteoarthritis Cartilage* **2004**, *12*, 336.
[42] L. Wu, H.-J. Prins, M. N. Helder, C. A. van Blitterswijk, M. Karperien, *Tissue Eng. Part A* **2012**, *18*, 1542.
[43] B. K. Hall, *Clin. Orthop. Relat. Res.* **1987**, *225*, 255.
[44] S. J. Bryant, T. T. Chowdhury, D. A. Lee, D. L. Bader, K. S. Anseth, *Ann. Biomed. Eng.* **2004**, *32*, 407.
[45] T. Hardingham, A. Fosang, *FASEB J* **1992**, *6*, 861.
[46] D. Huey, J. Hu, K. Athanasiou, *Science* **2012**, *6933*, 917.
[47] J. J. Yoo, D. A. Bichara, X. Zhao, M. A. Randolph, T. J. Gill, *J. Biomed. Mater. Res. A* **2011**, *99*, 102.

[48] B. A. Byers, R. L. Mauck, I. E. Chiang, R. S. Tuan, *Tissue Eng. Part A* **2008**, *14*, 1821.
[49] K. H. Chua, B. S. Aminuddin, N. H. Fuzina, B. H. I. Ruszymah, *Eur. Cell. Mater.* **2005**, *9*, 58.
[50] C. N. Salinas, K. S. Anseth, *Biomaterials* **2008**, *29*, 2370.
[51] I. Villanueva, C. A. Weigel, S. J. Bryant, *Acta Biomater.* **2009**, *5*, 2832.
[52] R. W. Farndale, C. A. Sayers, A. J. Barrett, *Connect. Tissue Res.* **1982**, *9*, 247.
[53] J. F. Woessner, *Arch. Biochem. Biophys.* **1961**, *93*, 440.
[54] J.-L. Ruan, N. L. Tulloch, V. Muskheli, E. E. Genova, P. D. Mariner, K. S. Anseth, C. E. Murry, *Tissue Eng. Part C. Methods* **2013**, *19*, 794.

Adv. Healthcare Mater. **2015**,
DOI: 10.1002/adhm.201400695

A Biosynthetic Scaffold that Facilitates Chondrocyte-Mediated Degradation and Promotes Articular Cartilage Extracellular Matrix Deposition

Balaji V. Sridhar, Eric A. Dailing, J. Logan Brock, Jeffrey W. Stansbury, Mark A. Randolph & Kristi S. Anseth

Regenerative Engineering and Translational Medicine

ISSN 2364-4133

Regen. Eng. Transl. Med.
DOI 10.1007/s40883-015-0002-3

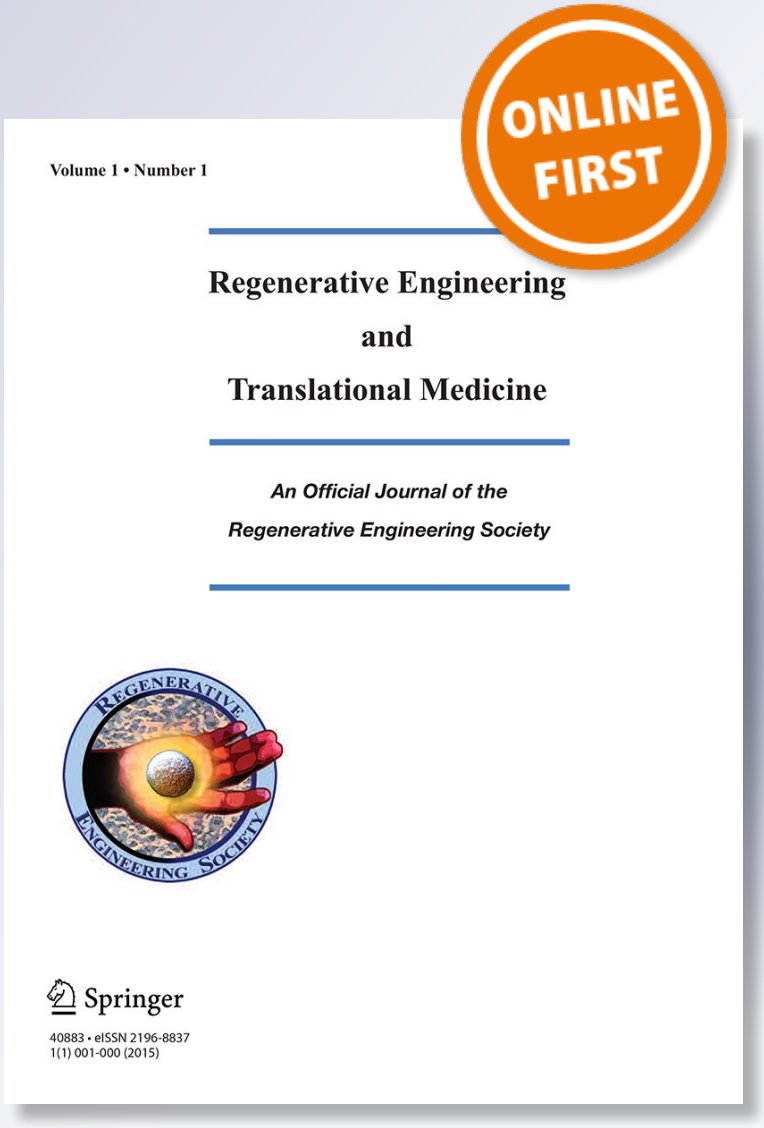

Springer

Regen. Eng. Transl. Med.
DOI 10.1007/s40883-015-0002-3

A Biosynthetic Scaffold that Facilitates Chondrocyte-Mediated Degradation and Promotes Articular Cartilage Extracellular Matrix Deposition

Balaji V. Sridhar[1,2] · Eric A. Dailing[1] · J. Logan Brock[1,2] · Jeffrey W. Stansbury[1,3] · Mark A. Randolph[4,5] · Kristi S. Anseth[1,2,6]

Received: 11 April 2015 / Accepted: 30 July 2015

Abstract
Articular cartilage remains a significant clinical challenge to repair because of its limited self-healing capacity. Interest has grown in the delivery of autologous chondrocytes to cartilage defects, and combining cell-based therapies with scaffolds that capture aspects of native tissue and allow cell-mediated remodeling could improve outcomes. Currently, scaffold-based therapies with encapsulated chondrocytes permit matrix production; however, resorption of the scaffold often does not match the rate of matrix production by chondrocytes, which can limit functional tissue regeneration. Here, we designed a hybrid biosynthetic system consisting of poly(ethylene glycol) (PEG) endcapped with thiols and crosslinked by norbornene-functionalized gelatin via a thiol-ene photopolymerization. The protein crosslinker was selected to facilitate chondrocyte-mediated scaffold remodeling and matrix deposition. Gelatin was functionalized with norbornene to varying degrees (~4–17 norbornenes/gelatin), and the shear modulus of the resulting hydrogels was characterized (<0.1–0.5 kPa). Degradation of the crosslinked PEG-gelatin hydrogels by chondrocyte-secreted enzymes was confirmed by gel permeation chromatography. Finally, chondrocytes encapsulated in these biosynthetic scaffolds showed significantly increased glycosaminoglycan deposition over just 14 days of culture, while maintaining high levels of viability and producing a distributed matrix. These results indicate the potential of a hybrid PEG-gelatin hydrogel to permit chondrocyte-mediated remodeling and promote articular cartilage matrix production. Tunable scaffolds that can easily permit chondrocyte-mediated remodeling may be useful in designing treatment options for cartilage tissue engineering applications.

Lay Summary
Articular cartilage remains a significant clinical challenge to repair because of its limited self-healing capacity. In this manuscript, a biosynthetic scaffold crosslinked by both gelatin and poly(ethylene glycol) (PEG) was developed to encapsulate primary cartilage cells, also known as chondrocytes. This hybrid scaffold facilitated cartilage-specific extracellular matrix (ECM) molecule deposition by permitting cell-mediated, localized degradation of the construct so that encapsulated chondrocytes had pericellular space to generate tissue. Furthermore, the data show that the mechanical properties of this gel can be easily modified and this system can be formed in situ at a defect site via a photopolymerizable reaction. The results of this manuscript indicate the potential of this novel system in designing treatment options for cartilage tissue regeneration applications.

Electronic supplementary material The online version of this article (doi:10.1007/s40883-015-0002-3) contains supplementary material, which is available to authorized users.

✉ Kristi S. Anseth
kristi.anseth@colorado.edu

[1] Department of Chemical and Biological Engineering, University of Colorado, Boulder, CO, USA

[2] BioFrontiers Institute, University of Colorado, Boulder, CO, USA

[3] Department of Craniofacial Biology, School of Dental Medicine, University of Colorado, Aurora, CO, USA

[4] Department of Orthopedic Surgery, Laboratory for Musculoskeletal Tissue Engineering, Massachusetts General Hospital, Harvard Medical School, Boston, MA, USA

[5] Plastic Surgery Research Laboratory, Division of Plastic Surgery, Massachusetts General Hospital, Harvard Medical School, Boston, MA, USA

[6] Howard Hughes Medical Institute, University of Colorado, Boulder, CO, USA

Published online: 30 September 2015

Keywords Cartilage tissue engineering · Chondrocytes · Gelatin · Local degradation · Hydrogel · Photopolymerization

Introduction

Articular cartilage has limited self-healing properties, which can necessitate clinical interventions to heal tissue defects. Chondrocytes, the sole, differentiated resident cells found in mature articular cartilage, are responsible for the generation and maintenance of tissue extracellular matrix (ECM) [1]. When combined with encapsulated chondrocytes, biofunctional scaffolds can facilitate cartilage ECM production and deposition. A variety of natural and synthetic materials have been examined as potential cell carriers and as therapeutic solutions for cartilage repair [2–5].

A limitation with many of the currently studied chondrocyte scaffold carriers is that their resorption rates do not match the rate of matrix deposition by encapsulated cells as found in native tissue [6]. Synthetic hydrogel carriers often limit deposition of chondrocyte-secreted matrix molecules to the space around the cell (i.e., the pericellular space) [7, 8]. To overcome this issue, hydrogels have been engineered to hydrolytically degrade at physiological pH, and while bulk degradation can be readily controlled, numerous material properties are highly coupled to this degradation. For example, high extents of degradation must occur before an ECM protein, like collagen, can assemble throughout hydrogel scaffolds, but this often coincides with a precipitous drop in gel mechanics [7, 9]. Alternatively, natural ECM proteins (e.g., collagen and hyaluronan) can form fibrillar hydrogel networks and provide numerous biological cues to guide tissue deposition by encapsulated cells [10]. These ECM proteins can also be easily degraded by encapsulated cells, which leads to a cell-mediated, local degradation mechanism [11]. However, natural protein-derived scaffolds are often mechanically weak, and it is difficult to control their reproducibility and degradation, which can necessitate synthetic modification to these materials to control their time-varying properties as well as facilitate the cell encapsulation process [12–14]. As a result, recent efforts in the field have included a focus on hybrid synthetic ECM mimics that have the potential to capture the tunability of synthetic scaffolds while integrating the properties of a cell-dictated degradation.

Previous work in our group demonstrated that cartilage cells encapsulated in poly(ethylene glycol) (PEG) hydrogels crosslinked by a collagen-derived peptide sequence (KCGPQG↓IWGQCK) generated constructs with increased, widespread articular cartilage-specific ECM compared to non-degradable gels [15]. These findings supported the hypothesis that local, cell-mediated degradation not only promotes cartilage tissue deposition but also maintains and in some cases increases scaffold mechanical integrity, in contrast to the decrease in bulk modulus typically found in hydrolytically cleavable scaffolds. However, it was found that enzymes secreted by encapsulated chondrocytes alone could not cleave the collagen-derived peptide linker with appropriate kinetics to enable a widespread distribution of matrix macromolecules. In fact, those constructs had the same pericellular matrix deposition pattern found in nondegradable scaffolds. Although previously, the Hubbell group engineered the collagen-derived peptide linker GPQG↓IWGQ to be more responsive to matrix metalloproteinases (MMPs) [16], chondrocytes were found to remodel synthetic scaffolds more appropriately in the presence of cartilage progenitor cells, mesenchymal stem cells (MSCs). Only when encapsulated in coculture with MSCs could the relatively metabolically inactive chondrocytes [17] readily degrade the sequence and then generate ECM throughout the scaffold. Furthermore, others have shown that cell-secreted MMPs are able to cleave a full-length protein at a greater rate than a peptide derived from that protein [18]. Collectively, these findings motivated the experiments reported herein, where we investigate whether a hybrid scaffold composed of PEG and a full-length protein, with a larger amount of collagenase-cleavable sequences per molecule than a peptide, would be responsive to chondrocyte-mediated local degradation and permit widespread matrix deposition.

Hybrid scaffolds that combine full-length proteins with synthetic linkers have been widely explored in tissue engineering applications. For example, fibrinogen [19–21] and collagen [22–24] have been chemically modified to allow covalent attachment to PEG by controlled reactions and thereby facilitate encapsulated cell development and proliferation. Collagen appears to be a good candidate material to use as a scaffold with chondrocytes since degradation of collagen is a rate-limiting step in cartilage remodeling [25]. However, collagen is resistant to most proteases and requires special collagenases for its enzyme hydrolysis. On the other hand, gelatin, a natural biomacromolecule derived from denatured collagen, is less antigenic, more cost-effective [26], and susceptible to more proteases than collagen [27]. These attributes potentially make gelatin an easier substrate to cleave by chondrocyte-secreted enzymes. Chondrocytes are also known to secrete gelatinases [28, 29], which can specifically cleave gelatin more efficiently than most proteases. Finally, gelatin has been successfully employed as a scaffold to promote articular cartilage-specific matrix production of encapsulated chondrocytes [30, 31], and hybrid PEG-gelatin networks have been developed for other tissue engineering applications with high cell viability under photopolymerization conditions [32–34].

In this work, we report the development of a gelatin network crosslinked with PEG for use with encapsulated chondrocytes and observe that the full-length protein is sensitive to local degradation cues and facilitates widespread cartilage-specific ECM deposition. Specifically, gelatin was

modified to contain pendant norbornene functionalities and reacted via a facile thiol-ene photopolymerization with PEG dithiols. The photoinitiated thiol-ene reaction is fast and highly efficient and permits precise spatial and temporal control of network formation [35].

Materials and Methods

Functionalization of Gelatin with Norbornene

Gelatin type A 300 bloom (1 wt% (*w*/*v*)) with M_n ~75 kDa [36] (Sigma-Aldrich), which contains around 21 primary amines per molecules, was dissolved in pH 8.5 sodium bicarbonate. 5-Norbornene-2-acetic acid succinimidyl ester (Sigma-Aldrich) was added to the gelatin solution (21 molar eq. to gelatin for 1:1 norbornene (NB):gelatin amine stoichiometric ratio, 10.5 molar eq. to gelatin for 0.5:1 NB:gelatin amine ratio, and 5.25 molar eq. to gelatin for 0.25:1 NB:gelatin amine ratio) and reacted with free amines on the gelatin molecule at 37 °C for 1 h. The functionalized gelatin was dialyzed against pH 8.5 sodium bicarbonate for 4 h at RT exchanging buffer every hour, using Slide-A-Lyzer™ G2 dialysis cassette MW 10 kDa (Thermo Scientific). After dialysis, solutions were frozen, lyophilized, and stored at −20 °C until use.

The degree of functionalization of gelatin with norbornene was quantified as previously described [32]. Briefly, the lysyl residue modification of gelatin was evaluated via the trinitrobenzenesulfonicacid assay (TNBSA, Thermo Scientific), which is a colorimetric assay that involves reacting the TNBSA reagent with primary amines on proteins for 2 h at 37 °C, stopping the reaction with 10 % SDS and 1 N HCl, and then reading the absorbance at λ=335 nm using a Synergy H1 microplate reader (BioTek). The functionalization efficiency was calculated using

$$\left(1-\frac{[\text{amines}]\text{after gelatin modification}}{[\text{amines}]\text{before gelatin modification}}\right)\times 100\ \%$$

Characterization of Degradation of the Functionalized Gelatin

To assess enzymatic cleavage of the norbornene-functionalized gelatin, 0.2 wt% gelatin solutions with varying extents of functionalization (1:1, 0.5:1, and 0.25:1 NB:gelatin amine molar ratios or unmodified gelatin) were dissolved in 0.1 M sodium nitrate (Sigma-Aldrich) and 0.1 M sodium dibasic phosphate (Sigma-Aldrich), so that the resulting solution could be assessed using aqueous mobile phase gel permeation chromatography (GPC) as previously described [37]. The gelatin solutions were incubated with either 20 units/mL (~0.1 mg/mL) type II collagenase (Worthington Biochemical) or chondrocyte-conditioned media from cells cultured for 3 days. The enzyme solutions were reacted with the functionalized gelatin for 1 h at 37 °C. GPC was performed using a Waters HPLC pump and refractive index detector, Polymer Standard Service Suprema columns (3000 and 100 A), and a linear PEG standard. All samples for GPC were prepared at a concentration of 0.2 wt% and filtered through a 0.4 μm filter. A mobile phase of 0.1 M sodium nitrate and 0.1 M sodium dibasic phosphate, injection volume of 25 mL, and flow rate of 0.5 mL/min were used for all samples.

PEG-Gelatin Network Formation and Mechanical Measurements

The photoinitiator lithium phenyl-2,4,6-trimethylbenzoylphosphinate (LAP) was synthesized as previously described [38]. Gelatin (2 wt% (*w*/*v*)) functionalized with varying amounts of norbornene was prepared in PBS. We used 2 wt% solutions since this is the critical chain overlap concentration above which gelatin can form physical gels at room temperature [39]. The gelatin macromolecules were crosslinked by 0.1 wt% (0.3 mM) 3.5 kDa PEG dithiol (JenKem Technology) via a photoinitiated thiol-ene polymerization with 0.05 wt% (1.7 mM) LAP and light (I_0=~3.5 mW/cm^2, λ=365 nm) for 30 s. For all experiments, 40 μL cylindrical gels (O.D. ~5 mm, height ~2 mm) were formed in the cut end of a 1 mL syringe (BD Medical).

The various gels were placed in cell culture media to swell overnight and weighed the next day. The volume swelling ratio Q was calculated by first solving for the mass swelling ratio q, which involved dividing the measured swollen mass by the theoretical dry mass (data not shown) and assuming that the density of the polymer was similar to that of its solvent. Parallel plate rheometry was performed on crosslinked gels that were formed with varied norbornene functionalization on the gelatin using an Ares 4400 DHR-3 shear rheometer (TA instruments) with 10 % strain frequency sweep and a 10 rad/s strain sweep. The shear modulus (G) of the constructs was determined when the gels were in the linear viscoelastic regime for both the frequency and the strain sweep. The final network crosslinking density ρ_{xL} was calculated from rubber elastic theory [40] where $\rho_{xL}=GQ^{1/3}(\text{RT})^{-1}$.

Cell Harvest and Expansion

Primary chondrocytes were isolated from articular cartilage of the femoral-patellar groove of 6-month-old Yorkshire swine as detailed previously [41]. Cells were grown in a T-75 culture flask with media as previously described [42] and were used directly after expansion, P0, for all cell-based experiments. Briefly, chondrocytes were grown in growth medium (high-glucose Dulbecco's modified Eagle's medium [DMEM]

supplemented with ITS+ Premix 1 % *v/v* (BD Biosciences), 50 mg/mL L-ascorbic acid 2-phosphate, 40 μg/mL L-proline, 0.1 μM dexamethasone, 110 μg/mL pyruvate, and 1 % penicillin-streptomycin-fungizone) with the addition of 10 ng/mL insulin-like growth factor (IGF-1) (Peprotech) to maintain cells in a dedifferentiated state. ITS was used because it can promote formation of articular cartilage from chondrocytes [43]. Cultures were maintained at 5 % CO_2 and 37 °C.

Chondrocyte Encapsulation and Viability Assessment

Chondrocytes were encapsulated at 40 million cells/mL in 40 μL cylindrical PEG-gelatin gels using gels formed from the 1:1 NB:gelatin amine synthesis conditions (~4.5 mM norbornene per gelatin chain). This macromolecule formulation degraded readily in response to chondrocyte-secreted enzymes. Cell-laden gels were immediately placed in 1-mL DMEM growth medium in 48-well nontreated tissue culture plates. Media was changed every 3 days. At days 1, 7, and 14, cell viability and cellularity were assessed using a LIVE/DEAD® (Life Technologies) membrane integrity assay and confocal microscopy with ImageJ (NIH) for assessment of cell circularity.

Biochemical Analysis of Cell-Hydrogel Constructs

On days 1,7, and 14, gels were removed from culture (n=3), weighed directly to determine the wet weight, snap frozen in LN_2, and stored at −70 °C prior to biochemical analysis. Hydrogels were digested in 500 μL enzyme buffer (125 μg/mL papain [Worthington Biochemical] and 10 mM cysteine) and homogenized using 5 mm steel beads in a TissueLyser (Qiagen). Homogenized samples were digested overnight at 60 °C.

Digested constructs were analyzed for biochemical content. DNA content, as an indicator of cell number, was measured using a PicoGreen assay (Life Technologies), and the results were expressed as the amount of DNA (μg) per chondrocyte-laden gel. Sulfated glycosaminoglycan (sGAG) content was assessed using a dimethylmethylene blue assay as previously described with results presented in equivalents of chondroitin sulfate [44]. As a cell-free control, digested acellular gels were assessed by the colorimetric assays, and the resulting values were subtracted from their respective cell-laden sample values. GAG content was expressed as a percentage of the wet weight of the respective gels.

Histology and Immunofluorescence Analysis

On day 14, constructs (n=3) were fixed in 10 % formalin for 30 min at RT and then snap frozen and cryosectioned to 20 μm sections as previously described [45]. At day 14, sections were stained for Safranin-O and Masson's trichrome on a Leica autostainer XL and imaged in bright field (20x objective) on a Nikon (TE-2000) inverted microscope.

For immunostaining, on day 14, sections were blocked with 5 % BSA and then analyzed by anti-type II collagen (1:50, US Biological) and anti-type I collagen (1:50, Abcam). Sections were pretreated with appropriate enzymes for 1 h at 37 °C: hyaluronidase (2080 U) for type II collagen and Pepsin A (4000 U) with Retrievagen A (BD Biosciences) treatment for type I collagen to help expose the antigen. Sections were probed with AlexaFluor 555-conjugated secondary antibodies (1:200, Life Technologies) and counterstained with DAPI to reveal cell nuclei. All samples were processed at the same time to minimize sample-to-sample variation. Images were collected on a Zeiss LSM710 scanning confocal microscope with a 20X objective using a z-stack maximum intensity projection of 4×5 μm slices of the 20 μm section using the same settings and postprocessing for all the images. The background gain was set to negative controls on acellular sections that received the same treatment. Positive controls were performed on porcine hyaline cartilage for type II collagen and porcine meniscus for type I collagen (Supplementary Fig. 2a, b).

Statistical Analysis

Data are shown as mean±standard deviation. One-way ANOVA with a two-tailed Bonferroni's multiple comparison posttest was used to assess differences in experimental outputs at different culture time points, since means of three samples are being compared simultaneously. α=0.05 was used for all analysis. Statistical calculations were performed on GraphPad Prism®. $p<0.05$ was considered to be statistically significant.

Results

Modifying PEG-Gelatin Network Properties

By varying the extent of norbornene functionalization of gelatin, we aimed to tune the crosslinking density of the final network and therefore the macroscopic properties of the resulting hydrogel. Figure 1a contains a schematic of gelatin functionalization with norbornene, along with the estimated amount of norbornenes attached to each gelatin molecule (based on calculations). Figure 1b depicts the photopolymerization between 2 wt% NB-functionalized gelatin with varying amounts of norbornene and 0.1 wt% PEG dithiol along with the concentrations of norbornene and thiol.

We characterized the efficiency of lysine modification on gelatin by the 5-norbornene-2-acetic acid succinimidyl ester reaction using the TNBSA assay, with data shown in Table 1 (n=5). The 1:1 norbornene:gelatin amine condition led to 75±

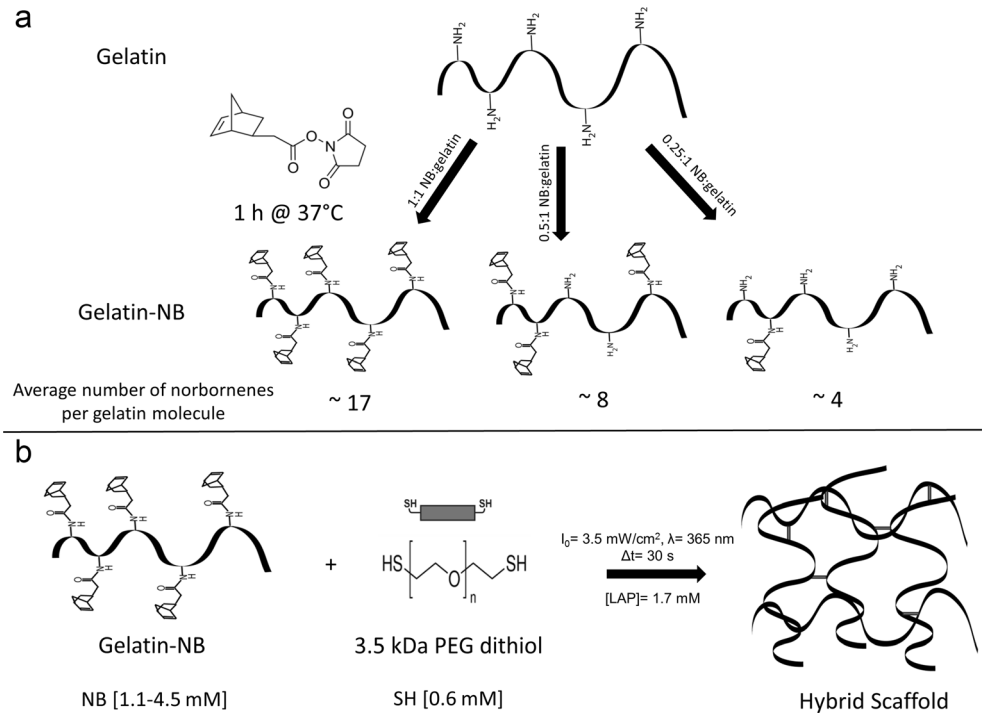

Fig. 1 Gelatin functionalization with norbornene and photopolymerization with PEG. **a** Depiction of the reaction of gelatin with varying molar amounts of norbornene succinimidyl ester. The reaction proceeded for 1 h at 37 °C and the amount of functionalization on the product was measured by TNBSA. The estimated amount of norbornenes per gelatin molecule is shown below based on functionalization efficiency calculations. **b** Photopolymerization scheme between 2 wt% norbornene-functionalized gelatin with varying amounts of norbornene (1.1–4.5 mM) and 0.1 wt% 3.5 kDa PEG dithiol with (0.6 mM) thiol to form a covalently crosslinked hybrid scaffold

6 % functionalization efficiency, which is similar to that observed with other studies using similar amine-modifying techniques [32, 33]. Lower stoichiometric ratios (0.5:1 and 0.25:1 norbornene/gelatin amine) led to corresponding decreases in the functionalization efficiency, 36±5 % and 19±5 %, respectively. The unmodified gelatin was measured to have ~21 amine groups per molecule, which was also confirmed by other studies [32, 36], and suggests that the synthesized gelatin macromolecules have on average ~17 (75 %), 8 (36 %), and 4 (19 %) norbornene pendent groups per molecule for crosslinking. The swollen shear modulus of the resulting acellular constructs was measured, and the crosslinking density of the scaffold was calculated. Consistent with the expected crosslinking reaction, both values increased with increasing amount of norbornene functionalization as shown in Table 1 (n=5).

Verification of Degradation of Modified Gelatin by Chondrocyte-Secreted Enzymes

Modification of proteins can alter their structure and change their susceptibility to enzymatic degradation since altered lysines may affect the way that an enzyme binds to its site to initiate cleavage. To verify that the modified gelatin could degrade in the response to chondrocyte-secreted enzymes, we performed a solution-based assay and tested the degradability of various modified gelatin macromolecules when exposed to either collagenase or chondrocyte-conditioned media. We chose chondrocyte-conditioned medium that was collected after 3 days of culture, since we have previously observed that the secreted enzymes can cleave a collagen-derived peptide sequence during that time frame [15]. After incubation of the modified gelatin with enzymes, GPC was

Table 1 Material properties of acellular hybrid scaffolds (n=5)

Molar ratio of norbornene succinimidyl ester reacted with gelatin amines	Norbornene functionalization efficiency (%)[a]	Calculated amount of norbornene on gelatin chain (mM)[b]	Thiol concentration (mM)	Swollen shear modulus G (kPa)	Crosslinking density ρ_{xL} (mM)[c]
0.25:1 Norbornene:gelatin amines	19±5	~1.1	0.6	<0.1	<0.18
0.5:1 Norbornene:gelatin amines	36±5	~2.2	0.6	0.2±0.1	0.36±0.04
1:1 Norbornene:gelatin amines	75±6	~4.5	0.6	0.5±0.1	0.90±0.05

[a] Norbornene functionalization efficiency was calculated using $\left(1-[\text{amines}]^{\frac{\text{after modification}}{\text{before modification}}}_{[\text{amines}]}\right)\times 100\ \%$

[b] Norbornene concentration per gelatin molecule was calculated by accounting for the amount of amines on type A gelatin (~21) and the norbornene functionalization efficiency for each condition assuming that only norbornenes replaced the gelatin amines

[c] Crosslinking density was calculated from the rubber elastic theory: $\rho_{xL}=GQ^{1/3}(\text{RT})^{-1}$

used to monitor the degradation of both unmodified and norbornene-substituted gelatin. The unmodified gelatin peak elutes at 18 min and is clearly distinguished from a large system peak at 20 min that occurs as a consequence of a small dissimilarity in composition, and thus a refractive index difference, between the injected buffer and the mobile phase. A substitution of 0.25:1 or 0.5:1 NB:gelatin amine resulted in no significant change in retention time compared to the unmodified gelatin, while the 1:1 NB:gelatin amine showed a distinguishable yet slightly shifted and significantly smaller peak. We hypothesize that this may be due to the formation of a slightly more hydrophobic macromolecule that may be more susceptible to interaction with the column stationary phase than the unmodified gelatin. When collagenase was added to each gelatin sample, the peak at 18 min completely disappears, indicating degradation of gelatin into smaller molecular weight fragments. A lower MW shoulder appears on the system peak, which corresponds to the gelatin degradation products. Finally, chondrocyte-conditioned medium was added to each gelatin sample to assess degradation in the presence of cell-secreted enzymes. Similar to treatment with collagenase, the gelatin peak was shifted to the low-molecular-weight shoulder, indicating that the norbornene-functionalized gelatin can be degraded by chondrocyte-secreted enzymes. Results are summarized in Supplementary Fig. 1, while Fig. 2 shows the effect of adding collagenase or chondrocyte-secreted enzymes to the most highly substituted gelatin (i.e., reacted at 1:1 NB:gelatin amines).

Chondrocyte Viability, Cellularity, and Morphology

Gelatin amines that were reacted at a 1:1 molar ratio with norbornene were used in all subsequent cell encapsulation experiments, since this formulation contained a higher amount of covalent crosslinks and thus could retain a gel structure for a longer period of time for the slow-growing chondrocytes. We chose a chondrocyte seeding density of 40 million cells/mL, as chondrocytes have been studied at this density for cartilage tissue engineering experiments using 3D scaffolds and shown to secrete an elaborate ECM at this concentration [46–48]. After chondrocytes were encapsulated, their viability, cellularity, and morphology were assessed at days 1, 7, and 14. In Fig. 3a, the chondrocytes retained spherical morphology at day 1 and begin to spread as observed on days 7 and 14, which suggests that the chondrocytes are able to locally remodel the environment. Image processing reveals that the circularity of the chondrocytes decreases from day 1 to day 7 and day 14 as shown in Fig. 3b, further corroborating the results seen in Fig. 3a.

Additionally, the cells retain high viability (calculated to be >95 %) at all the time points and appear to proliferate over time, as there are many more cells in the constructs at day 14 than there are at day 1. This increase in cellularity was quantified by the PicoGreen analysis that measures DNA content and shows a significant increase in cell number between day 1 and day 14 (p=0.01) (Fig. 3c). Collectively, these results suggest that chondrocytes can thrive, proliferate, and remodel their environment in this scaffold system.

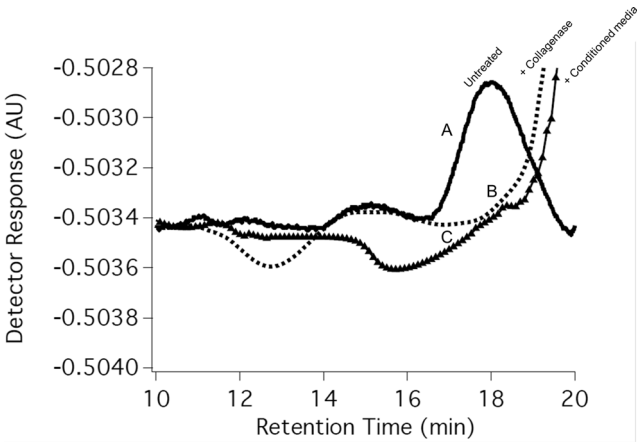

Fig. 2 GPC chromatogram of gelatin functionalized with norbornene at 1:1 NB:gelatin amine that is either untreated (*A*) or treated with 20 U/mL collagenase for 1 h at 37 °C (*B*) or treated with day 3 chondrocyte-conditioned media for 1 h at 37 °C (*C*). The untreated gelatin peak that is found at 18 min elution disappears after treatment with either collagenase or chondrocyte-conditioned media suggesting degradation of gelatin to smaller by-products by the enzymes

ECM Production and Deposition in Scaffolds

GAG content was assessed biochemically at days 1, 7, and 14, and the distribution of secreted matrix molecules was examined by staining sections with Safranin-O (GAG) and Masson's trichrome (collagen). Measured quantities of the matrix molecules were normalized to the wet weight of each construct. As Fig. 4a shows, at day 14, GAGs (red) were extensively distributed throughout the gel. Staining of an acellular construct revealed low background staining (Fig. 4b), indicating that staining was primarily from macromolecules secreted by the resident chondrocytes. Furthermore, quantitative analysis, as shown in Fig. 4c, supports the conclusion that the amount of sGAG deposition increased significantly from day 1 to day 14 (p=0.0004). A similar distribution pattern to what was seen with GAGs is observed with collagen (dark blue) as seen in Fig. 5a, b. Figure 5e depicts the scaffold as optically opaque, with a cartilaginous appearance after 14 days of culture, much more than either the acellular (Fig. 5c) or day 1 time point (Fig. 5d), further suggesting widespread ECM distribution in the scaffold [49]. This versatile PEG-crosslinked gelatin system appears to provide a scaffold that is readily degraded by chondrocytes and can support matrix deposition over time.

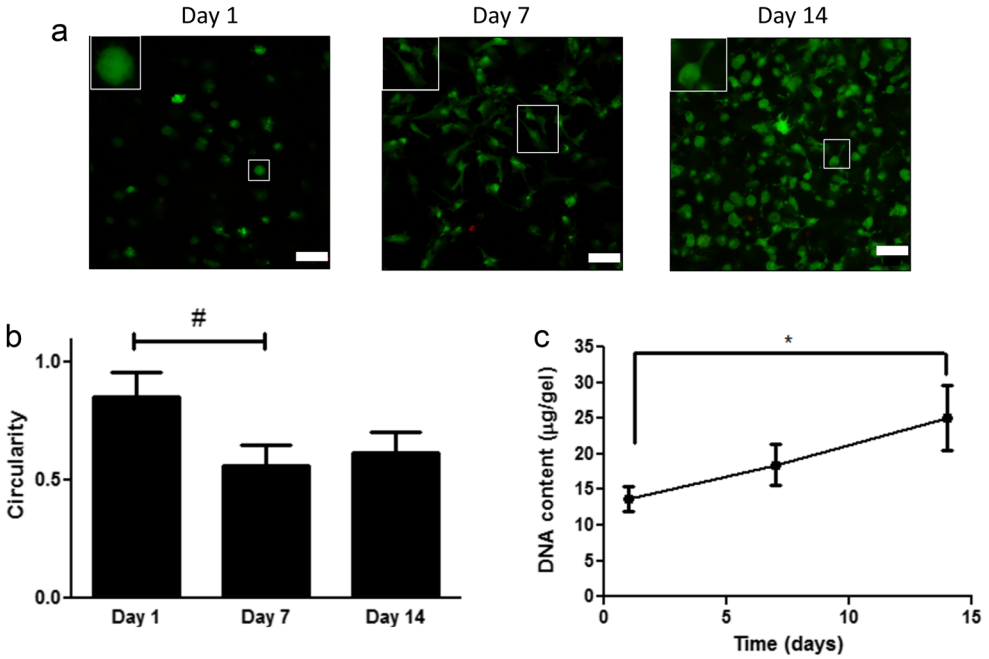

Fig. 3 Viability, morphology, and cellularity of 1:1 NB:gelatin amine hybrid scaffold. **a** Live (*green*)/dead (*red*) stains of encapsulated chondrocytes. Viability is calculated to be greater than 95 % at all the time points. *Insets* highlight single cells changing in morphology from rounded to more spread over time. *Scale bars* represent 50 μm. **b** Degree of circularity between 0 (not rounded) and 1(rounded) of the encapsulated cells. *A number sign with a line* indicates a statistically significant difference in circularity value between day 1 and day 7 (p=0.02). Results are presented as mean±SD (n=3). **c** DNA content (μg of DNA/gel) as measured by Picogreen assay over 14 days. *An asterisk with a line* indicates a statistically significant difference between day 1 and day 14 in DNA content (p=0.01). Results are presented as mean±SD (n=3)

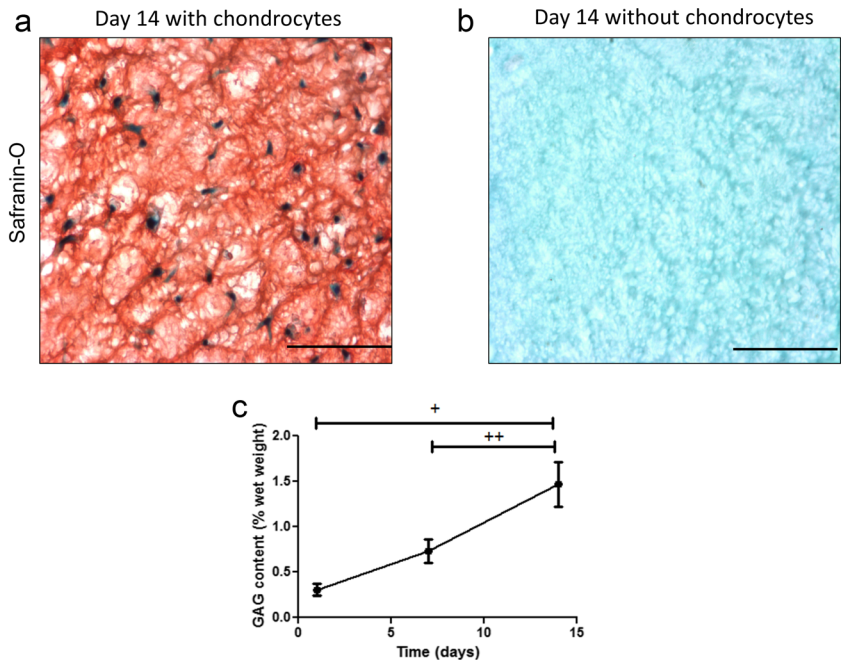

Fig. 4 Glycosaminoglycan distribution and production in a 1:1 NB:gelatin amine hybrid scaffold. **a** Section with encapsulated chondrocytes at day 14 stained for GAGs with nuclei stained *black* and GAGs stained *red*. **b** Acellular section stained for GAGs at day 14. *Scale bars* represent 100 μm. **c** Total GAG content expressed as a percentage of the respective construct wet weight assessed at days 1, 7, and 14. *A plus sign with a line* indicates a statistically significant difference in GAG content between day 1and day 14 (p=0.0004), and *two plus signs* with a line indicates a statistically significant difference in GAG content between day 7 and day 14 (p=0.001). Results are presented as mean± SD (n=3)

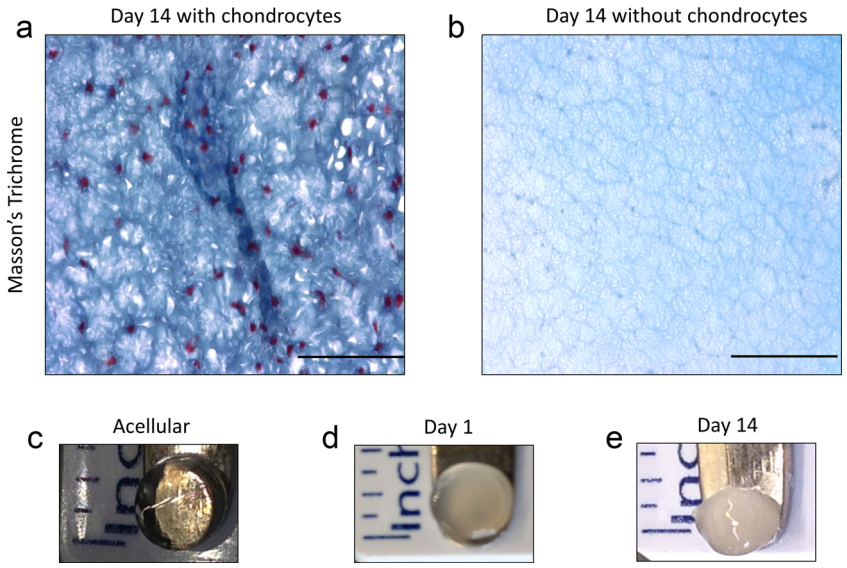

Fig. 5 Collagen and ECM distribution in a 1:1 NB:gelatin amine hybrid scaffold. **a** Section with encapsulated chondrocytes at day 14 stained for collagen with nuclei stained *violet* and collagen stained *blue*. **b** Acellular section stained for collagen at day 14. *Scale bars* represent 100 μm. **c** Gross image of a transparent acellular scaffold at day 1. **d** Gross image of a translucent scaffold with encapsulated chondrocytes at day 1. **e** Gross image of an opaque scaffold with encapsulated chondrocytes at day 14 that has a cartilaginous appearance

Quality of Collagen Generated by Chondrocytes in the Scaffold

To verify that the collagen generated by the chondrocytes had an articular cartilage phenotype, we qualitatively assessed the ratio of type II collagen to type I collagen on gel immunostained sections. Images revealed that at day 14, negligible type I collagen (red) was observed, but robust type II collagen (red) was observed throughout the scaffold as seen in Fig. 6.

Discussion

Engineering a clinically viable scaffold to promote cartilage regeneration is challenging. By using a novel, tunable hybrid biological-synthetic system, we have shown quantitatively and qualitatively, in vitro, that encapsulated chondrocytes generate highly distributed cartilage-specific ECM molecules. We showed that chondrocyte-secreted enzymes can degrade norbornene-functionalized gelatin and further demonstrated that cells are viable when embedded in the hydrogel formulation. The chondrocytes appear to spread throughout the scaffold, suggesting that encapsulated cells are locally remodeling their environment and facilitate the eventual deposition of matrix throughout the scaffold. Future investigations with this scaffold could prove useful in designing a cell carrier system to promote cartilage regeneration in vivo.

Modulus studies confirmed that these PEG-gelatin scaffolds could be tuned to adjust their crosslinking density and macroscopic properties that depend on this parameter (Table 1). In general, it can be more difficult to change material properties of pure protein-based gels, so covalent crosslinking can lead to higher mechanical properties [22]. If the crosslinking density can be adjusted by the user, it can also alter the amount of tissue deposition [9, 50]. Gel properties,

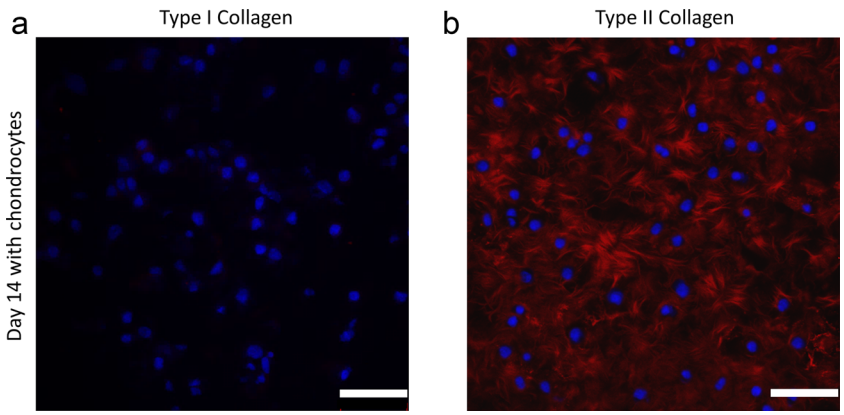

Fig. 6 Type I collagen versus type II collagen distribution assessed by immunofluorescence in a 1:1 NB/gelatin amine hybrid construct with encapsulated chondrocytes at day 14. **a** Gel section stained for type I collagen. **b** Gel section stained for type II collagen. Sections were stained for both anti-collagen type I and anti-collagen type II antibodies (*red*) and were counterstained with DAPI (*blue*) for cell nuclei. *Scale bars* represent 50 μm

degradation, and ECM deposition might be further tuned by changing the network connectivity using different molecular weight PEG crosslinkers or multiarm PEG crosslinkers depending on whether a more tightly or loosely crosslinked network is desired.

We confirmed that chondrocyte-secreted enzymes could degrade norbornene-functionalized gelatin by visualizing the degradation products with GPC (Fig. 2). GPC data suggest that norbornene-functionalized gelatin is degraded to smaller molecular weight products in the presence of chondrocyte-conditioned media. This confirms that norbornene-functionalized gelatin is a viable platform for the formation of chondrocyte-specific cellularly degradable hydrogels. We demonstrated these results in a solution-based assay, but a complementary study has shown that functionalized and crosslinked gelatin can be degraded by cell-secreted enzymes as well [51]. Here, we observe this indirectly by changes in the chondrocyte morphology (Fig. 3a); however, there are alternate ways to design systems that might respond to chondrocyte-secreted enzymes. One idea would be to include an aggrecanase-based cleavable peptide linker [52]. We selected the full-length protein gelatin for this study, as we hypothesized that its multiple MMP-cleavable sites would lead to more facile cleavage by chondrocytes than small peptide sequences as suggested by other groups [18]. In fact, the gelatin molecule contains about six MMP-sensitive sequences per molecule [27], which appears to be readily cleaved by chondrocyte-secreted enzymes at the cell density studied.

Viability results revealed that chondrocytes thrive and proliferate in the hybrid network. Cellularity in the gel quantitatively increased, which was confirmed by PicoGreen, and the cells spread over time (Fig. 3). Part of the reason for this change in cell morphology is likely because the chondrocytes are binding to adhesion factors present on the protein [26]. Another explanation is that the cells are degrading the network by a cell-mediated mechanism and spreading [51], which could facilitate the observed widespread matrix deposition. Future studies could focus on improving methods to verify that local degradation is occurring, which could include monitoring the cell-based degradation using microrheological techniques, such as microparticle tracking [53].

Cartilage-specific matrix produced by chondrocytes was distributed throughout the entire scaffold as it was in other cell-mediated degradable scaffolds [15] (Figs. 4a and 5a). Additionally, the GAG production from this scaffold was comparable to what was seen in a cellularly degradable cartilage tissue engineering scaffold with a similar cell seeding density [15]; however, this system did not need to tether a growth factor, such as TGF-β, to the network in order to elicit a response from chondrocytes. A possible explanation for the robust secretory properties might relate to the fact that gelatin can bind to growth factors released by cells and perhaps present them to embedded chondrocytes in a local and sustained manner [1].

The encapsulated chondrocytes have a lower circularity at day 14, which can be suggestive of a hypertrophic phenotype that generate higher amounts of type I collagen and functionally inferior cartilage tissue [54]. Interestingly, the collagen produced by the encapsulated cells maintained a higher quality articular cartilage phenotype, as indicated by the collagen typing result with a high type II collagen:type I collagen ratio (Fig. 6).

In a potential clinical application as a scaffold, this system could be advantageous since it is easy to tune formation of this network. Currently, collagen-based materials are used as scaffolds in the clinic and have yielded variable success, partly due to high variations in network formation [55]. The hybrid system presented in this manuscript can be easily tuned and permits the widespread elaboration of cartilage-specific ECM molecules over a short period of time. It would be interesting to see how matrix production is affected as the length of culture time is extended, especially in an in vivo environment where the presence of macrophages could help stimulate chondrocyte gelatinase secretion [28].

Conclusions

In summary, a novel hydrogel system based on crosslinking a full-length protein, gelatin, by PEG was designed to increase control over network formation and permit local chondrocyte-mediated degradation for cartilage tissue engineering applications. The hydrogel increases chondrocyte cellularity and facilitates cartilage ECM production via cell-mediated degradation in a manner that promotes widespread matrix deposition in just 14 days. The materials' approach was to modify gelatin with norbornene functionalities that were crosslinked with PEG dithiols via a photoinitiated thiol-ene reaction. Results confirmed that the final PEG-gelatin gel properties could be altered by modifying the amount of norbornene functionalization, while maintaining susceptibility to enzymatic degradation. Culture of chondrocyte-laden hydrogel scaffolds led to ECM molecules distributed throughout the construct and resembled articular cartilage with respect to gross appearance of the generated matrix molecules and collagen typing (high type II collagen:type I collagen ratio). This biosynthetic system may prove useful in clinical applications as a scaffold to promote cartilage regeneration.

Acknowledgments The authors acknowledge Amanda Meppelink for providing knees on which chondrocyte isolations were performed as well as Kathryn Morrissey for help with setting up GPC experiments. The authors would also like to thank Jason Silver, Dr. William Wan, and Dr. Malar Azagarsamy for assistance on experimental design. Funding for these studies was provided by the Howard Hughes Medical Institute, National Institutes of Health (R01 DE016523-10), and Department of Defense (W81XWH-10-1-0791). The US Army Medical Research

Acquisition Activity, 820 Chandler Street, Fort Detrick, MD, 21702-5014, USA, is the awarding and administering acquisition office.

Conflicts of Interest The authors have no conflicts of interest to declare.

References

1. Adolphe M. Biological regulation of the chondrocytes. Boca Raton: CRC Press; 1992.
2. Kim IL, Mauck RL, Burdick JA. Hydrogel design for cartilage tissue engineering: a case study with hyaluronic acid. Biomaterials. 2011;32:8771–82.
3. Hutson CB, Nichol JW, Aubin H, Bae H, Yamanlar S, Al-Haque S, et al. Synthesis and characterization of tunable poly(ethylene glycol): gelatin methacrylate composite hydrogels. Tissue Eng A. 2011;17:1713–23.
4. Kock L, van Donkelaar CC, Ito K. Tissue engineering of functional articular cartilage: the current status. Cell Tissue Res. 2012;347:613–27.
5. Spiller KL, Maher SA, Lowman AM. Hydrogels for the repair of articular cartilage defects. Tissue Eng B. 2011;17:281–99.
6. Forsyth CB, Cole A, Murphy G, Bienias JL, Im H-J, Loeser RF. Increased matrix metalloproteinase-13 production with aging by human articular chondrocytes in response to catabolic stimuli. J Gerontol A Biol Sci Med Sci. 2005;60:1118–24.
7. Nicodemus GD, Skaalure SC, Bryant SJ. Gel structure has an impact on pericellular and extracellular matrix deposition, which subsequently alters metabolic activities in chondrocyte-laden PEG hydrogels. Acta Biomater. 2011;7:492–504.
8. Sridhar BV, Doyle NR, Randolph MA, Anseth KS. Covalently tethered TGF-β1 with encapsulated chondrocytes in a PEG hydrogel system enhances extracellular matrix production. J Biomed Mater Res A. 2014;102:4464–72.
9. Bryant SJ, Anseth KS. Hydrogel properties influence ECM production by chondrocytes photoencapsulated in poly(ethylene glycol) hydrogels. J Biomed Mater Res A. 2002;59:63–72.
10. Lee KY, Mooney DJ. Hydrogels for Tissue Engineering. Chem Rev. 2001;101:1869–80.
11. Lutolf MP, Hubbell JA. Synthetic biomaterials as instructive extracellular microenvironments for morphogenesis in tissue engineering. Nat Biotechnol. 2005;23:47–55.
12. Bryant SJ, Anseth KS. Controlling the spatial distribution of ECM components in degradable PEG hydrogels for tissue engineering cartilage. J Biomed Mater Res A. 2003;64:70–9.
13. Zhao W, Jin X, Cong Y, Liu Y, Fu J. Degradable natural polymer hydrogels for articular cartilage tissue engineering. J Chem Technol Biotechnol. 2013;88:327–39.
14. Kretlow JD, Mikos AG. From material to tissue: biomaterial development, scaffold fabrication, and tissue engineering. AIChE J. 2008;54:3048–67.
15. Sridhar BV, Brock JL, Silver JS, Leight JL, Randolph MA, Anseth KS. Development of a cellularly degradable PEG hydrogel to promote articular cartilage extracellular matrix deposition. Adv Healthc Mater. 2015;4:635–781.
16. Patterson J, Hubbell JA. Enhanced proteolytic degradation of molecularly engineered PEG hydrogels in response to MMP-1 and MMP-2. Biomaterials. 2010;31:7836–45.
17. Lin Z, Willers C, Xu J, Zheng M-H. The chondrocyte: biology and clinical application. Tissue Eng. 2006;12:1971–84.
18. Fields GB, Van Wart HE, Birkedal-hansent H. Sequence specificity of human skin fibroblast collagenase: evidence for the role of collagen structure in determining the collagenase cleavage site. J Biol Chem. 1987;262:6221–6.
19. Schmidt O, Mizrahi J, Elisseeff J, Seliktar D. Immobilized fibrinogen in PEG hydrogels does not improve chondrocyte-mediated matrix deposition in response to mechanical stimulation. Biotechnol Bioeng. 2006;95:1061–9.
20. Almany L, Seliktar D. Biosynthetic hydrogel scaffolds made from fibrinogen and polyethylene glycol for 3D cell cultures. Biomaterials. 2005;26:2467–77.
21. Mironi-Harpaz I, Wang DY, Venkatraman S, Seliktar D. Photopolymerization of cell-encapsulating hydrogels: crosslinking efficiency versus cytotoxicity. Acta Biomater. 2012;8:1838–48.
22. Gonen-Wadmany M, Oss-Ronen L, Seliktar D. Protein-polymer conjugates for forming photopolymerizable biomimetic hydrogels for tissue engineering. Biomaterials. 2007;28:3876–86.
23. Appelman TP, Mizrahi J, Elisseeff JH, Seliktar D. The influence of biological motifs and dynamic mechanical stimulation in hydrogel scaffold systems on the phenotype of chondrocytes. Biomaterials. 2011;32:1508–16.
24. Singh RK, Seliktar D, Putnam AJ. Capillary morphogenesis in PEG-collagen hydrogels. Biomaterials. 2013;34:9331–40.
25. Manicourt DH, Devogelaer JP, Thonar EJ. Products of cartilage metabolism. In: Seibel M, Robins SP, Bilezikian JP, editors. Dynamics of bone and cartilage metabolism. 2nd ed. Burlington: Elsevier Science; 2006. p. 421–39.
26. Rice JJ, Martino MM, De Laporte L, Tortelli F, Briquez PS, Hubbell JA. Engineering the regenerative microenvironment with biomaterials. Adv Healthc Mater. 2013;2:57–71.
27. Gorgieva S, Kokol V. Collagen-vs. gelatine-based biomaterials and their biocompatibility: review and perspectives. In: Pignatello R, editor. Biomaterials applications for nanomedicine. Croatia: InTech, 2011; p. 17–52.
28. Dreier R, Wallace S, Fuchs S, Bruckner P, Grassel S. Paracrine interactions of chondrocytes and macrophages in cartilage degradation: articular chondrocytes provide factors that activate macrophage-derived pro-gelatinase B (pro-MMP-9). J Cell Sci. 2001;114:3813–22.
29. Mohtai M, Smith RL, Schurman DJ, Tsuji Y, Torti FM, Hutchinson NI, et al. Expression of 92-kD type IV collagenase/gelatinase (gelatinase B) in osteoarthritic cartilage and its induction in normal human articular cartilage by interleukin 1. J Clin Invest. 1993;92:179–85.
30. Wang C-C, Yang K-C, Lin K-H, Wu C-C, Liu Y-L, Lin F-H, et al. A biomimetic honeycomb-like scaffold prepared by flow-focusing technology for cartilage regeneration. Biotechnol Bioeng. 2014;111:2338–48.
31. Mazaki T, Shiozaki Y, Yamane K, Yoshida A, Nakamura M, Yoshida Y, et al. A novel, visible light-induced, rapidly cross-linkable gelatin scaffold for osteochondral tissue engineering. Sci Rep. 2014;4:4457.
32. Fu Y, Xu K, Zheng X, Giacomin AJ, Mix AW, Kao WJ. 3D cell entrapment in crosslinked thiolated gelatin-poly(ethylene glycol) diacrylate hydrogels. Biomaterials. 2012;33:48–58.
33. Daniele MA, Adams AA, Naciri J, North SH, Ligler FS. Interpenetrating networks based on gelatin methacrylamide and PEG formed using concurrent thiol click chemistries for hydrogel tissue engineering scaffolds. Biomaterials. 2014;35:1845–56.
34. Mũnoz Z, Shih H, Lin C-C. Gelatin hydrogels formed by orthogonal thiol–norbornene photochemistry for cell encapsulation. Biomater Sci. 2014;2:1063.
35. Hoyle CE, Bowman CN. Thiol-ene click chemistry. Angew Chem Int Ed Engl. 2010;49:1540–73.
36. Einerson NJ, Stevens KR, Kao WJ. Synthesis and physicochemical analysis of gelatin-based hydrogels for drug carrier matrices. Biomaterials. 2003;24:509–23.

37. Waldeck H, Kao WJ. Effect of the addition of a labile gelatin component on the degradation and solute release kinetics of a stable PEG hydrogel. J Biomater Sci Polym Ed. 2011;23:1595–611.
38. Fairbanks BD, Schwartz MP, Bowman CN, Anseth KS. Photoinitiated polymerization of PEG-diacrylate with lithium phenyl-2,4,6-trimethylbenzoylphosphinate: polymerization rate and cytocompatibility. Biomaterials. 2009;30:6702–7.
39. Mohanty B, Bohidar HB. Microscopic structure of gelatin coacervates. Int J Biol Macromol. 2005;36:39–46.
40. Bryant SJ, Anseth KS. Photopolymerization of hydrogel scaffolds. In: Ma PX, Ellisseeff J, editors. Scaffolding in tissue engineering. Boca Raton: CRC Press; 2006. p. 1–45.
41. Yoo JJ, Bichara DA, Zhao X, Randolph MA, Gill TJ. Implant-assisted meniscal repair in vivo using a chondrocyte-seeded flexible PLGA scaffold. J Biomed Mater Res A. 2011;99:102–8.
42. Byers BA, Mauck RL, Chiang IE, Tuan RS. Transient exposure to transforming growth factor beta 3 under serum-free conditions enhances the biomechanical and biochemical maturation of tissue-engineered cartilage. Tissue Eng A. 2008;14:1821–34.
43. Chua KH, Aminuddin BS, Fuzina NH, Ruszymah BHI. Insulin-transferrin-selenium prevent human chondrocyte dedifferentiation and promote the formation of high quality tissue engineered human hyaline cartilage. Eur Cell Mater. 2005;9:58–67.
44. Farndale RW, Sayers CA, Barrett AJ. A direct spectrophotometric microassay for sulfated glycosaminoglycans in cartilage cultures. Connect Tissue Res. 1982;9:247–8.
45. Ruan J-L, Tulloch NL, Muskheli V, Genova EE, Mariner PD, Anseth KS, et al. An improved cryosection method for polyethylene glycol hydrogels used in tissue engineering. Tissue Eng Part C Methods. 2013;19:794–801.
46. Silverman RP, Passaretti D, Huang W, Randolph MA, Yaremchuk MJ. Injectable tissue-engineered cartilage using a fibrin glue polymer. Plast Reconstr Surg. 1999;103:1809–18.
47. Passaretti D, Silverman RP, Huang W, Kirchhoff CH, Ashiku S, Randolph MA, et al. Cultured chondrocytes produce injectable tissue-engineered cartilage in hydrogel polymer. Tissue Eng. 2001;7:805–15.
48. Ibusuki S, Papadopoulos A, Ranka M, Halbesma G, Randolph M, Redmond R, et al. Engineering cartilage in a photochemically crosslinked collagen gel. J Knee Surg. 2010;22:72–81.
49. Gu Y, Chen P, Yang Y, Shi K, Wang Y, Zhu W, et al. Chondrogenesis of myoblasts in biodegradable poly-lactide-co-glycolide scaffolds. Mol Med Rep. 2013;7:1003–9.
50. Bryant SJ, Chowdhury TT, Lee DA, Bader DL, Anseth KS. Crosslinking density influences chondrocyte metabolism in dynamically loaded photocrosslinked poly(ethylene glycol) hydrogels. Ann Biomed Eng. 2004;32:407–17.
51. Benton JA, DeForest CA, Vivekanandan V, Anseth KS. Photocrosslinking of gelatin macromers to synthesize porous hydrogels that promote valvular interstitial cell function. Tissue Eng A. 2009;15:3221–30.
52. Skaalure SC, Chu S, Bryant SJ. An enzyme-sensitive peg hydrogel based on aggrecan catabolism for cartilage tissue engineering. Adv Healthc Mater. 2014;4:420–31.
53. Schultz KM, Anseth KS. Monitoring degradation of matrix metalloproteinases-cleavable PEG hydrogels via multiple particle tracking microrheology. Soft Matter. 2013;9:1570.
54. Huey D, Hu J, Athanasiou K. Unlike bone, cartilage regeneration remains elusive. Science. 2012;6933:917–21.
55. Kon E, Verdonk P, Condello V, Delcogliano M, Dhollander A, Filardo G, et al. Matrix-assisted autologous chondrocyte transplantation for the repair of cartilage defects of the knee: systematic clinical data review and study quality analysis. Am J Sports Med. 2009;37:1565–665.

TISSUE ENGINEERING: Part A
Volume 22, Numbers 13 and 14, 2016

DOI: 10.1089/ten.tea.2015.0577

termis
Tissue Engineering
& Regenerative Medicine
International Society

ORIGINAL ARTICLE

Hyaline Articular Matrix Formed by Dynamic Self-Regenerating Cartilage and Hydrogels

Amanda M. Meppelink, BS,[1] Xing Zhao, MD, MS, PhD,[1] Darvin J. Griffin, PhD,[2] Richard Erali, MA,[3] Thomas J. Gill, MD,[4] Lawrence J. Bonassar, PhD,[2] Robert W. Redmond, PhD,[5] and Mark A. Randolph, MAS[3]

Injuries to the articular cartilage surface are challenging to repair because cartilage possesses a limited capacity for self-repair. The outcomes of current clinical procedures aimed to address these injuries are inconsistent and unsatisfactory. We have developed a novel method for generating hyaline articular cartilage to improve the outcome of joint surface repair. A suspension of 10^7 swine chondrocytes was cultured under reciprocating motion for 14 days. The resulting dynamic self-regenerating cartilage (dSRC) was placed in a cartilage ring and capped with fibrin and collagen gel. A control group consisted of chondrocytes encapsulated in fibrin gel. Constructs were implanted subcutaneously in nude mice and harvested after 6 weeks. Gross, histological, immunohistochemical, biochemical, and biomechanical analyses were performed. In swine patellar groove, dSRC was implanted into osteochondral defects capped with collagen gel and compared to defects filled with osteochondral plugs, collagen gel, or left empty after 6 weeks. In mice, the fibrin- and collagen-capped dSRC constructs showed enhanced contiguous cartilage matrix formation over the control of cells encapsulated in fibrin gel. Biochemically, the fibrin and collagen gel dSRC groups were statistically improved in glycosaminoglycan and hydroxyproline content compared to the control. There was no statistical difference in the biomechanical data between the dSRC groups and the control. The swine model also showed contiguous cartilage matrix in the dSRC group but not in the collagen gel and empty defects. These data demonstrate the survivability and successful matrix formation of dSRC under the mechanical forces experienced by normal hyaline cartilage in the knee joint. The results from this study demonstrate that dSRC capped with hydrogels successfully engineers contiguous articular cartilage matrix in both nonload-bearing and load-bearing environments.

Introduction

A number of tissue-engineered approaches are being developed to address the shortcomings in articular cartilage repair. These approaches generally can be grouped into three methods: (1) cell suspension, (2) cell-seeded scaffolds, and (3) cellular self-assembly. The cell suspension approach is currently used clinically in autologous chondrocyte implantation (ACI), where a suspension of autologous chondrocytes is injected into cartilage defects and covered with a periosteal patch.[1] Based on this concept, synovial stem cell and bone marrow mesenchymal stem cell suspensions have also been shown to provide symptomatic relief in cartilage lesions in clinical studies.[2–4] However, the primary limitation of cell suspensions is there is no immediate biomechanical support and the tissue generated is often fibrocartilage as opposed to hyaline articular cartilage.

The concept behind cell-seeded scaffold therapies is that incorporating scaffolds into cartilage defects will provide immediate mechanical integrity and promote hyaline cartilage matrix formation. Numerous *in vitro* studies using dispersed chondrocytes encapsulated in various hydrogels have shown elevated collagen type II gene expression with some pericellular areas of hyaline cartilage matrix formation and improved biomechanical properties with increased culture time.[5–7] Nonload-bearing *in vivo* studies in mice with dispersed cells have also demonstrated islands of matrix production and biochemically immature cartilage constructs with evidence that the neotissue does integrate with native cartilage.[8–11] However, the constructs often cannot retain their

[1]Plastic Surgery Research Laboratory, Department of Surgery, Massachusetts General Hospital, Boston, Massachusetts.
[2]Meinig School of Biomedical Engineering, Cornell University, Ithaca, New York.
[3]Laboratory of Musculoskeletal Tissue Engineering, Massachusetts General Hospital, Boston, Massachusetts.
[4]Boston Sports Medicine and Research Institute, Dedham, Massachusetts.
[5]Wellman Center for Photomedicine, Harvard Medical School, Massachusetts General Hospital, Boston, Massachusetts.

volume *in vivo* due to the scaffold's unreliable degradation profile and lack of mechanical integrity with host tissue.[6,10] When these cell-seeded scaffolds have been applied to load-bearing defects *in vivo* in large animals, they commonly generate inconsistent pockets of articular matrix rather than contiguous new cartilage.[12,13]

The self-assembly approach to tissue-engineered cartilage utilizes the ability of chondrocytes in suspension to aggregate in culture and generate hyaline-like cartilage tissue with biochemical and biomechanical characteristics similar to native cartilage.[14–18] These self-assembled constructs have been tested extensively *in vitro* to assess ideal cellular concentration[19] and culture time.[15] They have been shown to generate hyaline-like tissue faster than chondrocytes encapsulated in agarose.[14] To the best of our knowledge, however, these self-assembled constructs have not been tested *in vivo* in articular defects.

To overcome the issues described with current technologies, our group has developed a new hybrid technology to generate durable hyaline articular cartilage matrix with autologous cells to improve the outcome of joint surface repair. A suspension of freshly harvested chondrocytes is cultured *in vitro* for 14 days to allow self-assembly and early extracellular matrix (ECM) formation, thus forming dynamic self-regenerating cartilage (dSRC). The dSRC is then placed in the defect and capped with a hydrogel to ensure the cells stay in the injury and provide integrity until more ECM is deposited and the mechanical integrity improves. The first step of this study was to assess the cartilage matrix formation of dSRC capped with hydrogel in a subcutaneous nonload-bearing rodent cartilage defect repair model. Based on those encouraging results, a pilot study was then performed to examine the cartilage tissue regeneration of dSRC in a load-bearing environment in a swine model.

Materials and Methods

The Institutional Animal Care and Use Committee (IACUC) of the Massachusetts General Hospital (MGH) approved all animal procedures and the collection of discarded tissues. All chemicals were purchased from Sigma (St. Louis, MO) unless otherwise noted.

Cartilage harvest and cell isolation

Articular cartilage with normal, undamaged appearance was harvested from the entire femoral condyle of 3- to 4-month-old Yorkshire swine knees under sterile conditions ($n=29$ knees total). The knees were collected from the discarded tissue of carcasses from other studies at Massachusetts General Hospital. The cartilage was excised, rinsed in phosphate-buffered saline (PBS), minced into 1-mm^3 pieces, and then digested at 37°C on a shaker for 14–18 h in Ham's F-12 media (Invitrogen, Carlsbad, CA) containing 0.1% collagenase type 2 (Worthington Biochemical, Freehold, NJ) and 1% antibiotic/antimycotic solution. The digested tissue was filtered using a 100-μm filter to remove any undigested tissue. The resulting cell suspension of isolated chondrocytes was centrifuged at 250 *g* for 10 min and washed three times in growth media consisting of Ham's F-12 media supplemented with 10% fetal bovine serum (Invitrogen), 1% antibiotic/antimycotic solution, 1% nonessential amino acids (Invitrogen), and 50 μg/mL ascorbic acid. The cell count per milliliter was determined using a hemocytometer and trypan blue to exclude dead cells. Only chondrocyte harvests with a viability of 90% or greater were used in the study.

dSRC construction

To form the dSRC, a cell suspension of 10^7 freshly isolated chondrocytes in 5 mL of growth media was placed into a 15-mL polypropylene tube. The tubes were placed in conical tube racks, laid horizontally, and cultured under horizontal reciprocating motion at 40 cycles per minute for 14 days at 37°C. Media changes were performed every 3–4 days.

Construct preparation and implantation in murine model

To simulate a cartilage defect, rings (8.5 mm outer diameter and 6 mm inner diameter) were punched from swine articular cartilage of the femoral condyle using tubular chisels (Smith & Nephew, London, United Kingdom) and then underwent five freeze/thaw cycles for devitalization.[20] The cartilage rings were devitalized to prevent the chondrocytes in the existing native cartilage from potentially influencing the formation of new cartilage matrix by the dSRC. Any live cells or neomatrix formation must therefore arise from the dSRC chondrocytes.

Before *in vivo* implantation, the dSRC was placed into the center of devitalized cartilage rings and capped with a hydrogel. The dSRC nearly filled the rings (85 mm^3), so ~60 μL of fibrin or collagen gel was added on top of the dSRC to fill the ring and keep the construct in place. To make the fibrin gel, a 110 mg/mL solution of bovine fibrinogen in saline was mixed in equal volume with a 20 U/mL solution of thrombin (King Pharmaceuticals, Bristol, TN) in saline. The collagen gel consisted of bovine collagen type I gel (Invitrogen) diluted to 4% using distilled water, 1 M NaOH, and 10×PBS (resulting pH = 7.2). Based on previous work in our laboratory, a control group consisted of freshly isolated swine chondrocytes that were immediately encapsulated in fibrin gel as a cell suspension of 4×10^7 cells per mL[21] and injected into the center of devitalized rings. All constructs ($n=9$ per group) were implanted into subcutaneous pockets on the backs of nude mice (*nu/nu* mice; Massachusetts General Hospital) and harvested at 6 weeks postimplantation.

Pilot studies in swine model

MGH miniature swine were used for the large animal experiments. These animals are particularly suitable as they are syngeneic and allow nonautologous cellular transplantation without immunosuppression.[22] Chondrocytes were harvested from the femoral condyle articular cartilage of a donor swine, chopped, digested, and cultured as dSRC for 2 weeks before implantation, as described earlier. To examine cartilage matrix formation in a load-bearing environment, chondral defects were created in swine knees ($n=4$ swine). Under sterile conditions, sixteen 2-mm-diameter holes were created using a biopsy punch in the patellar groove of each MGH miniature swine to a depth of 5 mm. The defects in each of the four swine were filled with four different treatments ($n=4$ per group): (1) dSRC capped with collagen gel; (2) collagen gel alone; (3) empty as a negative control; and (4) 2 mm osteochondral plug as a positive control. Collagen gel was used because it is better tolerated and

generates less of an inflammatory response in the swine knee (unpublished observation, Massachusetts General Hospital). Osteochondral plugs were collected while creating the defects and used for the positive control. The knee was harvested at 6 weeks postsurgery.

Histological analysis

Two constructs from each group in the murine study were randomly selected and placed in 10% phosphate-buffered formalin for 48 h, embedded in paraffin, and sectioned. The defects from the swine knees were fixed in 10% phosphate-buffered formalin, decalcified using EDTA, and then embedded in paraffin for histological analysis. In addition, dSRC samples after 14 days of *in vitro* culture and native swine articular cartilage from the femoral condyle were fixed in 10% phosphate-buffered formalin, embedded in paraffin, and sectioned. Sections from animal models, *in vitro* samples, and native swine cartilage were stained with hematoxylin and eosin (H&E) to assess the morphology of the engineered tissue. Following deparaffinization and hydration, sections were stained with hematoxylin (Leica, Buffalo Grove, IL) for 10 min followed by brief exposure to 0.25% acid alcohol, distilled water washes, bluing reagent (StatLab, McKinney, TX) for 1 min, additional washes in distilled water, 95% ethanol for 30 s, and finally, eosin (Leica) for 90 s.

Additional sections from animal models, *in vitro* samples, and native swine cartilage were stained with Safranin-O to qualitatively analyze the production of sulfated glycosaminoglycans (GAG). Sections were deparaffinized, hydrated, then stained with hematoxylin for 5 min, washed in distilled water, differentiated briefly in 1% acid-alcohol, and rinsed again in distilled water. The slides were then exposed to 0.02% Fast Green for 1 min, 1% acetic acid for 30 s, and finally, 1% Safranin-O for 30 min. After dehydration and clearing, both H&E and Safranin-O sections were coverslipped using Permount (Fisher, Pittsburg, PA).

For immunohistochemical analysis of animal models and native swine cartilage sections, the rabbit anti-pig collagen type I (COL I) antibody (Abcam, Cambridge, MA) and rabbit anti-pig collagen type II (COL II) antibody (Abcam) were used. The antibodies were diluted 1:1000 in 10% goat serum and 3% bovine serum albumin blocking buffer before use. For antigen retrieval, sections were treated with 2% bovine testicular hyaluronidase for 30 min and then BLOXALL (Fisher) for 5 min to inactivate endogenous peroxidase. After 30 min in the blocking buffer, the sections were incubated with the primary antibody for 60 min. In negative controls, no primary antibody was used on the section. Sections were washed extensively in PBS, incubated with a rabbit-labeled polymer-HRP secondary antibody (Dako, Glostrup, Denmark) for 30 min, and washed again in PBS (3×5 min). The immunoreaction was detected using 3,3′-diaminobenzidine (DAB) chromogen solution (Dako) for 3 min. Finally, sections were washed in distilled water and counterstained with hematoxylin to visualize the cell nuclei.

Biochemical analysis

The biochemical content of constructs in the murine model and native swine articular cartilage harvested from the femoral condyle was quantified using GAG and hydroxyproline assays ($n=5$–8 per group GAG, $n=7$–10 per group hydroxyproline). First, each construct was weighed and digested with papain solution [20 μg/mL papain, 100 mM sodium acetate, 10 mM EDTA, and 5 mM L-cysteine in 0.2 M sodium phosphate buffer (pH 6.4)] at 60°C for 16 h. The digested sample was then used for both assays.

The total content of sulfated proteoglycans and GAG per construct was measured using the dimethylene blue method.[23] After incubation with the dye reagent (Biocolor, Carrickfergus, United Kingdom) containing 1,9-dimethyl-methylene blue, the dissociation reagent (Biocolor) containing the sodium salt of an anionic surfactant was added to dissociate the sGAG-dye complex and enhance the spectrophotometric absorption profile. The absorbance was measured at 656 nm. A standard curve was generated using authentic bovine tracheal chondroitin 4-sulfate (Biocolor).

The hydroxyproline level, used as an indicator of collagen content, per construct was determined by the chloramine-T method.[24] The papain digests were hydrolyzed with equal volumes of 12 M hydrochloric acid at 120°C for 3 h. Addition of the chloramine T oxidation buffer mixture was followed by addition of 4-(dimethylamino)benzaldehyde (DMAB) diluted with perchloric acid to the hydrolyzed samples. The absorbance was measured at 560 nm, and a standard curve was generated using standard hydroxyproline provided in the kit. All samples were tested in triplicate and standards run in duplicate. The content of each construct was reported as percentage of wet tissue weight.

Biomechanical analysis

Methods for analysis of the compressive properties of constructs in the murine model were based on those described previously.[25] Full-thickness cylindrical plugs (3 mm diameter) were harvested from the constructs using a biopsy punch (Miltex, York, PA) applied perpendicular to the articular surface ($n=4$–9 per group). The plugs were thawed in a bath of PBS containing protease inhibitors (Invitrogen). Before testing, sample heights were measured using a caliper. Samples were placed in a 3 mm confining chamber, covered with a porous plug and PBS with protease inhibitors (Sigma-Aldrich, St. Louis, MO), and mounted to an EnduraTEC ELF 3200 (Bose, Eden Prairie, MN) for testing. A series of 5% steps in compressive strain were imposed on each sample up to a total of 40% strain. For each step, the resultant load was measured for 10 min using a Honeywell 50lb load cell (Bose) at a frequency of 1 Hz. The stress–relaxation curves were fit to a poroelastic model and analyzed using custom MATLAB code to calculate aggregate modulus (Ha).[26,27]

Statistical analysis

Biochemical and biomechanical results were compared between each of the dSRC groups and the control group using a Student's *t*-test with unpaired data and unequal variance. The level of significance was set at $p<0.05$ in all statistical tests. Mean values were reported with standard deviation.

Results

Histological evaluation of constructs in murine model

The dSRC was hypercellular with respect to native cartilage and appeared to generate cartilage matrix after 14 days of *in vitro* culture as evidenced by slight cytoplasmic positive

Safranin-O staining for proteoglycans and GAG (Fig. 1). After a further 6 weeks *in vivo*, the dSRC constructs capped with fibrin and collagen hydrogels generated extensive, contiguous cartilage matrix as demonstrated in Figure 2. Grossly, dSRC capped with hydrogels generated tissue, which filled the cartilage rings and resembled native articular cartilage in appearance, texture, and resistance to compression when pressed by forceps as opposed to the thin, clear tissue produced by the control group of chondrocytes encapsulated in fibrin gel. Intense Safranin-O staining showed greater proteoglycan and GAG content in the dSRC groups compared to chondrocytes encapsulated in fibrin gel.

Immunohistochemical staining confirmed that the new matrix formed in all experimental groups was similar to native articular cartilage and consisted predominantly of collagen type II and no collagen type I, typical of hyaline normal cartilage (Fig. 2). In addition, there was evidence of neocartilage penetrating into the surrounding cartilage ring (Fig. 3). There were very few gaps and very minimal collagen type I staining observed at the interface of the generated cartilage matrix of the dSRC groups and the native cartilage rings. More prevalent gaps were seen in the control group where additional fibrous connective tissue was evident interposing between the construct and native cartilage ring. Qualitatively, the dSRC group had a higher cellular density than native cartilage, but the cell morphology is similar to that in native cartilage with some early evidence of lacunae formation.

Biochemical analysis of constructs in murine model

The amount of GAG in the dSRC group capped with fibrin gel was 19.89 ± 10.1 μg/mg wet tissue and the dSRC group capped with collagen gel was 17.81 ± 11.7 μg/mg wet tissue (Fig. 4) after 6 weeks *in vivo*. This was 32% and 28% of the amount measured in mature native swine articular cartilage (61.97 ± 0.5 μg/mg wet tissue), respectively. Both dSRC groups showed a statistically significant increase in GAG content compared to the control group of chondrocytes encapsulated in fibrin gel, 5.95 ± 2.6 μg/mg wet tissue ($p = 0.005$ fibrin, $p = 0.02$ collagen).

The amount of hydroxyproline measured was 1.61 ± 0.6 μg/mg wet tissue in the dSRC constructs capped with fibrin gel and 2.41 ± 1.4 μg/mg wet tissue in the dSRC constructs capped with collagen gel compared to 1.01 ± 0.3 μg/mg wet tissue in the encapsulated chondrocyte control group (Fig. 4). This was a statistically significant increase for both hydrogel-capped dSRC groups compared to the control, $p = 0.02$. The dSRC capped with fibrin gel measured 39% and the collagen gel-capped constructs measured 58% of the hydroxyproline content found in native cartilage (4.18 ± 0.3 μg/mg wet tissue).

Biomechanical analysis of constructs in murine model

The aggregate modulus was found to be $2.10 \times 10^5 \pm 1.7 \times 10^5$ Pa per construct for dSRC samples capped with fibrin gel, $1.87 \times 10^5 \pm 0.2 \times 10^5$ Pa per construct for dSRC samples capped with collagen gel, and $2.89 \times 10^5 \pm 1.5 \times 10^5$ Pa per construct for encapsulated chondrocyte control group (Fig. 4). There was no statistical difference observed between each dSRC group and the control of cells encapsulated ($p = 0.1$ fibrin, $p = 0.06$ collagen).

Pilot study in swine model: histological evaluation

Following the promising results of dSRC constructs in the nonload-bearing and immunocompromised mouse model study, a collagen gel was used in the pilot *in vivo* swine model as opposed to fibrin because the former is better tolerated and generates less of an inflammatory response in the swine knee. The osteochondral defects filled with dSRC and capped with collagen gel showed enhanced contiguous cartilage matrix after 6 weeks *in vivo* in a load-bearing environment compared to defects filled with collagen gel alone and those left empty (Fig. 5). The illustrative images in Figure 5 show that the dSRC group produced a smooth and intact articular cartilage surface as opposed to the acellular collagen gel group and empty group, which generated an uneven articular surface and an unequal distribution of the cartilage tissue. In all groups, no gaps were observed between the neotissue and subchondral bone. The positive control group of osteochondral plugs filled the defects with existing articular cartilage as the example shows in Figure 5, but in many of the plug-filled defects, the articular surface remained uneven (results not shown).

Immunohistochemical staining demonstrated that the neocartilage formed in the dSRC defects was predominantly collagen II with no evidence of collagen I present. The collagen gel defects were filled with fibrous tissue as evident by positive collagen I staining, while the empty defects demonstrated variable staining with some areas staining positive for collagen II, hyaline cartilage, and some areas for collagen I, fibrous tissue. There is variation among all the defects, but the images shown in Figure 5 are representative of the defects in all four swine.

Continuous lateral integration between the neotissue and the native cartilage borders of the defect was observed in all groups (Fig. 6). All experimental groups were hypercellular compared to native cartilage likely because of the bone marrow cells released from the bleeding of the subchondral bone during creation of the defects. In addition, lacunae were evident in the dSRC-filled, empty, and plug-filled defects. Lacunae were not evident in the collagen gel-filled defects.

Discussion

Articular cartilage is avascular and has little ability to heal or regenerate, which makes restoration of the articular surface after injury particularly challenging. Although various methods are used clinically, as yet, there is no ideal method for generating hyaline articular cartilage for joint surface repair. In this study, a new approach that involves generation of dSRC *in vitro* and then hydrogel capping in an articular cartilage defect model was found to generate extensive cartilage matrix in a nonload-bearing *in vivo* environment in rodents. The generated tissue was found to have morphological, histological, and biochemical characteristics of native articular cartilage.

Histological analysis demonstrated that dSRC constructs capped with fibrin and collagen gel generated noticeably improved hyaline articular cartilage compared to isolated chondrocytes encapsulated in fibrin gel. In addition, the thin area surrounding all constructs staining positive for collagen I (Fig. 2) was remnant connective tissue that encapsulated the constructs *in vivo*. It is important to note in the collagen-

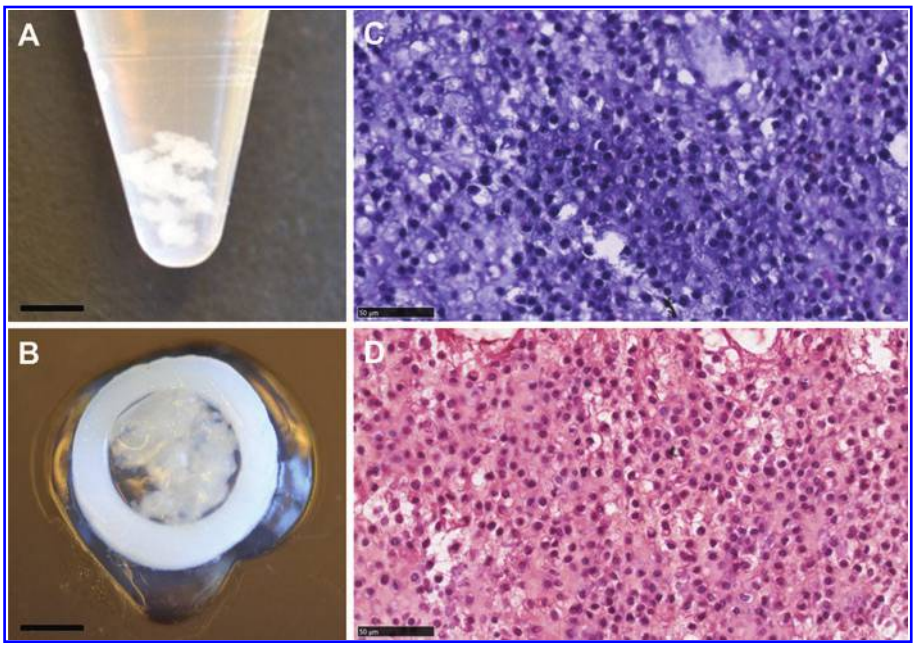

FIG. 1. dSRC formation in culture tube following 14 days of dynamic reciprocating culture **(A)**, and then, dSRC in decellularized swine cartilage ring capped with fibrin gel and ready for implantation in mouse **(B)**. After *in vitro* culture, H&E **(C)** staining shows a high cellularity and the beginning of lacunae formation, and Safranin-O **(D)** shows slightly positive cytoplasmic staining indicative of cartilage matrix formation. Scale bars = 3 mm **(A, B)** and 50 μm **(C, D)**. dSRC, dynamic self-regenerating cartilage; H&E, hematoxylin and eosin.

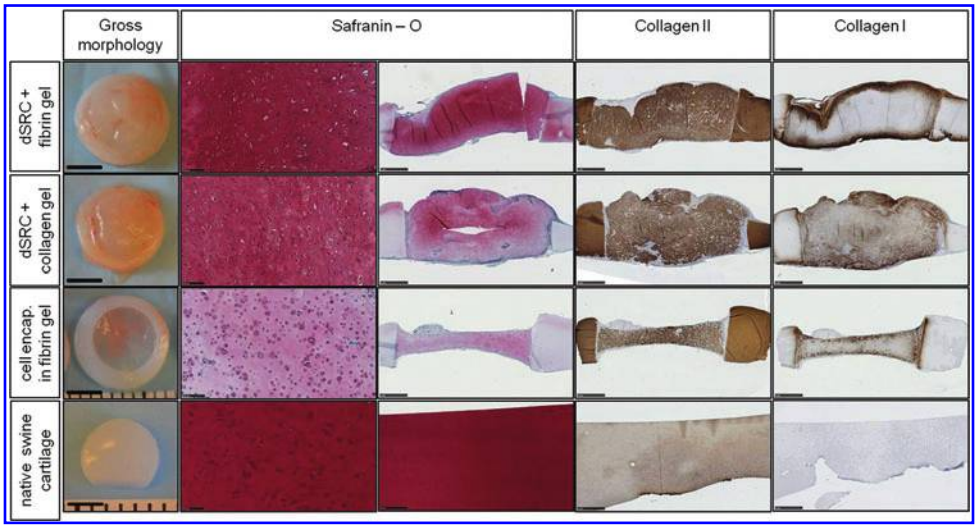

FIG. 2. Histological evaluation of constructs after 6 weeks in murine model. Gross morphology, Safranin-O staining, and immunohistochemical staining for collagen II and collagen I of experimental groups—dSRC capped with fibrin gel, dSRC capped with collagen gel, and chondrocytes encapsulated in fibrin gel—compared to native swine articular cartilage. Scale bars = 3 mm, gross morphology; 100 μm, Safranin-O *column I*; 1 mm, Safranin-O *column II*, collagen II, and collagen I.

capped dSRC group that the observed slightly positive staining for collagen type I is due to the type I bovine collagen gel used initially to cap the dSRC constructs. Biochemical analyses further demonstrated that the dSRC constructs produced significantly more ECM components than the control group with values characteristic of articular cartilage.

Biomechanical analysis is an important indication of a construct's likelihood to withstand the mechanical forces of the joint. The testing performed on the nonload-bearing

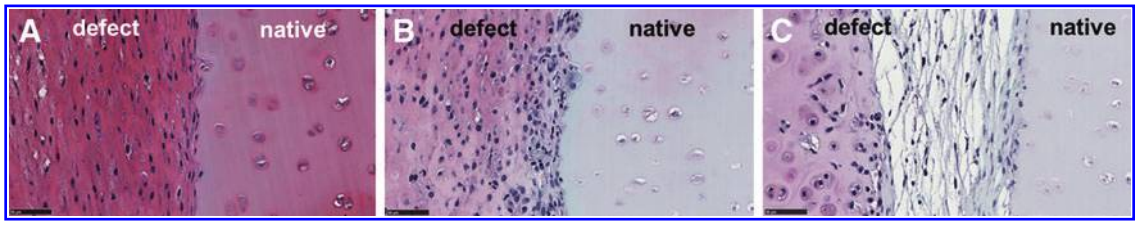

FIG. 3. As indicated by Safranin-O staining, evidence of dSRC capped with fibrin gel **(A)** and collagen gel **(B)** integrating with native cartilage after 6 weeks in murine model. Larger gaps were observed between chondrocytes encapsulated in fibrin gel **(C)** and the native ring. Scale bars = 50 μm.

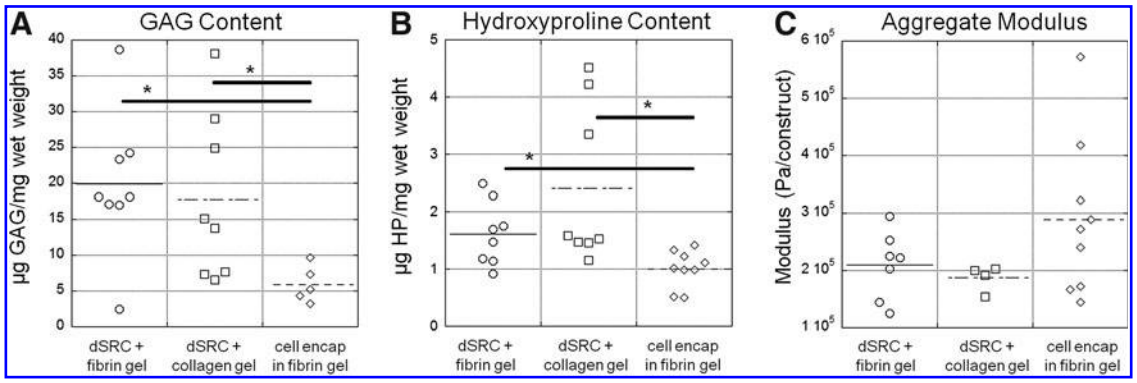

FIG. 4. Biochemical and biomechanical results after 6 weeks in murine model. Dot plots of the **(A)** GAG content, **(B)** hydroxyproline content, **(C)** aggregate modulus for dSRC capped with fibrin and collagen gel and chondrocytes encapsulated in fibrin gel. There was a statistically significant difference in GAG content and hydroxyproline content between the dSRC groups and the cell-encapsulated control. No statistical difference in aggregate modulus. $*p < 0.05$. GAG, glycosaminoglycans.

in vivo samples in this study resulted in wide-ranging aggregate modulus values. These variable data are likely because the constructs implanted in subcutaneous pockets on nude mice were not subject to mechanical forces, thus resulting in mechanically immature cartilage matrix and partially because of the inherent variability of biological samples. Despite the inconclusive results, the constructs subsequently demonstrated they are capable of generating matrix under the normal mechanical forces in the *in situ* load-bearing environment of the swine model.

An important distinction between chondrocytes encapsulated in hydrogel and dSRC constructs is the time-dependent progression of matrix formation. As depicted in the cartoon schematic of Figure 7, cells suspended in a gel have not begun to generate matrix after 14 days *in vitro* and the matrix formed after 6 weeks *in vivo* is isolated around the individual cells. In comparison, cells cultured in suspension under motion begin generating pockets of hypercellular matrix *in vitro* after 14 days and as the neomatrix develops, the cellular density becomes lower and the matrix formation is more expansive after 6 weeks *in vivo*. The enhanced cell-to-cell communication and resulting matrix formation distinguish dSRC constructs from other tissue-engineered approaches and this likely explains the consistent, extensive production of cartilage matrix by dSRC constructs.

To date, self-assembly studies are limited to *in vitro* culture conditions, and hence, it is challenging to draw parallel comparisons between prior results and the current study. The dSRC method for cartilage formation differs from other self-assembly methods because the cell suspension is subjected to constant reciprocating motion during culture, as opposed to static culture.[14,16] In pilot studies, we found that a cell suspension under motion resulted in homogeneous matrix formation after 6 weeks *in vivo*, but that was not seen following culture of the same cell suspension without motion (data not shown). This observation was consistent with other studies that noted nonuniform Safranin-O staining after *in vitro* culture.[16] The biochemical composition of the constructs using a static self-assembly method *in vitro* was one-third that of native articular cartilage, which is less than the *in vivo* results of this study.[14] In addition, the constructs generated were very thin and would be unable to fill chondral defects in the knee joint.[14] On the contrary, our dSRC study demonstrated a robust ability to generate neocartilage that filled a model chondral defect.

The murine study in this work served as a screening tool to assess the potential effectiveness of the dSRC constructs before beginning a swine study. The positive *in vivo* results of dSRC treatments in the nonload-bearing murine model indicated that the constructs had the potential to be effective in swine. Whereas many tissue-engineered approaches are not reproducible under true load-bearing conditions, this approach was successfully applied in a swine pilot study.[12,13] The hydrogel-capped dSRC constructs in swine osteochondral defects demonstrated contiguous new hyaline articular cartilage matrix and seamless integration with native cartilage under the normal mechanical forces of the swine knee.

These initial findings suggest that the dSRC method may successfully address the shortcomings of current clinical therapies. OATS, the transfer of osteochondral plugs of nonweight-bearing cartilage to a chondral defect, can result in surface irregularities of the lesion due to plug placement.[28] This inadequacy was seen in nearly all plug-filled defects in our study, but in very few dSRC-filled injuries. In microfracture, small holes created in the subchondral bone are thought to release bone marrow cells to populate the cartilage defect; however, long-term results are poor because the fibrocartilage that forms wears down under the mechanical forces of the knee.[29] This limitation was seen in the empty defects of this pilot study where the defects filled inconsistently with hyaline and fibrocartilage. ACI is another clinical therapy known to result in fibrous cartilage despite the injection of previously extracted chondrocytes into the chondral defect under a periosteum patch.[1,30] However, dSRC-filled defects did not suffer the same shortcomings of the current clinical therapies and consistently regenerated with hyaline cartilage matrix.

These promising early results of dSRC with hydrogel capping provide motivation for additional load-bearing *in vivo* studies with larger, critical-sized defects and longer regeneration times. The results with 2 mm defects demonstrate that dSRC constructs produce hyaline cartilage that is capable of withstanding normal loads and integrates with

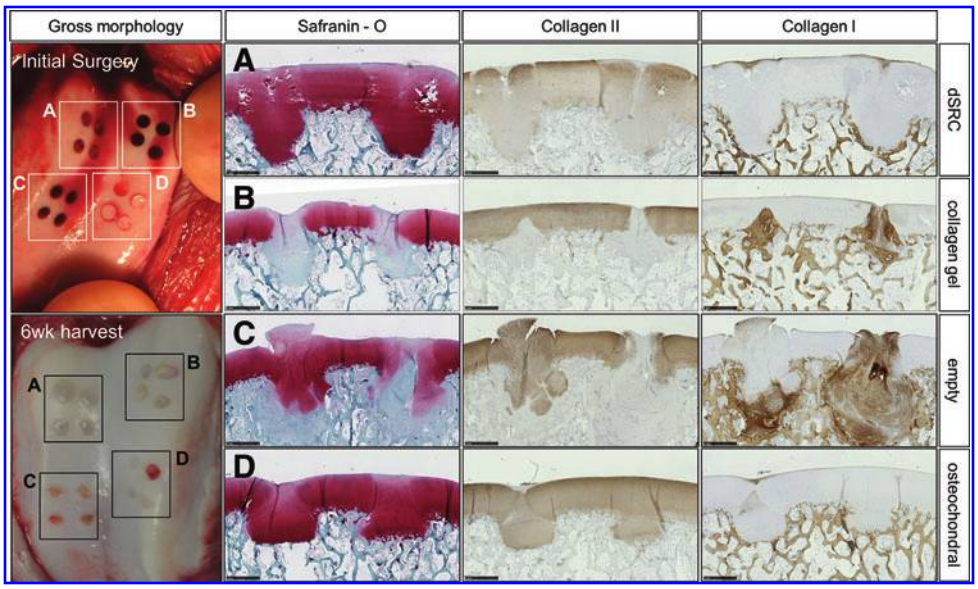

FIG. 5. Histological evaluation of osteochondral defects after 6 weeks in swine model. Gross morphology of defects at time of surgery and at 6 weeks of harvest. Safranin-O staining and collagen II and collagen I immunohistochemical staining of defects filled with **(A)** dSRC and capped with collagen gel, **(B)** filled with collagen gel, **(C)** left empty, and **(D)** filled with osteochondral plug. Scale bars = 1 mm. Fragments of sections missing are histological artifacts.

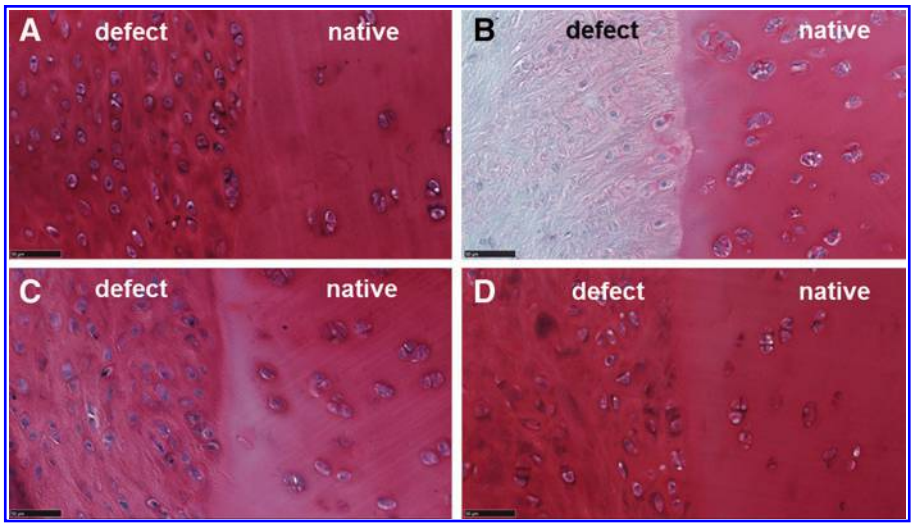

FIG. 6. Integration of osteochondral defects and native cartilage after 6 weeks in swine model as evidenced by Safranin-O staining. Continuous lateral integration of native articular cartilage and defects filled with **(A)** dSRC and capped with collagen gel, **(B)** filled with collagen gel, **(C)** left empty, and **(D)** filled with osteochondral plug. In addition, the cell morphology in the neocartilage of the dSRC group **(A)** is similar although hypercellular compared to native cartilage. Scale bars = 50 μm.

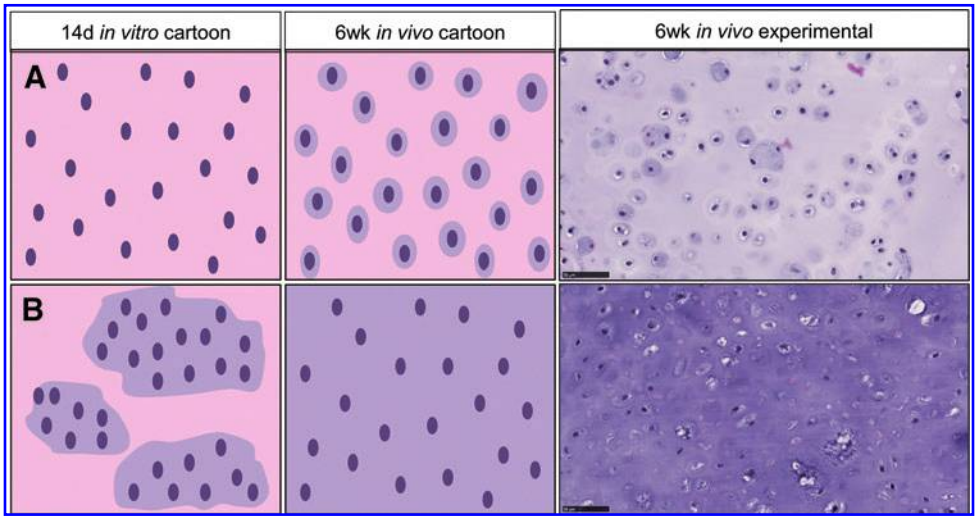

FIG. 7. Comparison of chondrocyte and dSRC matrix formation. **(A)** Chondrocytes encapsulated in fibrin gel generated no cartilage matrix after 14 days of *in vitro* culture and matrix formed in pockets around the cells after 6 weeks *in vivo* as depicted in cartoon schematics and supported by experimental H&E histology. **(B)** dSRC capped with fibrin gel began generating cartilage matrix during *in vitro* culture, and neocartilage was expansive after 6 weeks *in vivo* as depicted in the cartoon schematics and supported by experimental constructs. Scale bars = 10 μm.

native tissue, but success in larger defects over a longer duration is paramount for clinical translation. It would also be interesting to examine the mechanical effects of using photocrosslinked hydrogel as the capping scaffold to determine if that improves hyaline matrix formation. We have now initiated a large controlled study of larger defects in a swine model to address these questions.

Conclusion

In conclusion, this study demonstrates that dSRC capped with a hydrogel successfully generates contiguous hyaline articular cartilage *in vivo* in nonload-bearing and load-bearing environments. This novel method utilizing autologous cells has the potential to improve the outcome of joint surface repair.

Acknowledgments

This study was supported by a grant from the Department of Defense (Award Number W81XWH-10-1-0791). The content of the articles does not necessarily reflect the position or the policy of the Government, and no official endorsement should be inferred. Special thanks to Tricia Della Pelle and Nicole Brousides for their work in histological processing as well as Jie Zhao, MD, PhD, for her help with the immunohistochemical staining. The authors also thank Joseph Locascio, PhD, for assistance on the statistical analysis.

Disclosure Statement

No competing financial interests exist.

References

1. Brittberg, M., Lindahi, A., Nilsson, A., Ohlsson, C., Isaksson, O., and Peterson, L. Treatment of deep cartilage defects in the knee with autologous chondrocyte transplantation. N Engl J Med **331,** 889, 1994.
2. Sekiya, I., Muneta, T., Horie, M., and Koga, H. Arthroscopic transplantation of synovial stem cells improves clinical outcomes in knees with cartilage defects. Clin Orthop Relat Res **473,** 2316, 2015.
3. Wakitani, S., Okabe, T., Horibe, S., Mitsuoka, T., Saito, M., Koyama, T., *et al.* Safety of autologous bone marrow-derived mesenchymal stem cell transplantation for cartilage repair in 41 patients with 45 joints followed for up to 11 years and 5 months. J Tissue Eng Regen Med **5,** 146, 2011.
4. Nejadnik, H., Hui, J.H., Feng Choong, E.P., Tai, B.C., and Lee, E.H. Autologous bone marrow-derived mesenchymal stem cells versus autologous chondrocyte implantation: an observational cohort study. Am J Sports Med **38,** 1110, 2010.
5. Kang, J.Y., Chung, C.W., Sung, J.H., Park, B.S., Choi, J.Y., Lee, S.J., *et al.* Novel porous matrix of hyaluronic acid for the three-dimensional culture of chondrocytes. Int J Pharm **369,** 114, 2009.
6. Ibusuki, S., Halbesma, G.J., Randolph, M.A., Redmond, R.W., Kochevar, I.E., and Gill, T.J. Photochemically crosslinked collagen gels as three-dimensional scaffolds for tissue engineering. Tissue Eng **13,** 1995, 2007.
7. Lee, C.S., Gleghorn, J.P., Won Choi, N., Cabodi, M., Stroock, A.D., and Bonassar, L.J. Integration of layered chondrocyte-seeded alginate hydrogel scaffolds. Biomaterials **28,** 2987, 2007.
8. Zhao, X., Bichara, D.A., Ballyns, F.P., Yoo, J.J., Ong, W., Randolph, M.A., *et al.* Properties of cartilage engineered from elderly human chondrocytes for articular surface repair. Tissue Eng Part A **18,** 1490, 2012.
9. Papadopoulos, A., Bichara, D.A., Zhao, X., Ibusuki, S., Randolph, M.A., Anseth, K.S., *et al.* Injectable and photopolymerizable tissue-engineered auricular cartilage using poly(ethylene glycol) dimethacrylate copolymer hydrogels. Tissue Eng Part A **17,** 161, 2011.
10. Passaretti, D., Silverman, R., Huang, W., Kirchhoff, H., Ashiku, S., Randolph, M.A., *et al.* Cultured chondrocytes produce injectable tissue-engineered cartilage in hydrogel polymer. Tissue Eng **7,** 805, 2001.
11. Johnson, T., Xu, J., Zaporojan, V., Mesa, J.M., Weinand, C., Randolph, M.A., *et al.* Integrative repair of cartilage with articular and nonarticular chondrocytes. Tissue Eng **10,** 1308, 2004.
12. Filova, E., Jelinek, F., Handl, M., Lytvynets, A., Rampichova, M., Varga, F., *et al.* Novel composite hyaluronan/type I collagen/fibrin scaffold enhances repair of osteochondral defect in rabbit knee. J Biomed Mater Res B Appl Biomater **87,** 415, 2008.
13. Pulliainen, O., Vasara, A.I., Hyttinen, M.M., Tiitu, V., Valonen, P., Kellomaki, M., *et al.* Poly-L-D-lactic acid scaffold in the repair of porcine knee cartilage lesions. Tissue Eng **13,** 1347, 2007.
14. Mesallati, T., Buckley, C.T., and Kelly, D.J. A comparison of self-assembly and hydrogel encapsulation as a means to engineer functional cartilaginous grafts using culture expanded chondrocytes. Tissue Eng Part C Methods **20,** 52, 2014.
15. Ofek, G., Revell, C.M., Hu, J.C., Allison, D.D., Grande-Allen, K.J., and Athanasiou, K.A. Matrix development in self-assembly of articular cartilage. PLoS One **3,** e2795, 2008.
16. Hu, J.C., and Athanasiou, K.A. A self-assembling process in articular cartilage tissue engineering. Tissue Eng **12,** 969, 2006.
17. Kraft, J.J., Jeong, C., Novotny, J.E., Seacrist, T., Chan, G., Domzalski, M., *et al.* Effects of hydrostatic loading on a self-aggregating, suspension culture-derived cartilage tissue analog. Cartilage **2,** 254, 2011.
18. Novotny, J.E., Turka, C.M., Jeong, C., Wheaton, A., Li, C., Presedo, A., *et al.* Biomechanical and magnetic resonance characteristics of cartilage-like equivalent generated in a suspension culture. Tissue Eng **12,** 2755, 2006.
19. Revell, C.M., Reynolds, C.E., and Athanasiou, K.A. Effects of initial cell seeding in self assembly of articular cartilage. Ann Biomed Eng **36,** 1441, 2008.
20. Tognana, E., Chen, F., Padera, R.F., Leddy, H.A., Christensen, S.E., Guilak, F., *et al.* Adjacent tissues (cartilage, bone) affect the functional integration of engineered calf cartilage in vitro. Osteoarthritis Cartilage **13,** 129, 2005.
21. Silverman, R., Passaretti, D., Huang, W., Randolph, M.A., and Yaremchuk, M.J. Injectable tissue-engineered cartilage using fibrin glue polymer. Plast Reconstr Surg **103,** 1809, 1999.
22. Mezrich, J.D., Haller, G.W., Arn, J.S., Houser, S.L., Madsen, J.C., and Sachs, D.H. Histocompatible miniature swine: an inbred large-animal model. Transplantation **75,** 904, 2003.

23. Taylor, K., and Jeffree, G. A new basic metachromatic dye, 1:9-dimethyl methylene blue. Histochem J **1,** 199, 1969.
24. Reddy, G., and Enwemeka, C. A simplified method for the analysis of hydroxyproline in biological tissues. Clin Biochem **29,** 225, 1996.
25. Griffin, D.J., Bonnevie, E.D., Lachowsky, D.J., Hart, J.C., Sparks, H.D., Moran, N., *et al.* Mechanical characterization of matrix-induced autologous chondrocyte implantation (MACI(R)) grafts in an equine model at 53 weeks. J Biomech **48,** 1944, 2015.
26. Gleghorn, J.P., Jones, A.R.C., Flannery, C., and Bonassar, L. Boundary mode frictional properties of engineered cartilaginous tissues. Eur Cell Mater **14,** 20, 2007.
27. Chang, S.C.N., Rowley, J.A., Tobias, G., Genes, N.G., Roy, A.K., Mooney, D.J., *et al.* Injection molding of chondrocyte/alginate constructs in the shape of facial implants. J Biomed Mater Res **55,** 503, 2001.
28. Berta, A., Duska, Z., Toth, F., and Hangody, L. Clinical experiences with cartilage repair techniques: outcomes, indications, contraindications and rehabilitation. Eklem Hastalik Cerrahisi **26,** 84, 2015.
29. Kreuz, P.C., Steinwachs, M.R., Erggelet, C., Krause, S.J., Konrad, G., Uhl, M., *et al.* Results after microfracture of full-thickness chondral defects in different compartments in the knee. Osteoarthritis Cartilage **14,** 1119, 2006.
30. Richardson, J., Caterson, B., Evans, E., Ashton, B., and Roberts, S. Repair of human articular cartilage after implantation of autologous chondrocytes. J Bone Joint Surg Am **81-B,** 1064, 1999.

Address correspondence to:
Mark A. Randolph, MAS
Plastic Surgery Research Laboratory
Massachusetts General Hospital
15 Parkman Street
WAC 435
Boston, MA 02114

E-mail: marandolph@mgh.harvard.edu

Received: December 23, 2015
Accepted: June 17, 2016
Online Publication Date: July 1, 2016

APPENDIX 6

The Characterization Of Local Interfacial Mechanics in an Articular Cartilage Defect Repair Model

[1]*Darvin J. Griffin,* [2]*Amanda M. Meppelink,* [3]*Mark A. Randolph,* [4]*Itai Cohen,* [1,5]*Lawrence J. Bonassar*

[1]*Nancy E. and Peter C. Meinig School of Biomedical Engineering, Cornell University, Ithaca, NY*

[2]*Plastic Surgery Research Laboratory, Department of Surgery, Massachusetts General Hospital, Boston, MA*

[3]*Laboratory for Musculoskeletal Tissue Engineering, Massachusetts General Hospital, Boston, MA*

[4]*Department of Physics, Cornell University, Ithaca, NY*

[5]*Sibley School of Mechanical and Aerospace Engineering, Cornell University, Ithaca, NY*

***Bonassar, Lawrence, Ph.D.**

Address: 149 Weill Hall, Cornell University, Ithaca, NY, 14853, USA

Email: lb244@cornell.edu; Phone: (607)255-9381; Fax: 607-255-7330

*Corresponding Author

Running Title: Local interfacial mechanics of cartilage

Key words: Cartilage repair • ACI • Confocal Strain mapping

Word Count: 4187

ABSTRACT

The lack of lateral anchoraging and integration of grafted cartilage makes the tissue more susceptible to mechanical failure. Recently, our lab has developed a novel system for measuring the microscale mechanics of native and repaired tissue on the length scale of 20μm. This approach would provide new information about the mechanical environment at the interface of repaired and host native cartilage. The objective of this study was to detect and characterize the local mechanics at the interface of repaired and native articular cartilage. Either fresh cells or cell clusters formed over 14 days were placed in a cartilage ring with a 6mm inner diameter, implanted subcutaneously in female nude mice and harvested at 12 weeks. Samples of the interface were cut into ~2mm cubes (Fig. 2B) and prepared for confocal strain mapping(Fig. 2C, D). Localized strains were measured using particle image velocimetry (PIV) as described previously. Shear deformation was induced by displacing the moveable plate in the direction parallel to the articular surface to produce 1% shear strain. Vector maps and plots of γ_{xy} and ε_{yy} exhibited large strains at the interface. γ_{xy} were lower near the articular surface, and higher in the deep zone. ε_{yy} were higher near the articular surface and remained consistently high in the deep zone(Fig. 3). Additionally, there was a high degree of peeling along the interface, which could infer a new probable delaminating mechanism(Fig. 4). These results shed more light on the mechanical properties for strategic engineered constructs to withstand physiological loads and promote integration in cartilage repair.

INTRODUCTION

Currently, a number of techniques are used for articular cartilage repair, such as subchondral penetration[1,2,3], osteochondral transplantation[4,5,6], autologous chondrocyte transplantation[7,8,9], as well as tissue-engineered grafts[10,11,12]. A major challenge in achieving successful cartilage repair is the integration of repaired cartilage with the adjacent native cartilage. The lack of lateral anchorage and integration of repair or graft tissue leaves the graft susceptible to mechanical failure that could lead to poor prognosis[13,14,15,16,17]. This problem has motivated a great deal of research into methods of enhancing the integration of repair tissue with the surrounding host cartilage.

In vivo studies normally evaluate cartilage repair with biochemical assays and histological methods [5,18,11]; however, the biomechanical behavior of this interface is poorly understood. There have been many studies that measured strength of the integration of cartilage-graft interfaces, including *in vitro* model, subcutaneous or heterotopic *in vivo* models, and orthotropic transplants into joint defects. Such studies have measured integration strength with lap-shear tests[8,13], tensile tests[19] and push out model tests[17,16]. Only a handful of studies have characterized the compressive properties of repair tissue through confined compression[11], indentation[13] and one paper reporting integration strength and tensile properties of repaired tissue from an *in vivo* joint defect[15]. Generally these studies have investigated bulk tissue properties; such as failure strength, stiffness, and failure strain[11,13,15].

This lack of data is in part due to the fact that previous techniques are unable to measure local deformations at such interfaces. As such there is essentially no information on the local deformations that occur at these interfaces during failure. Measuring the deformations would help to identify local mechanisms of tissue failure as well as locate regions of this interface that may be particularly susceptible to failure. Such knowledge would provide a valuable tool for assessing the efficacy of cell-based cartilage repair methods and then inform techniques to improve functional cartilage graft

integration.

Our group has developed a novel system for measuring the local mechanics of native and repaired cartilage via confocal elastography[2,10,20,1,5]. Specifically this technique has measured local shear properties of cartilage on length scale of 20-40μm[22,23,24,25], and has identified large regional variations in mechanical properties along the depth of the tissue. However to date these techniques have not been applied to understanding local mechanics of cartilage-graft interfaces. Therefore the objectives of this study were to: 1) characterize the local mechanics at the interface of repaired and native articular cartilage in a subcutaneous heterotopic transplant model; and 2) assess the effect of chondrocyte culture conditions on the mechanical behavior of the interface.

METHODS

Tissue Preparation & Implantation

Integration of the engineered tissue with existing native cartilage was examined in a system in which engineered cartilage was grown in a cylindrical defect punched in an articular cartilage explant (Fig. 1A, B). All procedures involving animals were approved by the Institutional Animal Care and Use Committee of the Massachusetss General Hospital following the National Institutes of Health Guide for the Care and Use of Laboratory Animals. Articular cartilage was aseptically harvested from the knees of Yorkshire pigs. Articular cartilage was dissected sharply from the underlying bone and minced into 1- to 2-mm fragments under sterile conditions. The cartilage was then digested with 0.1 w/v% collagenase type II (Worthingon, Freehold, NJ) for 12 to 18 hours at 37°C. After digestion, chondrocytes were rinsed and washed twice with chondrocyte growth media. Cell number was determined using the trypan blue dye test. After isolation, the chondrocytes were combined with fibrin gel by two different methods. In the first group, $10x10^6$ cells were placed into a 15 cc polypropylene tube and cultured statically at

37°C for 14 days; producing cell clusters. Chondrocyte growth media containing Ham's F-12 media (Invitrogen, Carlsbad, CA) supplemented with 10% fetal bovine serum (Invitrogen), 1% non-essential amino acids (Invitrogen), 1% antibiotic antimycotic solution (Sigma, St. Louis, MO) and 0.005% ascorbic acid (Sigma) was used for cell culture and changed every 3 to 4 days. Cell clusters were placed in the center of a devitalized 6mm inner diameter swine articular cartilage ring and capped with fibrin gel (Sigma)[12](Fig. 1B). In the control group, fresh chondrocytes containing no pre-culture were immediately encapsulated in fibrin gel as a cell suspension of 40 million cells per mL and injected into the center of devitalized swine articular cartilage ring.

To assess the maturation of the interface between new cartilage and native cartilage, constructs generated as described above were implanted subcutaneously in nude female mice. As described previously, although not a load-bearing model subcutaneous implantation enables rapid construct development under *in vivo* conditions[26,27]. Filled cartilage rings were implanted subcutaneously in the dorsum of nude female mice (*nu/nu* mice; Massachusetts General Hospital, Boston, MA) and harvested at 12 weeks (n=5). The center of the cartilage disk was removed using a 3mm biopsy punch leaving a ring of engineered and native matrix(Fig. 2A). The rings were sliced into 2mm cubes and prepared for mechanical testing to observe local deformations under shear (Fig. 2B).

Histology

Constructs from each group were randomly selected and fixed in 10% phosphate-buffered formalin for 48 hours. Samples were embedded in paraffin and 5μm sections were cut from the middle of the constructs. Sections were stained with hematoxylin and eosin (H&E) to assess morphology of the engineered constructs and integration of the constructs with the cartilage ring. Briefly, sections were stained with hematoxylin (Leica, Buffalo Grove, IL) for 10 minutes, followed by brief exposure to

0.25% acid alcohol and vintage bluing reagent (StatLab, McKinney, TX), and finally stained with eosin (Leica) for 90 seconds.

Confocal Elastography

2mm cubes were placed into a 7 μg/mL of 5-isomer of fluorescein dichlorotriazine (5-DTAF) (Molecular Probes®, Grand Island, NY) solution for 30 min to fluorescently stain the cartilage extracellular matrix[1,2,3,4]. The deep zone of the cubes were glued to a tissue deformation imaging stage (TDIS) and compressed to 7% axial strain (Fig. 2C). The TDIS was mounted on an inverted Zeiss Live 5 confocal microscope and imaged using a 488 nm laser (Fig. 2D). Sinusoidal shear deformations were induced by displacing the moveable plate in the direction parallel to the articular surface by 20μm, yielding an effective shear strain of 1% shear strain, and frequency of 1 Hz. Localized strains were measured using a particle image velocimetry (PIV) algorithm implemented in MATLAB[1]. After each increment of shear strain, multiple snapshots 512×512μm were taken throughout the sample and tiled in order to obtain an image spanning the entire tissue. Images were divided into a grid with 50×50 μm spacing. Using this grid, the displacement fields in the vertical (u) and horizontal (v) directions were calculated by performing particle image velocimetry analysis on confocal images before and after application of shear. These displacement fields used to calculate shear strain γ_{xy} (du/dy)(Fig. 3A) and axial strain ε_{yy} (dv/dy)(Fig. 4A) throughout the sample. To assess spatial variation in local mechanics between samples (n=4), γ_{xy} and ε_{yy} were averaged across y at x= 75μm, 300μm, and 900μm.

RESULTS

Histology

The H&E staining (Fig. 1) confirmed the formation of new cartilage in both chondrocyte groups, but matrix staining in repaired cartilage was different from that of native cartilage. Constructs created using fresh chondrocytes showed dense cellular tissue (Fig. 1C), created a close interface between the repaired and native cartilage. Specifically, outgrowths of new cartilage matrix were observed penetrating or migrating into the native cartilage matrix disc. In contrast, the pre-culture group showed some apparent integration, but not as marked as that observed when the fresh chondrocytes were used (Fig. 1C).

Confocal Elastography

Local deformations of the interface between native and engineered tissue were easily visualized using confocal microscopy (Fig. 2E). Based on images of the undeformed and deformed states, local deformation tensors were obtained using particle image velocimetry and differentiated to calculate strain tensors. Specifically, shear strain applied parallel to the articular surface resulted 2 modes of deformation at the interface: 1) sliding, as quantified by γ_{xy} (du/dy) (Fig. 3) and 2) peeling, as quantified as ε_{yy} (dv/dy) (Fig. 4) at the interface. Intriguingly, sliding (γ_{xy}) did occur at interface despite the applied orthogonal 1% shear strain. Furthermore, sliding was confined to ~100μm near the interface with a peak strain of ~0.5%, nearly half of the applied orthogonal shear strain. Qualitatively, both fresh and pre-culture γ_{xy} vector maps were similar; however averaged peak strains were lower the for fresh group (.002) than pre-culture group (.003) ($p<.05$). In both culture groups sliding was more pronounced deeper in the tissue γ_{xy} ~.002-.003) compared to the tissue surface ($p<.0001$), where γ_{xy} ~.001 (Fig. 5).

Shear loading also induced peeling ε_{yy} (dv/dy) at the interface. Peeling was localized to within

~50μm of interface with a peak strain of ~1.8-2% which was greater than applied shear strain (Fig 4B). The pre-culture group displayed more peeling at interface compared to fresh group (Fig. 4B) ($p<.05$) peak values for pre-culture were >1% at interface and <.25% at interface for the fresh group. Deeper regions of the interface displayed less peeling than the articular surface (Fig. 5) ($p<.05$).

DISCUSSION

Understanding the mechanical properties at the interface of tissue-engineered cartilage is important for improving integrative repair. The goals of the present study were to characterize the local mechanics at the interface of repaired and native cartilage and to determine if different culture conditions affect the mechanical environment at the interface. The results from this study reveal that shear loading induces a complex, spatially heterogeneous response at the interface between repaired and native cartilage. There were two distinct modes of failure identified at the interface: the sliding along the repaired/native cartilage interface and peeling along the direction of shear. In both fresh and pre-culture groups, there was significant sliding along the interface (Fig. 3). The high compliance of this region suggests a lack of anchorage of engineered tissue to the native tissue. Even though histology indicated a well-bonded interface in the fresh group (Fig. 1C), γ_{xy} values at the interface were as high as .005 (Fig. 3). Additionally, there was minimal peeling in fresh samples, but a high degree of peeling for the pre-culture group (Fig. 4). These data indicate that chondrocyte culture conditions can affect the quality of integration and mode of mechanical failure.

Many studies routinely evaluate the quality of repair tissue with qualitative or quantitative assays of tissue structure such as gross observations, histology, and immunohistochemistry[28–30]. Such studies have rated integration using histological scoring systems based on continuity of tissue interfaces generated *in vitro* as well as in heterotopic (subcutaneous) or orthotopic *in vivo* transplantation

models[15,28,30–33]. Such studies have revealed the importance of matrix synthesis and cell migration in generating continuous interfaces. However, relatively few studies have focused on mechanical evaluation of these interfaces in subcutaneous implantation models. For example, previous studies report time dependent increase in tensile strength, failure strain, failure energy, and tensile modulus to values 5–30% of normal articular cartilage[19.27,28]. Further studies by Gratz et al.[33] and Fujie et al.[34], have reported integration mechanical properties from orthotopic *in vivo* cartilage repair models. In an equine model, Gratz et al.[33] reported the bulk tensile properties of the interface indicating that modulus and strength were 12% and 40% of native tissue respectively. A recently published study by Fujie et al.[34] investigated zone-specific integration properties of repaired articular cartilage defects treated in a porcine model. The authors reported an average tensile strengths of the integration boundary compared to normal cartilage were 12%, 25%, and 45% at the superficial, middle, and deep layers, respectively. Although it was possible to determine the depth-dependent strength of the interface by cartilage zone, this technique involves cutting a full-thickness specimen into three pieces and testing each piece individually. A unique feature of the present study is that no sectioning was required and this technique allows spatially continuous assessment of 2D strain fields throughout the depth of cartilage. Because our measurement resolution was 20μm, we were able detect mechanical signatures that may have been obscured at the bulk level. Specifically, we were able to identify two mechanisms of failure based on how the tissue deforms at the interface.

Histological assessments are useful in the analysis of integration, but our results suggest that just the appearance of the interface alone may not be enough to predict effective integration. More importantly, the extracellular matrix constituents may play an important role in the mechanical behavior of repairing the interface. For example, previous studies have suggested that collagen[14] and proteoglycans[17] were important for mechanical integration, but these studies used bulk biochemical and

mechanical assessments. Thus exploring of structure-function relationship across the interface of engineered and native cartilage might be critical for optimum integration. Previously, we have reported combining confocal elastography, with Fourier-transform infrared imaging (FTIR) to identify key structure-property relationships in the local shear behavior of articular cartilage[21]. Applying this approach of measuring both local composition and mechanics may reveal key factors necessary for robust integration of cartilage implants.

Limitations of this study include an evaluation of cartilage integration in murine subcutaneous model. These models are not optimal as the subcutaneous environment is different from the load bearing native cartilage environment. However, the subcutaneous model have been extensively characterized in helping bridge the gap between *in vitro* and *in vivo* load bearing models in larger animals[19,26,27,35]. Additionally, we do note the sample number was n=4. However, even at low numbers we still identified differences in spatial patterns and culture technique.

In conclusion, this study successfully detected the local interfacial mechanics in a subcutaneous defect repair model. The mechanical characterization of the interface of engineered and native tissue provides us with a powerful tool for studying cartilage integration. These results shed more light on the necessary mechanical properties for strategic engineered constructs to withstand physiological loads and promote integration in cartilage repair.

CONFLICT OF INTEREST STATEMENT

There are no conflicts of interest to declare.

ACKNOWLEDGMENTS

This study was supported by a Cornell University, Meing School of Biomedical Engineering, the Department of Defense (award number W81XWH-10-1-0791). The authors would like to thank Lena Bartell for her experimental support.

REFERENCES:

1. Hangody L, Kárpáti Z. 1994. [New possibilities in the management of severe circumscribed cartilage damage in the knee]. [Internet].Magy. Traumatol. Ortop. Kezseb. Plasztikai Seb. 37(3):237–43[cited 2015 Nov 30] Available from: http://www.ncbi.nlm.nih.gov/pubmed/7920908.
2. Nehrer S, Spector M, Minas T. 1999. Histologic analysis of tissue after failed cartilage repair procedures. [Internet].Clin. Orthop. Relat. Res. (365):149–62[cited 2015 Apr 20] Available from: http://www.ncbi.nlm.nih.gov/pubmed/10627699.
3. Jackson DW, Lalor PA, Aberman HM, Simon TM. 2001. Spontaneous repair of full-thickness defects of articular cartilage in a goat model. A preliminary study. [Internet].J. Bone Joint Surg. Am. 83-A(1):53–64[cited 2015 Apr 20] Available from: http://www.ncbi.nlm.nih.gov/pubmed/11205859.
4. Hallal PC, Wells JCK, Bertoldi AD, et al. 2005. A shift in the epidemiology of low body mass index in Brazilian adults. [Internet].Eur. J. Clin. Nutr. 59(9):1002–6[cited 2015 Nov 30] Available from: http://www.ncbi.nlm.nih.gov/pubmed/15970943.
5. Hangody L, Kish G, Kárpáti Z, et al. 1997. Arthroscopic autogenous osteochondral mosaicplasty for the treatment of femoral condylar articular defects. A preliminary report. [Internet].Knee Surg. Sports Traumatol. Arthrosc. 5(4):262–7[cited 2015 Apr 20] Available from: http://www.ncbi.nlm.nih.gov/pubmed/9430578.
6. Mow VC, Ratcliffe A, Rosenwasser MP, Buckwalter JA. 1991. Experimental studies on repair of large osteochondral defects at a high weight bearing area of the knee joint: a tissue engineering study. [Internet].J. Biomech. Eng. 113(2):198–207[cited 2015 Apr 24] Available from: http://www.ncbi.nlm.nih.gov/pubmed/1875694.
7. Peterson L, Brittberg M, Kiviranta I, et al. 2002. Autologous Chondrocyte Transplantation: Biomechanics and Long-Term Durability [Internet].Am. J. Sport. Med. 30(1):2–12[cited 2015 May 13] Available from: http://ajs.sagepub.com/content/30/1/2.short.
8. Henderson I, Lavigne P, Valenzuela H, Oakes B. 2007. Autologous chondrocyte implantation: superior biologic properties of hyaline cartilage repairs. [Internet].Clin. Orthop. Relat. Res. 455:253–61[cited 2015 Feb 5] Available from: http://www.ncbi.nlm.nih.gov/pubmed/16980901.
9. Peterson L, Brittberg M, Kiviranta I, et al. Autologous chondrocyte transplantation. Biomechanics and long-term durability. [Internet].Am. J. Sports Med. 30(1):2–12[cited 2015 Feb 5] Available from: http://www.ncbi.nlm.nih.gov/pubmed/11798989.
10. Griffin D, Bonnevie E, Lachowsky D, et al. 2015. Mechanical Characterization of Matrix-Induced Autologous Chondrocyte Implantation (MACI®) Grafts in an Equine Model at 53 weeks [Internet].J. Biomech. [cited 2015 Apr 18] Available from: http://www.sciencedirect.com/science/article/pii/S0021929015002262.
11. Chu CR, Dounchis JS, Yoshioka M, et al. 1997. Osteochondral repair using perichondrial cells. A 1-year study in rabbits. [Internet].Clin. Orthop. Relat. Res. (340):220–9[cited 2015 Apr 24] Available from: http://www.ncbi.nlm.nih.gov/pubmed/9224260.
12. Madry H, Kaul G, Zurakowski D, et al. 2013. Cartilage constructs engineered from chondrocytes overexpressing IGF-I improve the repair of osteochondral defects in a rabbit model. [Internet].Eur. Cell. Mater. 25:229–47[cited 2015 May 13] Available from:

http://www.ncbi.nlm.nih.gov/pubmed/23588785.

13. Reindel ES, Ayroso AM, Chen AC, et al. 1995. Integrative repair of articular cartilage in vitro: adhesive strength of the interface region. [Internet].J. Orthop. Res. 13(5):751–60[cited 2015 Apr 9] Available from: http://www.ncbi.nlm.nih.gov/pubmed/7472754.

14. DiMicco MA, Waters SN, Akeson WH, Sah RL. 2002. Integrative articular cartilage repair: dependence on developmental stage and collagen metabolism. [Internet].Osteoarthritis Cartilage 10(3):218–25[cited 2015 Apr 23] Available from: http://www.sciencedirect.com/science/article/pii/S1063458401905023.

15. Gratz KR, Wong VW, Chen AC, et al. 2006. Biomechanical assessment of tissue retrieved after in vivo cartilage defect repair: tensile modulus of repair tissue and integration with host cartilage. [Internet].J. Biomech. 39(1):138–46[cited 2015 Apr 20] Available from: http://www.jbiomech.com/article/S0021929004005330/fulltext.

16. van de Breevaart Bravenboer J, In der Maur CD, Bos PK, et al. 2004. Improved cartilage integration and interfacial strength after enzymatic treatment in a cartilage transplantation model. [Internet].Arthritis Res. Ther. 6(5):R469–76[cited 2015 Apr 23] Available from: http://arthritis-research.com/content/6/5/R469.

17. Obradovic B, Martin I, Padera RF, et al. 2001. Integration of engineered cartilage. [Internet].J. Orthop. Res. 19(6):1089–97[cited 2015 Apr 24] Available from: http://www.ncbi.nlm.nih.gov/pubmed/11781010.

18. Brittberg M, Lindahl A, Nilsson A, et al. 1994. Treatment of deep cartilage defects in the knee with autologous chondrocyte transplantation. [Internet].N. Engl. J. Med. 331(14):889–95[cited 2015 Mar 1] Available from: http://www.ncbi.nlm.nih.gov/pubmed/8078550.

19. Peretti GM, Bonassar LJ, Caruso EM, et al. 1999. Biomechanical analysis of a chondrocyte-based repair model of articular cartilage. [Internet].Tissue Eng. 5(4):317–26[cited 2015 Apr 24] Available from: http://www.ncbi.nlm.nih.gov/pubmed/10477854.

20. Buckley MR, Gleghorn JP, Bonassar LJ, Cohen I. 2008. Mapping the depth dependence of shear properties in articular cartilage. [Internet].J. Biomech. 41(11):2430–2437[cited 2014 Feb 7] Available from: http://www.ncbi.nlm.nih.gov/pubmed/18619596.

21. Silverberg JL, Barrett AR, Das M, et al. 2014. Structure-function relations and rigidity percolation in the shear properties of articular cartilage. [Internet].Biophys. J. 107(7):1721–30[cited 2015 Feb 5] Available from: http://www.cell.com/article/S0006349514008546/fulltext.

22. Buckley MR, Bonassar LJ, Cohen I. 2012. Localization of Viscous Behavior and Shear Energy Dissipation in Articular Cartilage Under Dynamic Shear Loading [Internet].J. Biomech. Eng. 135(3):31002[cited 2014 Jan 30] Available from: http://www.ncbi.nlm.nih.gov/pubmed/24231813.

23. Griffin DJ, Vicari J, Buckley MR, et al. 2014. Effects of enzymatic treatments on the depth-dependent viscoelastic shear properties of articular cartilage. [Internet].J. Orthop. Res. 32(12):1652–7[cited 2015 Jan 13] Available from: http://www.ncbi.nlm.nih.gov/pubmed/25196502.

24. Silverberg JL, Dillavou S, Bonassar L, Cohen I. 2013. Anatomic variation of depth-dependent mechanical properties in neonatal bovine articular cartilage. [Internet].J. Orthop. Res. 31(5):686–91[cited 2014 Feb 12] Available from: http://www.ncbi.nlm.nih.gov/pubmed/23280608.

25. Michalek AJ, Buckley MR, Bonassar LJ, et al. 2009. Measurement of local strains in intervertebral disc anulus fibrosus tissue under dynamic shear: contributions of matrix fiber orientation and elastin content. [Internet].J. Biomech. 42(14):2279–2285[cited 2014 Jan 21] Available from: http://www.pubmedcentral.nih.gov/articlerender.fcgi?artid=2757465&tool=pmcentrez&rendertype=abstract.

26. Spangenberg KM, Peretti GM, Trahan CA, et al. 2002. Histomorphometric analysis of a cell-based model of cartilage repair. [Internet].Tissue Eng. 8(5):839–46[cited 2015 Dec 7] Available from: http://online.liebertpub.com/doi/abs/10.1089/10763270260424196.

27. Peretti GM, Zaporojan V, Spangenberg KM, et al. 2003. Cell-based bonding of articular cartilage: An extended study. [Internet].J. Biomed. Mater. Res. A 64(3):517–24[cited 2015 Dec 7] Available from: http://www.ncbi.nlm.nih.gov/pubmed/12579566.

28. Fortier LA, Mohammed HO, Lust G, Nixon AJ. 2002. Insulin-like growth factor-I enhances cell-based repair of articular cartilage. [Internet].J. Bone Joint Surg. Br. 84(2):276–88[cited 2015 Apr 23] Available from: http://www.ncbi.nlm.nih.gov/pubmed/11922373.

29. Strauss EJ, Goodrich LR, Chen C-T, et al. 2005. Biochemical and biomechanical properties of lesion and adjacent articular cartilage after chondral defect repair in an equine model. [Internet].Am. J. Sports Med. 33(11):1647–53[cited 2015 Feb 5] Available from: http://www.ncbi.nlm.nih.gov/pubmed/16093540.

30. Ortved KF, Begum L, Mohammed HO, Nixon AJ. 2015. Implantation of rAAV5-IGF-I transduced autologous chondrocytes improves cartilage repair in full-thickness defects in the equine model. [Internet].Mol. Ther. 23(2):363–73[cited 2015 Apr 20] Available from: http://www.ncbi.nlm.nih.gov/pubmed/25311491.

31. Proffen BL, Sieker JT, Murray MM, et al. 2015. Extracellular matrix-blood composite injection reduces post-traumatic osteoarthritis after anterior cruciate ligament injury in the rat. [Internet].J. Orthop. Res. [cited 2015 Dec 9] Available from: http://www.ncbi.nlm.nih.gov/pubmed/26629963.

32. Faschingbauer M, Renner L, Waldstein W, Boettner F. 2015. Are lateral compartment osteophytes a predictor for lateral cartilage damage in varus osteoarthritic knees? : Data from the Osteoarthritis Initiative. [Internet].Bone Joint J. 97-B(12):1634–9[cited 2015 Dec 9] Available from: http://www.ncbi.nlm.nih.gov/pubmed/26637677.

33. Gratz KR, Wong VW, Chen AC, et al. 2006. Biomechanical assessment of tissue retrieved after in vivo cartilage defect repair: tensile modulus of repair tissue and integration with host cartilage. [Internet].J. Biomech. 39(1):138–46[cited 2015 Apr 20] Available from: http://www.ncbi.nlm.nih.gov/pubmed/16271598.

34. Fujie H, Nansai R, Ando W, et al. 2015. Zone-specific integrated cartilage repair using a scaffold-free tissue engineered construct derived from allogenic synovial mesenchymal stem cells: Biomechanical and histological assessments. [Internet].J. Biomech. 48(15):4101–8[cited 2015 Nov 19] Available from: http://www.ncbi.nlm.nih.gov/pubmed/26549765.

35. Malda J, Kreijveld E, Temenoff JS, et al. 2003. Expansion of human nasal chondrocytes on macroporous microcarriers enhances redifferentiation. [Internet].Biomaterials 24(28):5153–61[cited 2015 Dec 14] Available from: http://www.ncbi.nlm.nih.gov/pubmed/14568432.

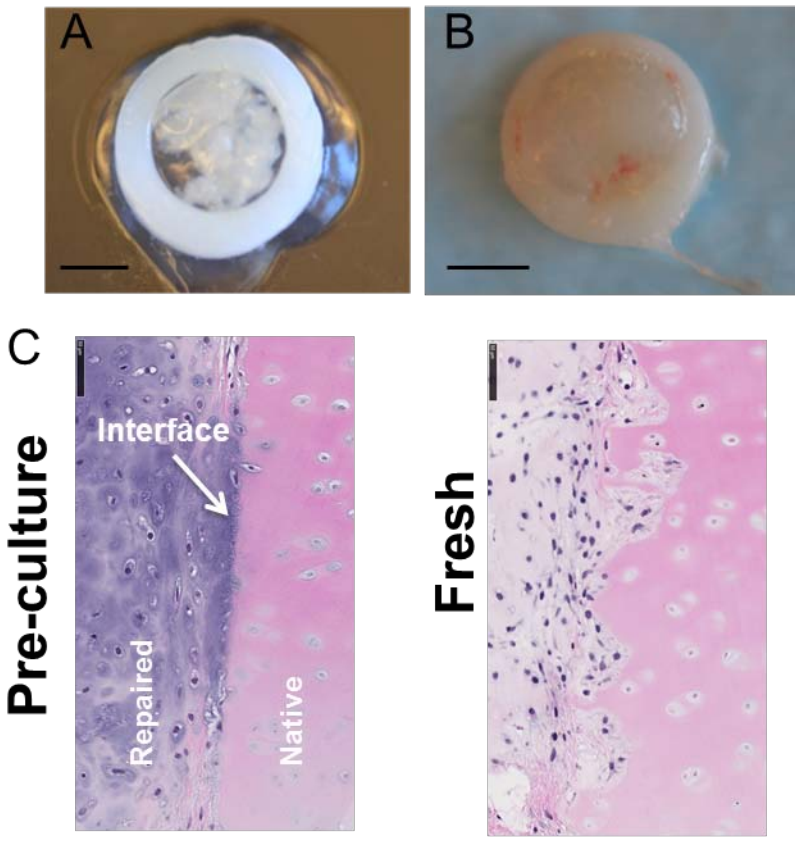

Figure 1. Cell clusters capped with fibrin gel in the center of cartilage ring prior to implantation (A) and after harvest after 12 weeks (B). Scale bars = 300μm. H&E stain, showing interface of repaired and native articular cartilage in the murine model (C) Scale bar = 1mm.

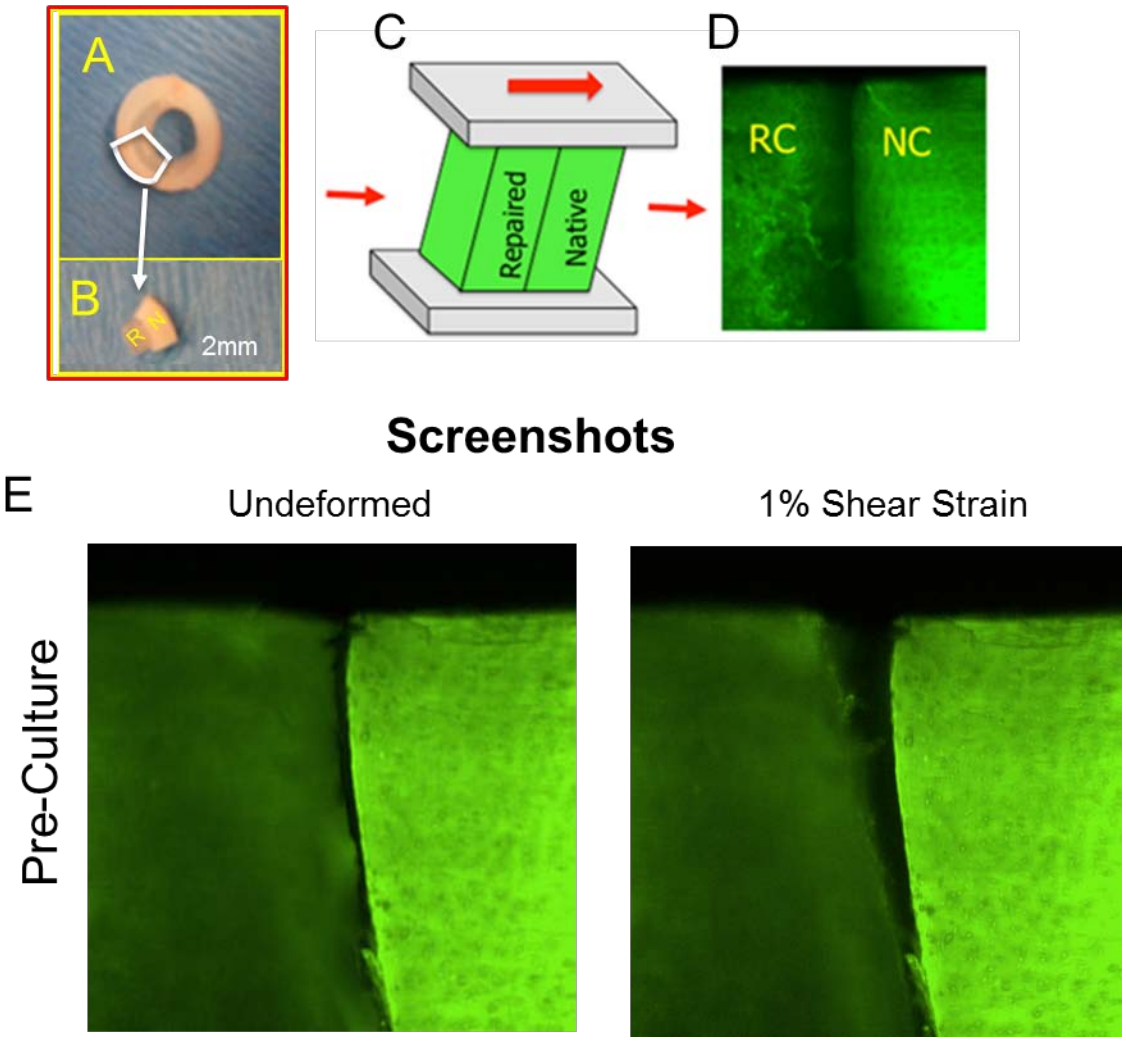

Figure 2. Articular rings of repaired and native cartilage were cut into cubes (A, B) representative schematic of how the sample is loaded in the tissue deformation imaging stage (C) confocal micrograph taken at the interface of repaired cartilage (RC) and native cartilage (NC) (D) screenshots of

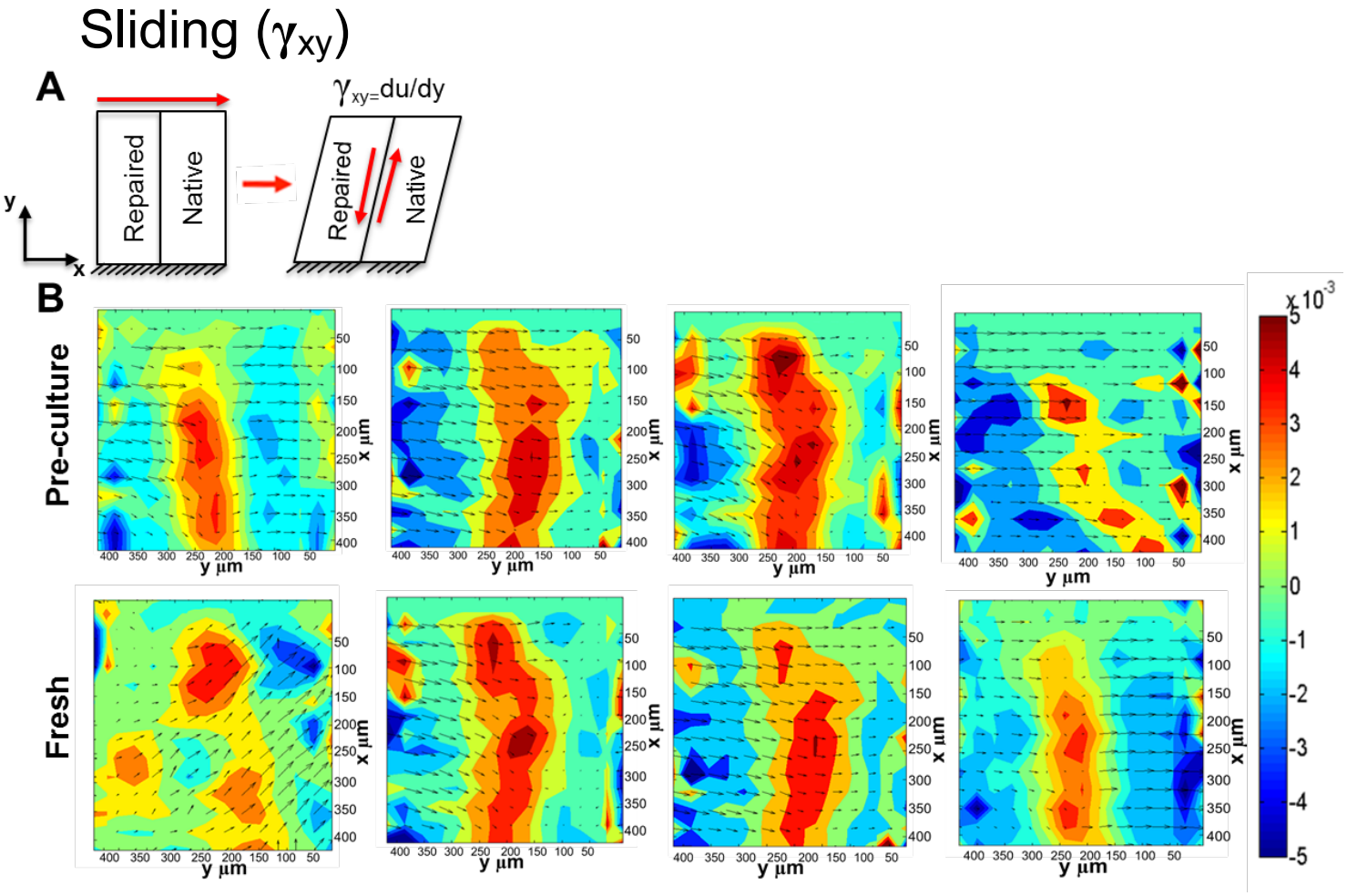

Figure 3. Representative schematics of sliding at the interface (A) PIV Vector Maps for Sliding (B) Shear strain applied parallel to the articular surface direction, was found to induce sliding (γ_{xy}) at the interface. Two-dimensional vector maps of γ_{xy} exhibited large strains at the interface for both groups.

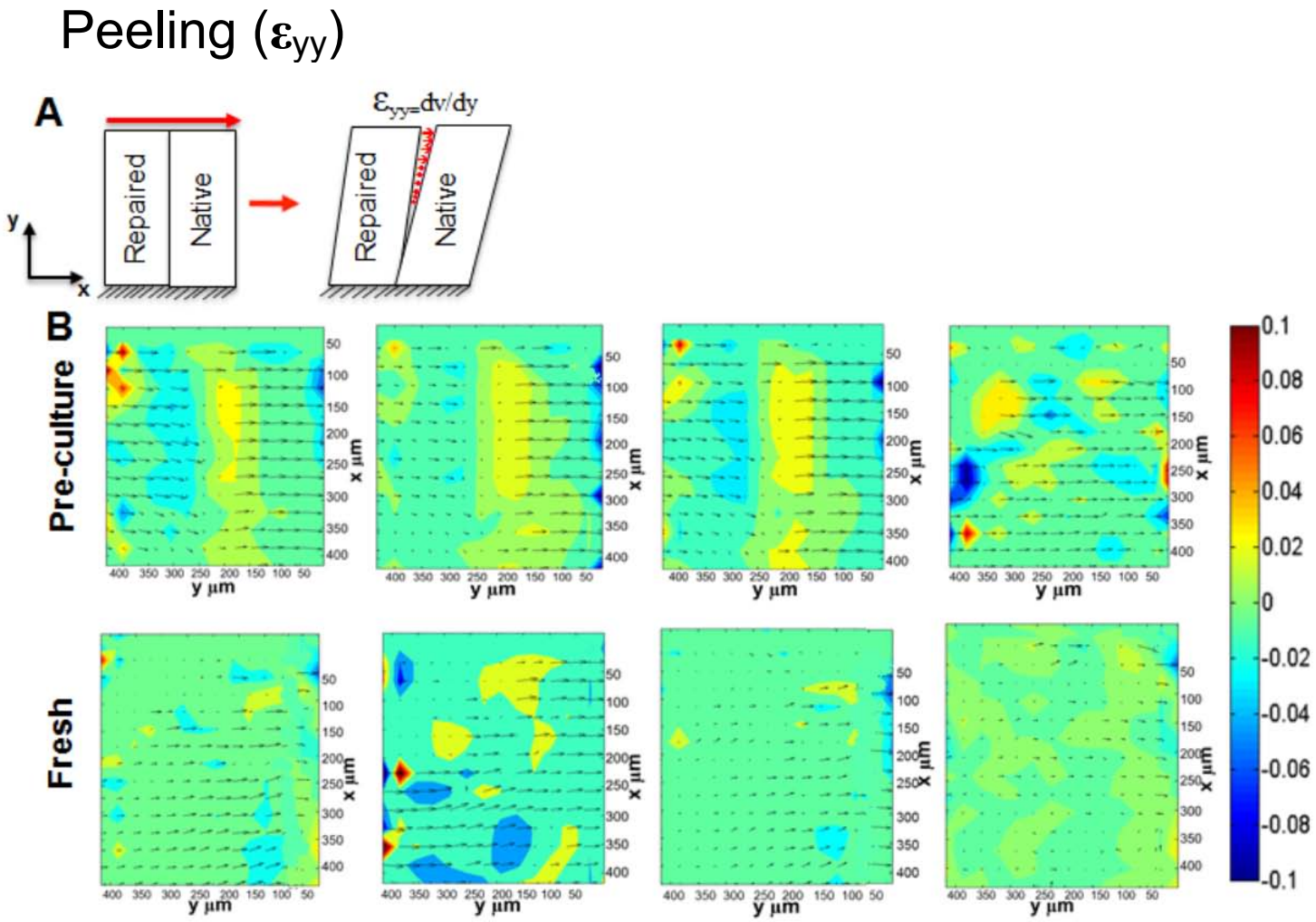

Figure 4. Representative schematics of sliding at the interface (A) PIV Vector Maps for Peeling (B) Shear strain applied parallel to the articular surface direction, was found to induce peeling (ε_{yy}) at the interface. Pre-culture group displayed more peeling at interface compared to fresh group. Integration appeared more prevalent near the surface, but was poorly integrated at deeper depths.

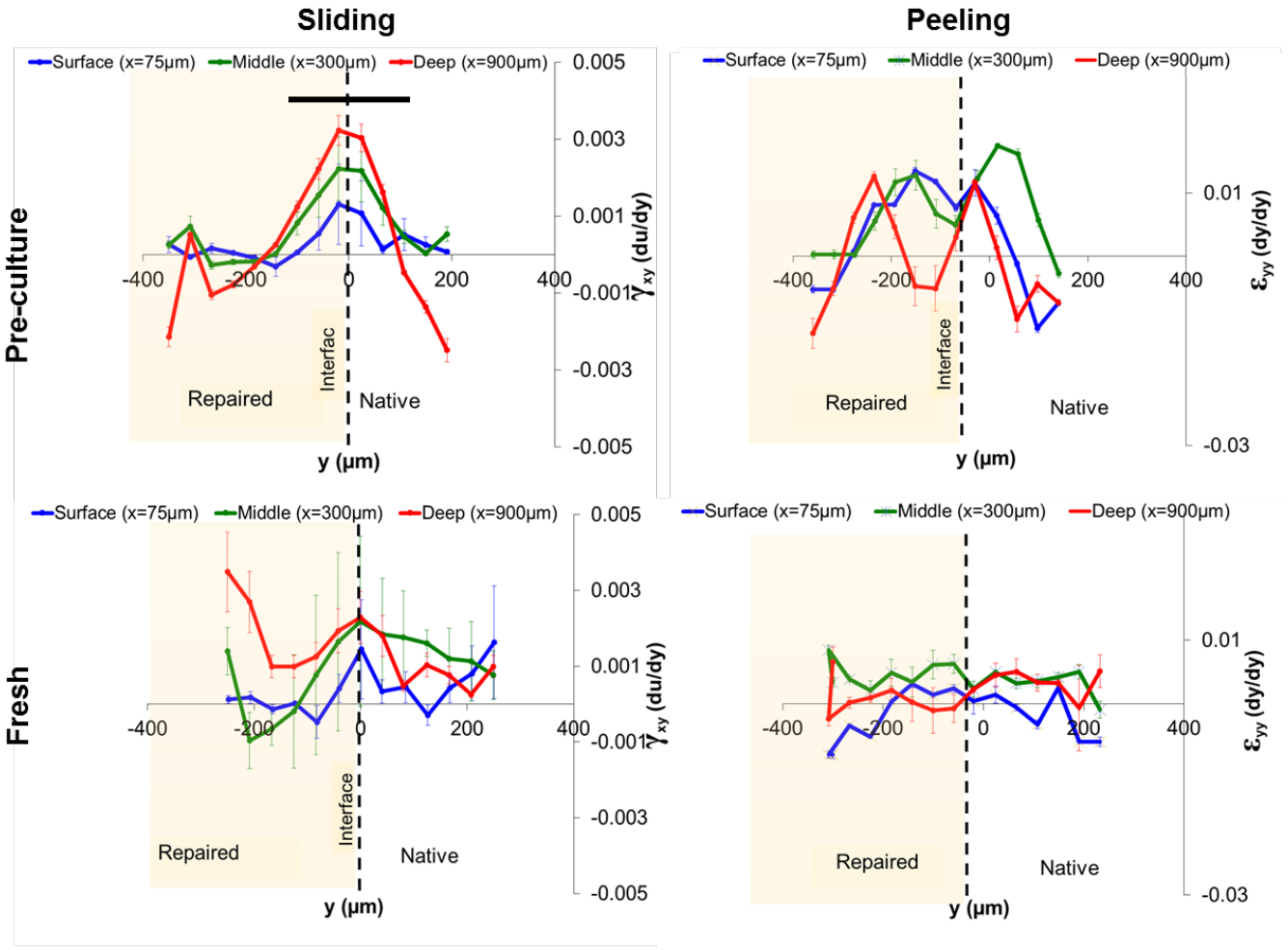

Figure 5. Depth-Dependent Interfacial Profiles: The interface in both groups demonstrated very similar sliding features, but was different in peeling. γ_{xy} values were lower at the articular surface, but increased by a factor of 2 at higher depths (300-900μm). ε_{yy} values were higher at the surface and remained relatively high throughout the entire depth of tissue. Bar denotes statistical difference.